Reconstruction of Paleoenvironmental Conditions and Temporal Patterns of Ancient Mining on Isle Royale using Biochemical and Trace Metal Analyses of Lake Sediment

A Thesis

SUBMITTED TO THE FACULTY OF

UNIVERSITY OF MINNESOTA

BY

Kathryn G. Vall

IN PARTIAL FULFILLMENT OF THE REQUIREMENTS

FOR THE DEGREE OF

MASTER OF SCIENCE

Dr. Byron Steinman

November 2018

Acknowledgements

I would like to thank my advisor, Byron Steinman, for the incredible opportunity to visit Isle Royale, and so many other breath-taking places. It has been a joy to take part in such an interesting and worth-while master's project, and I am extremely grateful for all the guidance he has given me. I would like to thank Dave Pompeani, Dan Bain, and Seth Depasqual for collaborating on this project and discussing literature and results with me. These discussions spurred a lot of scientific intrigue and helped me develop the driving questions of my research and identify what was most significant to me. I am grateful to Katie Schreiner and Howard Mooers for reviewing this work as members of my committee and taking such a keen interest in my endeavors.

I would also like to acknowledge the staff, faculty, and graduate students of the Geology Department and the Large Lakes Observatory for their help and encouragement. Specifically, Julie Halbur, whose patience and diligence was instrumental (pun intended) in my many laboratory preparations, and Zach Wagner for being an excellent counterpart in the lab, in the field, on road trips, and in the classroom.

Finally, I would like to thank my husband, Dylan, and the rest of my family for their endless moral support and encouragement.

This project was funded by the National Park Service and the Geological Society of America.

Abstract

Isle Royale and the Keweenaw Peninsula of Michigan are home to some of the oldest examples of native North American metalworking and land use. The overarching objective of this research is to produce a reconstruction of the timing, spatial patterns, and environmental impacts of mining activities on Isle Royale through sedimentological and biogeochemical analysis of lacustrine sediments. We also seek to produce a parallel record of paleoenvironmental conditions to assess the potential impacts of environmental change on ancient mining cultures.

In 2016, we collected a 7.5 m long sediment core sequence from Lily Lake on Isle Royale, MI. Lily Lake lies approximately 100 m above the current water level of Lake Superior and formed approximately ~11,000 years before present following the retreat of the Laurentide ice sheet. Lily Lake has been exposed to very little human land use change relative to other lakes on Isle Royale (e.g. there are no ancient mine pits in the immediate catchment), and thus is well suited for reconstructing past environmental changes. We analyzed weakly sorbed metal concentrations using ICP-MS to test hypotheses on the timing and transport mechanisms of potential metal pollution derived from ancient mining activities. In addition, we conducted EA-IRMS analysis (including carbon/nitrogen ratios, and the isotopic composition of organic C and N) on bulk organic sediment to provide a record of natural paleoenvironmental changes.

Preliminary results from the metals analysis provide evidence of Middle Archaic mining activity that is temporally consistent with radiocarbon dated artifacts and similar evidence from other lakes located adjacent ancient mine pits on Isle Royale and the Keweenaw Peninsula of Michigan. Additional work is required to assess the relative influence of natural versus anthropogenic processes that may have influenced metal concentrations in Lily Lake sediment and to determine a transport mechanism for the putative mining related pollution.

This research is significant to the continued understanding of temporal and spatial patterns of mining on Isle Royale and will therefore be of use to archaeologists. This research will also inform studies on the transport

mechanisms of pollution and how pollution signals are expressed in lake sediment. There is also a great need to understand more about the ability of Lake Superior (and potentially other great lakes) to ameliorate broad scale climate change, which has major implications for future ecological responses to climate.

Table of Contents

Introduction

Isle Royale and the Keweenaw Peninsula, Michigan, are home to extensive copper deposits (Bornhorst and Barron 2011) that were extensively mined in both historical and ancient times. Recent research suggests that the oldest occurrences of metal working in the world occurred there approximately 8000 calendar years before present (BP) (Pompeani et al. 2013a, 2014; Reardon 2014). Archaeological surveys in the early 20th century were the first to identify ancient pit mines and artifacts (Dustin 1957; Holmes 1901; Lathrop 1901). LiDAR imagery has greatly improved surveys of these areas, by revealing numerous tailing piles and pit mines that were not discovered using traditional surveying methods (Gallagher and Josephs 2008). Determining the age of the pit mines and tailings piles, and hence the time when the mining occurred, has been a long standing question in archaeology, with most of the focus applied to radiocarbon dating artifacts and other organic material associated with features and sites (Beukens et al. 2006). Recent paleolimnological research has provided valuable information regarding the timing of these events through trace metal and radiocarbon analysis of lake sediment. These studies produced evidence suggesting that prehistoric mining activities likely produced metal pollution that was deposited in lakes and incorporated into sediment at concentrations exceeding background levels (Pompeani et al. 2013a, 2014). These analyses have been used to identify the timing and duration of copper procurement, and to validate archaeological data acquired through radiocarbon dating of artifacts and features. Determining the timing, intensity, and spatial patterns of ancient mining on Isle Royale and the Keweenaw Peninsula is of cultural and societal significance, as it sheds light on the social complexity and technological capabilities of Archaic North American civilization, a time period and location for which human history is largely unknown.

Two Holocene timescale studies on the paleoclimate of Isle Royale have been conducted, of which both rely principally on analyses of pollen in lake sediment (Flakne 2003; Potzger 1954). The Flakne et al. (2003) study was

focused on sediment from Lily Lake, with age constraint provided by six radiocarbon dates all produced using samples of bulk sediment (Flakne 2003). This method of radiocarbon dating has proven to yield ages with large uncertainties due to terrestrial carbon sequestration in soils (Grimm et al. 2009). Furthermore, although insightful, analysis of pollen abundance alone is insufficient for developing a complete reconstruction of past climate, as the differences in transport and preservation of pollen may result in misrepresentation of dominant vegetation types. Nevertheless, a transition to a dry climate during the mid-Holocene is inferred from palynological analysis of sediment from Lily Lake as well as Lake Ojibway on Isle Royale. Both records exhibit a shift in abundance of spruce pollen to pine pollen at this time (Flakne 2003). However, this transition appears much less dramatic in records from Isle Royale than in records from other lakes outside the climatic influence of Lake Superior (Davis et al. 2000). Pollen records from lakes on Isle Royale and from five other national parks located near the Great Lakes were compared to analyze the potential for lake effect climate to ameliorate a smaller lake's sensitivity to climate warming (Davis et al. 2000). This study found that the warm dry period recorded during the mid-Holocene was less pronounced in locations within greater proximity to the Great Lakes, such as Isle Royale National Park, and more pronounced in locations further away, such as Voyageurs National Park (Davis et al. 2000). Due to the complex nature of climate in the Great Lakes Region, there is a need for research to be conducted to evaluate the spatial heterogeneity of climate patterns across this region. A higher resolution record of vegetation response to climate in the Lily Lake catchment will provide a basis for comparison with other records in the Lake Superior Region and perhaps provide insight on the potential for Lake Superior to temporarily buffer future climate change in its immediate vicinity.

Paleolimnological research has demonstrated that the collection and analysis of sediment cores from multiple lakes throughout the Lake Superior region will potentially provide a clearer picture of human history through the Holocene, as well as changes in climate that may have affected civilization. To

these ends, we present a multi-proxy record spanning the past ~11,000 BP from Lily Lake based on trace metal concentration, the isotopic composition and amounts of lacustrine carbon and nitrogen ($\delta^{13}C$, %C, and C/N ratio), and lignin phenol analyses of sediment cores. This study focuses on the fraction of trace metals that are weakly sorbed to organic matter and other sediment constituents, because changes in concentration of this exchangeable fraction reflect anthropogenic inputs, such as aerosols that are released during combustion of rock, biomass, and fossil fuels. Because of its remote location and the lack of historical human land use in the surrounding catchment, Lily Lake is an ideal control site for providing context for changes in anthropogenic inputs and paleoenvironmental changes through the Holocene. Lily Lake is located at a high elevation (relative to the mean elevation of Isle Royale), far from shorelines, and has not been exposed to land use changes such as logging, habitation, or agriculture. Therefore, the record of vegetation changes in the Lily Lake catchment potentially provides a more accurate representation of climate change through the Holocene than other lakes on the island where vegetation has been affected by humans. Furthermore, Lily Lake does not contain ancient pit mines in its catchment and therefore can be used as a control site for determining the extent to which pollution associated with ancient mining activities was derived from atmospheric transport versus catchment runoff, with the latter having been hypothesized to be the principal transport mechanism for lakes containing mine pits (Pompeani et al. 2013a, 2014). This project provides complimentary records of changes through time in trace metal concentrations and various biogeochemical proxies in lake sediment that can be compared to other records from the region.

This record compliments the research of Flakne et al. (2003) and expands upon it through enhancement of the sampling resolution, the use of terrestrial organic macrofossils for age model development, and the application of a suite of additional sedimentological and biogeochemical analyses. Results from these proxies are used to infer the timing and magnitude of ancient mining, and climate variability effects on the source of organic matter (terrestrial vs. aquatic) and type

of vegetation in the catchment (gymnosperm vs. angiosperm and C3 vs. C4 plants).

The aim of this research on Isle Royale is twofold. Firstly, we aim to investigate the timing and magnitude of ancient mining activity; secondly, we aim to reconstruct the influence of Holocene climate variations on vegetation. Our hypotheses are that the Lily Lake sediment will contain a metal pollution signal distinguishable from background levels if mining occurred on a sufficient scale and pollution was transported atmospherically, and that vegetation analysis will show a cool climate in the Early Holocene, and a dry climate during the mid-Holocene. We will test the former hypothesis by conducting trace metal concentration analysis on sediments from Lily Lake and comparing results to other sediment records from Isle Royale and the Keweenaw Peninsula. To test the latter hypothesis, we will use analyze the C/N ratio and $\delta^{13}C$ values of bulk sediment and conduct lignin phenol biomarker analysis.

Study Site

Lily Lake

Lily Lake (W 47.91177˚ N 89.09109˚) is located on Isle Royale, MI in Lake Superior (Figure 1). The surface area of the lake is 0.095 km^2, and the maximum depth is approximately 4 m. The catchment of lily lake is 0.48 km^2 and contains old-growth hardwood forest composed of *Betula alleghaniensis* (yellow birch), *Acer saccharum* (sugar maple), *Pinus strobus* (white pine), *Thuja occidentalis* (eastern white-cedar), and *Quercus rubra* (red oak) (Flakne 2003). Floating bog mats occupy the entire perimeter of Lily Lake and extend into the lake approximately 10-20 m from the southern shore, and as much as 40 m from the western shore. The bogs are dominated by various species of sphagnum mosses, sedges, and shrubs, as well as carnivorous *Sarracenia purpurea*

(pitcher plants), carnivorous *Drosera rotundifolia* (sundew), and *Vaccinium oxycoccos* (bog cranberries). The lake has no major fluvial inputs or outputs.

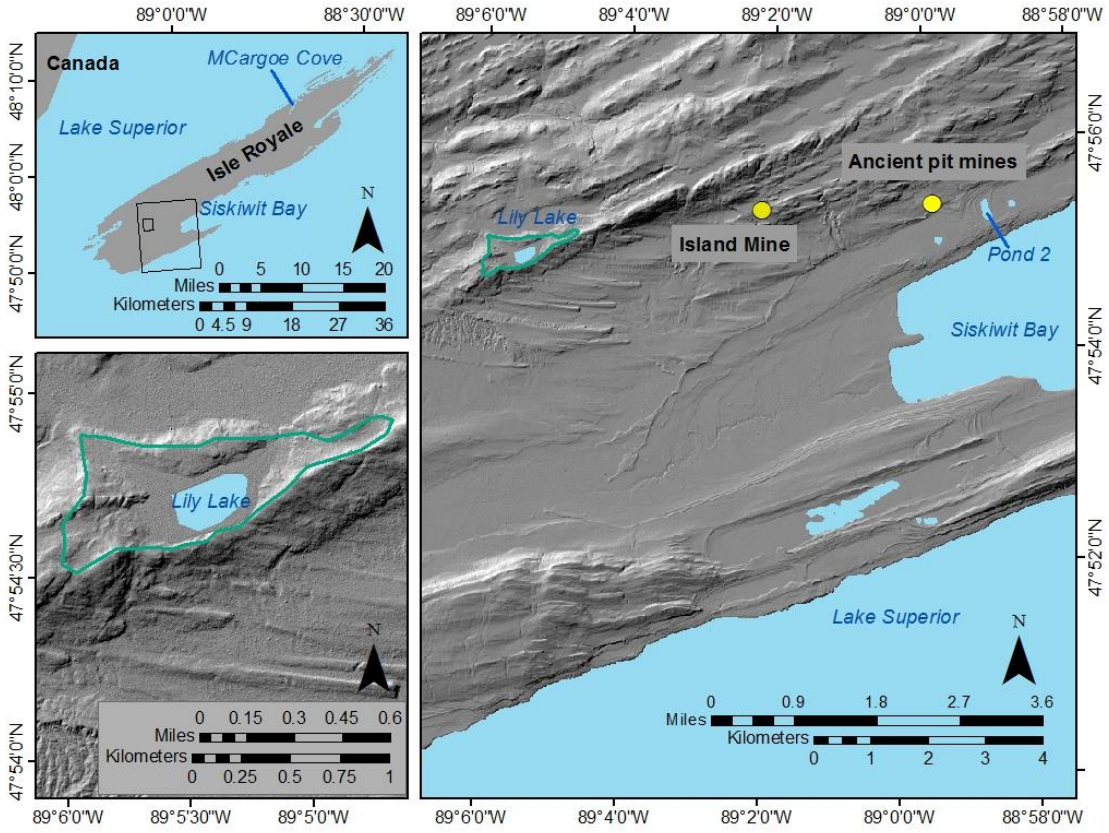

Figure 1. LiDAR map showing location of Lily Lake. Blue line indicates catchment boundary. Yellow dots indicate nearest locations of copper extraction.

Lily Lake lies atop the Red Oak Ridge, which rises approximately 120 m above the current level of Lake Superior (Figure 1). The Red Oak Ridge and other parallel ridges on the island are surface expressions of the southeast dipping beds that form the northern limb of the Lake Superior syncline (Rosenmeyer 2009). The southern limb of the syncline outcrops on the Keweenaw Peninsula in Michigan.

The parent material in the Lily Lake catchment is glacial material deposited following the retreat of the Laurentide ice sheet on Isle Royale approximately 11,000 years ago (Flakne 2003; Huber 1973; Lewis and Anderson

1989; Saarnisto 1974). The basin of Lily Lake was formed by glacial scour and inundated following the Marquette readvance (Farrand and Drexler, 1985). The retreat of the glacial lobe covering Isle Royale began relatively slowly, leaving deposits of till on the southwest end of the island. The glacier retreated much more rapidly over the central and northeastern portions of the island, resulting in extensive exposure of bedrock (Huber 1973). Due to its high elevation on the island, the basin of Lily Lake became isolated soon after deglaciation and was not submerged during the Minong or Nipissing glacial lake phases (Raymond et al. 1975).

The underlying bedrock in the Lily Lake catchment is the Portage Lake Volcanic Group, which is a series of amygdaloid basalt lava flows interbedded with sandstones and conglomerates. The Portage Lake Volcanics host rich native copper deposits which formed from hydrothermal fluid moving through fissures (Bornhorst and Barron 2011; Rosenmeyer 2009). These deposits are prevalent on Isle Royale and on the Keweenaw Peninsula and have been extensively mined. Lily Lake is approximately 4 km from Island Mine, which is the nearest known pit mine site (Figure 1). Island Mine is a historic mining location and was exploited post 1800 CE. The nearest presumed ancient pit mine sites are located 7 km southeast of Lily Lake near Hay Bay and Pond 2. Preliminary archaeological surveys suggest that these sites were mined during ancient times (Dustin 1957); however, the exact age has yet to be determined.

Isle Royale climate

Isle Royale is located near the northern shore of Lake Superior, and, because large bodies of water experience slower rates of temperature change than the surrounding atmosphere, climate on Isle Royale has less pronounced seasonality than the greater Midwest region (Davis et al. 2000). Average temperatures in July reach a high of 24˚C (75˚F) and a low of 12˚C (54˚F). In winter, average January temperatures are between -8 to -18˚C (0 to 18˚F) (NOAA, 2017). Average monthly precipitation on Isle Royale is ~8 cm during the summer months, and 3 to 7 cm during winter months. Isle Royale National park

is typically closed November through April due to the large amounts of snow, which make park operations difficult. Isle Royale Climate experiences less contrast between winter and summer temperatures than the regions inland from Lake Superior. This is due to the strong local influence of Lake Superior on lake surface temperatures and air temperature. For this reason, Isle Royale receives snow fall approximately two weeks later than inland areas, and temperatures on the island remain cold enough to sustain snow and ice several weeks later into the spring.

Methods

Sediment core collection

Two sediment cores (A-16, B-16) were collected from Lily Lake in August of 2016 using a modified Livingstone piston corer with driving rods (Wright, Mann, and Glaser 1984). Eleven drives from core A-16 (W 47.91177˚ N 89.09109˚) were collected using a 5.7 cm diameter, 1 m steel barrel at a water depth of 1.4 m and extruded into ABS tubing that was split lengthwise and lined with plastic wrap. Four drives from core B-16 (W 47.91177˚ N 89.09102˚) were collected using 6.7 cm diameter, 1.5 m polycarbonate tubes at a water depth of (1.4 m). The fifth section of Core B-16 was collected using the method for core A-16. Each drive was sealed for transportation using tape. A 1.5 m surface core was collected using 6.7 cm diameter polycarbonate tube from the location of core A-16. The core was carried vertically to shore and extruded into plastic bags at 1 cm intervals using a tray fitted to the top of the core barrel. All cores were stored in the dark at 4°C until sampling for analysis.

Initial core sampling and loss-on-ignition

All analyses were conducted on sediment core B-16. Each drive was split into halves and sampled for loss-on-ignition (LOI) and bulk density analysis at 3

cm intervals using a 2 cc volumetric sampler. The samples were frozen then lyophilized at -40° for a minimum of 24 hours. Following the lyophilization, the dry weight of the samples was recorded. Dry bulk density was determined as the dry weight divided by the volume of the sample.

The relative abundance of organic matter was determined using LOI using methods described in Dean (Dean 1974). Previously freeze-dried samples were homogenized using an agate mortar and pestle, weighed, and combusted at 550° C for 4 hours. Weights of the samples were recorded following the 550° burn. One run of LOI was conducted on drive 4 at 1000° C for 1 hour.

Core chronology

Samples for radiocarbon analysis were visually identified and collected from the sediment cores. Large samples were directly obtained from the cores, and smaller samples were processed by collecting ~3.5 cc samples from the cores and soaking them for 24 hours in 3% hydrogen peroxide (H_2O_2) to disaggregate sediment. The solution was then filtered through a 100-micron sieve and rinsed with tap water. Fine particles of charcoal, seeds, and wood, were collected under magnification using metal tweezers. All samples were stored in glass vials with deionized water. At Northern Illinois University radiocarbon samples were pre-treated using an acid-base-acid method (Abbott and Stafford 1996) and combusted at 200° C in vacuum sealed quartz tubes. The samples were analyzed at the W. M. Keck Carbon Cycle Accelerator Mass Spectrometry Laboratory at the University of California Irvine.

The Lily Lake age model was determined using 14 accelerator mass spectrometry (AMS) radiocarbon dates. The record spans 11,000 yr BP to present. Radiocarbon dates were acquired from terrestrial material such as wood, seeds, and leaves. One sample of aquatic material was used and produced an age that was consistent with the age model trend. The ages were calibrated using IntCal13 calibration curve (Reimer 2013). To produce a median age and probability distribution for the radiocarbon dates we used Bchron, a

Bayseian statistical age model software package for R (Parnell et al. 2008; Parnell, Buck, and Doan 2011). This software produces multiple iterations of the age model by sampling from the probability distribution based on analytical uncertainty, depth interval spanned by the sample, and the calibration curve of known ^{14}C concentrations in the atmosphere through time.

Metal analysis

Elemental analysis to determine concentrations of weakly sorbed trace metals such as copper, lead, iron etc. was conducted using a weak nitric acid digestion according to the methods outlined by Pompeani et al. (2013). 2 cc samples were collected from each drive and placed in plastic scintillation vials. The lower five drives were sampled every 3 cm, and the upper 140 cm surface core was sampled every 2 cm. Sediment samples were frozen, then lyophilized for a minimum of 24 hours at -40° C. Dried samples were homogenized using an agate mortar and pestle; all tools were cleaned with milliQ water prior to use on each sample. For each sample 0.10 to 0.20 g (± 0.005) of sediment was weighed and placed in a polypropylene tube under 6 mL of 10% HNO_3. The weight of the sediment-solution mixture was recorded. Samples were placed horizontally on a shaker table for 24 hours. The samples were then centrifuged at 4000 rpm for 15 minutes, and the resulting supernatant was pipetted into a new set of polypropylene tubes. The supernatant was refrigerated and transported to the University of Pittsburgh to be analyzed on a Perkin/Elmer Nexion 300X ICP-MS. Prior to being run on ICP-MS, subsamples of supernatant were diluted with 10 mL of 2% nitric acid and 0.08 mL of a solution containing the internal standards Ti, Ge, and Be. The supernatant was mixed by hand for 30 seconds prior to loading into the ICP-MS. The instrument was calibrated prior to each run using a set of standards to produce calibration curves. Blanks containing 10 mL of 2% HNO_3 and 0.08 mL of the internal standard were analyzed every tenth sample to determine a detection limit of <1 ppm for Mg, K, Ti, Fe, Ni, Cu, and <100 ppt for Pb. Duplicate dilutions were prepared and analyzed for every seventh sample

and were within 5% for the metals reported, except for K, which showed variability between duplicates of better than 17%. This high variability in K is likely because the lower limit of the calibration curve is 0.02 ppm, and values of K measured near this limit may be over extrapolated. The accuracy of measurements of K concentrations could be improved by rerunning the samples at a smaller dilution.

Bulk elemental analysis

Elemental analysis isotope ratio mass spectrometry (EA-IRMS) was conducted using a Costech CNS analyzer interfaced to a Thermo Delta Plus XP IRMS located at the Large Lakes Observatory to determine bulk organic carbon content, carbon to nitrogen ratio (C/N) and $\delta^{13}C$ values of sedimentary organic matter. The lower five drives of core B-16 from Lily Lake were sampled at a resolution of 6 cm. The surface core was sampled at 4 cm resolution. All samples were collected using methanol cleaned tools and placed in combusted glass jars. The samples were frozen, then lyophilized at -40°C for a minimum of 24 hours. The samples were homogenized using an agate mortar and pestle (cleaned with methanol prior to every sample), dried a second time overnight in an oven at 50° C, and stored in a desiccator until processing. The samples were not fumigated prior to analysis because of the lack of carbonates in the sediment. One blank tin capsule and one blank empty well were analyzed at the beginning of each EA-IRMS run to test for residual material in the instrument. Standards were run after every ten samples to determine analytical precision. The standards used included: 13C-labeled acetanilide (71.09% C, 10.36% N, δ13C = -33.83‰), caffeine (49.48% C, 28.85% N, δ13C = -38.53‰), natural-abundance sorghum (41.58% C, δ13C = -13.68‰) and low-organic content soil (1.61% C, 0.13% N, δ13C = -26.66‰). Analytical precision (1σ) was better than 1.1% and 1.3% for C and N content by weight, respectively, and better than 0.08‰ for $\delta^{13}C$.

Following the initial EA-IRMS run, five samples from approximately evenly spaced locations spanning the entire core were analyzed to evaluate the effect of

the acid- fumigation treatment. Using previous target weights, subsamples from this batch were loaded into silver capsules, and wetted with 10 microliters of carbon-free distilled water. The tray was placed in a glass desiccator chamber with an ungreased lid and no desiccant, along with a combusted glass beaker containing approximately 50 mL of hydrochloric acid. The samples were fumigated for 6 hours, before being removed and placed on a hot plate to dry for 48 hours, based on the protocol from Harris et al. (2001). The silver capsules were folded, then loaded into tin capsules and analyzed using the EA-IRMS. This test batch was also run with two sets of standards, a blank capsule, and a blank well. No duplicates were prepared.

A second test batch was prepared using the same set of five samples, which were re-homogenized using a mechanical grinding mill to produce the appropriate sediment fineness. For this batch, the sample set was duplicated three times, and each set was prepared using a different treatment method. The first set was non-fumigated, to test for potential effects associated with a lack of homogenization. The second set was treated with acid-fumigation, to test whether the degree of homogenization influenced the extent of the fumigation reaction. The third set was prepared according to a new method of direct acid application. For this treatment, subsamples weighing approximately three times the original target weight, were loaded into cold acid cleaned falcon tubes. Then, 5 mL of 1N hydrochloric acid was added to each polypropylene tube, mixed using a vortex mixer, and gently swirled on a shaker table for 4 hours, with intermittent remixing using the vortex mixer. The polypropylene tubes were centrifuged for 10 minutes at 3400 rpm and the waste removed. The sediment was rinsed using 10 mL of carbon-free distilled water, centrifuged for 10 minutes at 3400 rpm, and the waste removed. The rinsing process was repeated a second time, then the wet sediment was transferred into a combusted glass vial. The vials were covered with lint-free wipes and dried at 40° C for 72 hours. Once dry, the sediment was scraped and re-homogenized inside the jar using a methanol cleaned metal spatula. The dry sediment was then loaded into tin capsules and run through EA-

IRMS according to previous methods. This batch was run with two sets of standards, a blank capsule, a blank well, and no duplicates.

Lignin phenol analysis

Characterization of lignin phenol ratios in the sediment organic matter was conducted using gas chromatography - mass spectrometry (GC-MS) on the Agilent 6890 interfaced to an Agilent 5973 MS at the Large Lakes Observatory. Lignin phenols were extracted from freeze dried sediment samples using alkaline cupric oxide oxidation methods of Schreiner et al. (2013). Freeze dried sediment samples were weighed into methanol cleaned stainless steel vessels along with 330 ± 4 mg of combusted CuO powder. The vessels were filled with 2N NaOH and sealed in a glove box under N_2 atmosphere. The sealed vessels were placed in an oxidation oven for 3 hours at 155°C. Once oxidation was complete, 50 µL of TCAD was delivered to each of the vessels, and the vessels were shaken by hand. The vessels were then centrifuged at 3500 rpm for 2 minutes, and the liquid poured off the top into a combusted glass vial. This rinse was repeated for each vessel two additional times. Once all the liquid was transferred, 2.5 g of combusted NaCl and 3 mls of 6N HCl were added to each vial, and the vials were stored overnight at 5˚C. The next step was a liquid-liquid extraction to transfer the lignin phenols from the NaOH solution to ethyl acetate. For this step, 3 mls of ethyl acetate was dispensed into each of the vials, which were then shaken by hand for 1 minute and centrifuged for 2 minutes at 2500 rpm. The top layer of liquid was removed using a combusted glass pipette and transferred into a new combusted glass vial. This step was repeated two additional times. Approximately 2.5 g of sodium sulfate was added to each vial and left to dry for 30 minutes.

The liquid was removed from each vial using a combusted glass pipette and filtered through a glass pipette filled with glass wool. Each vial was rinsed twice with 2 mls of ethyl acetate and filtered through the glass wool pipette. A new combusted glass pipette and glass wool pipette were used for each sample

to prevent cross contamination. The vials of ethyl acetate were blow dried to ~1 ml under a constant stream of N_2, then transferred to 4 mL combusted glass vials and blown to dryness. Ethyl vanillin (EVAL) was used as the internal standard and was added to each vial along with 500 µL of pyridine then each vial was vortexed for 30 seconds. The solution was dispensed into glass inserts along with lignin standards and bis-(trimethylsilyl) trifluoroacetamid (BSTFA). The vials were mixed by hand and placed in a heating block at 70° C for 1 hour before being loaded into the autosampler. The sum in milligrams of these phenols is expressed relative to 100 mg of organic carbon (OC) and is referred to as lambda-8 (Λ_8).

Relative error for Λ_8 was within 15% of the theoretical values determined using long term average measurements in lab for NIST reference material #1944 (New York/ New Jersey waterway sediment). Analytical precision for individual lignin phenols was determined using the 1:40 concentration mixed standard plotted on a linear response curve, which resulted in errors within 10% of theoretical concentration for all compounds except acetosyringone, which was more than 100%.

Results

Age model

The glacial transition occurs at 7.44 m and is constrained to 11,000 yr BP (Flakne 2003; Huber 1973; Lewis and Anderson 1989; Saarnisto 1974). The age model produced using Bchron is show no age reversals (Figure 2). The average sedimentation rate is 0.005 g/cm^2/yr.

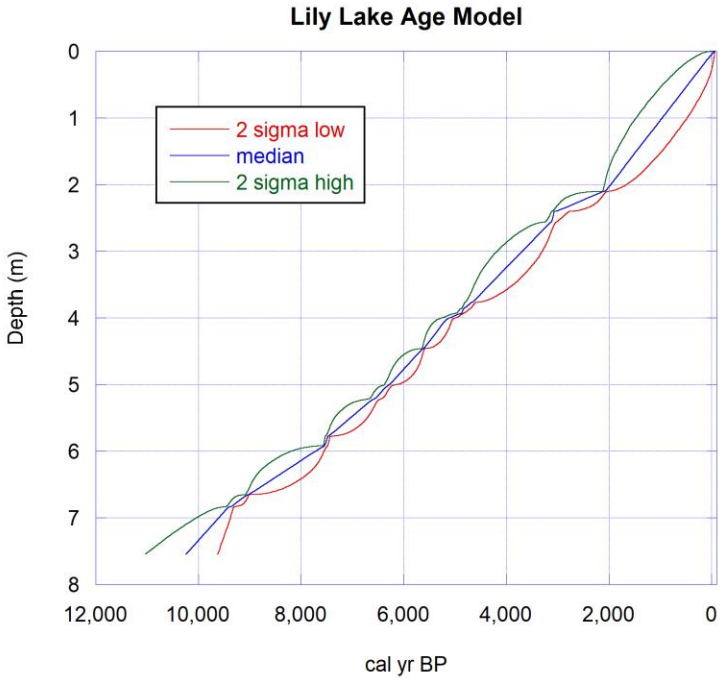

Figure 2. Bchron age model for Lily Lake

Bulk density

The values for bulk density at the base of the core (1.24 g/cm^3) at a depth of 7.55 m are very high compared to the rest of the record (Figure 3). Bulk density decreases abruptly to 0.20 g/cm^3 at about 7.4 m (10,000 BP), then continues to decrease until values reach approximately 0.05 g/cm^3 at 6.5 m. At 4.79 m there is a slight increase from 0.06 to 0.08 g/cm^3. Bulk density remains nearly constant through the remaining upper portions of the core.

Loss-on-ignition

The lowest samples are 98% mineral matter, then values decrease and vary between 63% and 85% through depths 7.34-7.22 m. (Figure 3). Values decrease to 21% at 6.00 m and stay within the range of 16-24% for depths 6.00 - 5.30 m. There is a sharp peak at 4.79 m where mineral matter reaches 63%. This peak corresponds to the slight positive excursion in the bulk density record (Figure 3). Above 4.79 m, values decrease to 29% and stay in the range of 20-30%.

Lead and potassium

Overall, Pb concentrations vary between 0.3 and 21.9 ppm (Figure 3). Background values are 1-2.5 ppm in the lower 4.5 m of the record, and >1.5 through depths 4.5 to 1.5 m. There are three large positive excursions with values of 6.4, 3.3, and 6.5 ppm centered on depths 6.81, 5.38, and 4.77 m. In the most recently deposited sediments, above 1 m, concentrations reach their highest values on record at a maximum of 22 ppm, which is 3 times greater than the maximum concentration measured in lower depths.

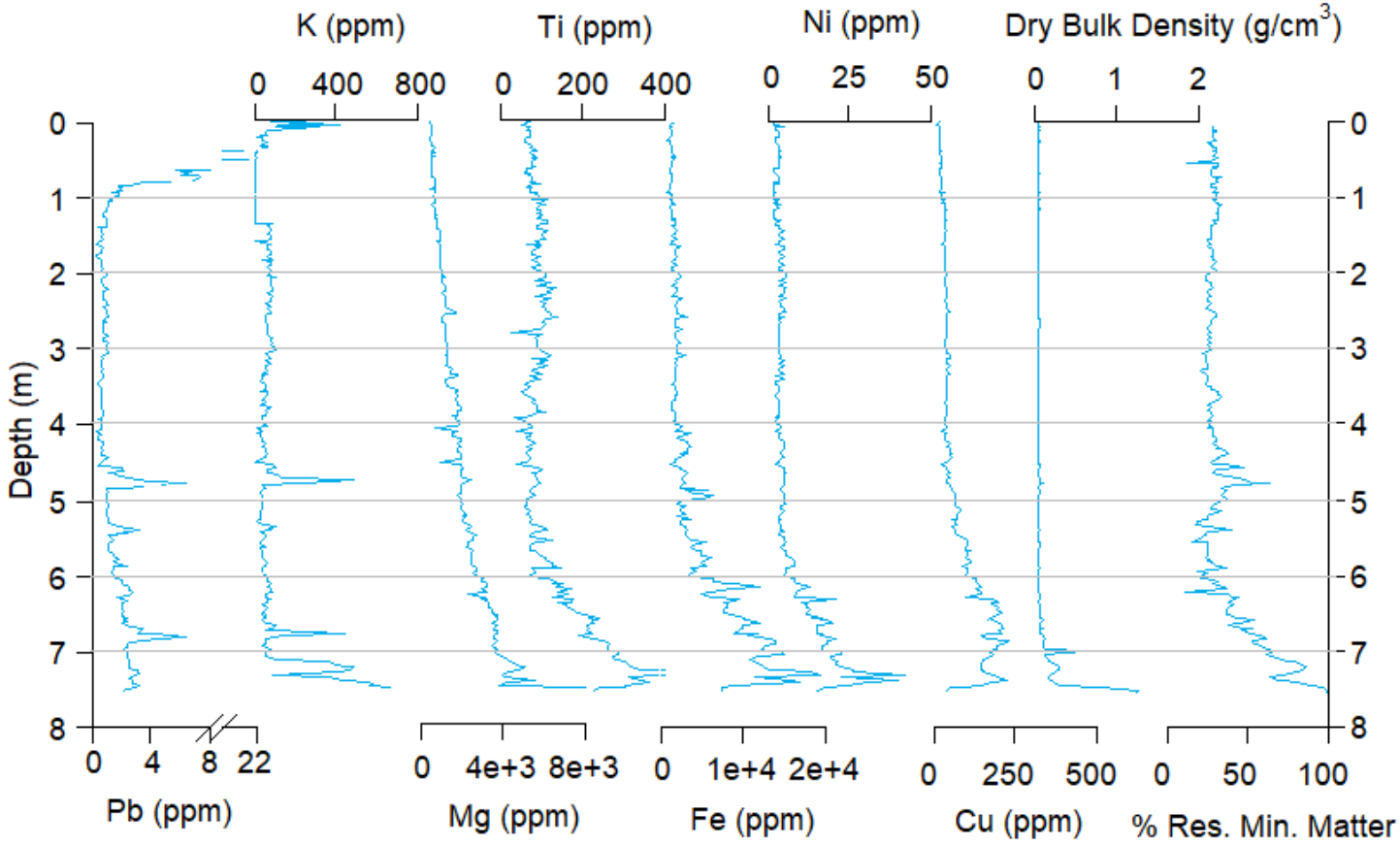

Figure 3. Summary of results from bulk density, loss-on-ignition, and trace metals analysis.

Pb concentrations near the base of the core from 7.53 m to 6.93 m vary between 2.2 - 3.1 ppm (Figure 3). The first Pb peak occurs at 6.81 m and is 6.4 ppm. The next peak spans a depth of 5.53 - 5.41 m, with the highest concentration of 3.3 ppm occurring at 5.38 m. The third Pb spike occurs between 4.89 and 4.53 m, with a peak concentration of 6.5 ppm centered on 4.77 m. Concentrations through the remaining upper ~0.5 to 0 m of the core are highly variable (~6 ppm between high and low points), but average values decrease from about 20 ppm at 0.5 m to about 12.8 ppm at 0 m.

Potassium concentrations vary between 0 and 650 ppm overall, with background values ranging approximately 10-70 ppm (Figure 3). There are four positive excursions in the lower sediments with concentrations of 480, 440, 106, and 480 ppm centered on depths 7.26, 6.81, 5.38, and 4.77 m. The highest concentration of the record, 650 ppm, occurs at the lowest depth, 7.53 m. The K peaks at 6.81, 5.38, and 4.77 m correspond to maximum concentrations of Pb at the same depths. Concentrations of K increase from <100 ppm to a maximum of 460 ppm through depths 1.45 to 0 m.

In sediments between 7 and 4 m, the peaks for Pb and K occur at similar depths and their magnitudes are 2 to 10 times higher than background concentrations. In surface sediments below 7 m and above 2 m increases in K and Pb are decoupled. There is a large increase in K at the base of the core, where no change in Pb is visible. Increases in concentrations of K in surface sediments occur at a shallower depth than Pb, and the magnitude of their maximum concentrations are proportionally less than in sediments between 7 to 4 m. The peaks that occur in sediments between 7 to 4 m show 3-4 times higher magnitude excursions of concentrations of K than Pb, but in surface sediments the K expression is less pronounced relative to Pb.

Iron, Titanium, and Nickel

All three of these elements show similar trends through the depth record, where concentrations of Fe, Ni, and Ti are low through 7.47 to 7.53 m (Figure 3).

Here iron is 7,500 ppm, Ni is 17 ppm, and Ti is 240 ppm. There is a positive excursion near 7.3 m, where concentrations increase to 19,000 ppm for Fe, 40 ppm for Ni, and 450 ppm for Ti. Then, concentrations of Fe decrease to 3,000 ppm, Ni to ~5 ppm, and Ti to ~90 ppm through depths 7.3 to 4.5 m. Concentrations vary between 1,000--4,000 ppm for Fe, 1-6 ppm for Ni, and 30-140 ppm for Ti.

Magnesium

The trend in magnesium concentrations is similar to those of Fe, Ni, and Ti in the upper portion of the core spanning 7 to 0 m (Figure 3). However, at the lowest part of the core (depth of 7.53 m), where concentrations of Fe, Ni, and Ti are low, the Mg concentration is high relative to the rest of the core (8,000 ppm). Average concentrations decrease from about 5,000 ppm at 7.4 m to 500 ppm at 0 m.

Copper

The lowest samples, at depths 7.53 and 7.5 m have concentrations of approximately 44 ppm. Concentration increase to 220 ppm through depths 7.5 to 7.4 m (Figure 3) and vary between 140 and 230 ppm through depths 7.4 to 6.4 m. Concentrations decrease to approximately 50 ppm between 6.4 and 4.5 m. Values in the uppermost sediments, between depths 4.5 to 0 m, vary between 15 and 60 ppm, except for one anomalous data point at 1.72 m depth, where concentrations exceed 10 times the average value for this part of the core. We concluded this to be an analytical anomaly and have removed it from the figures presented in this work.

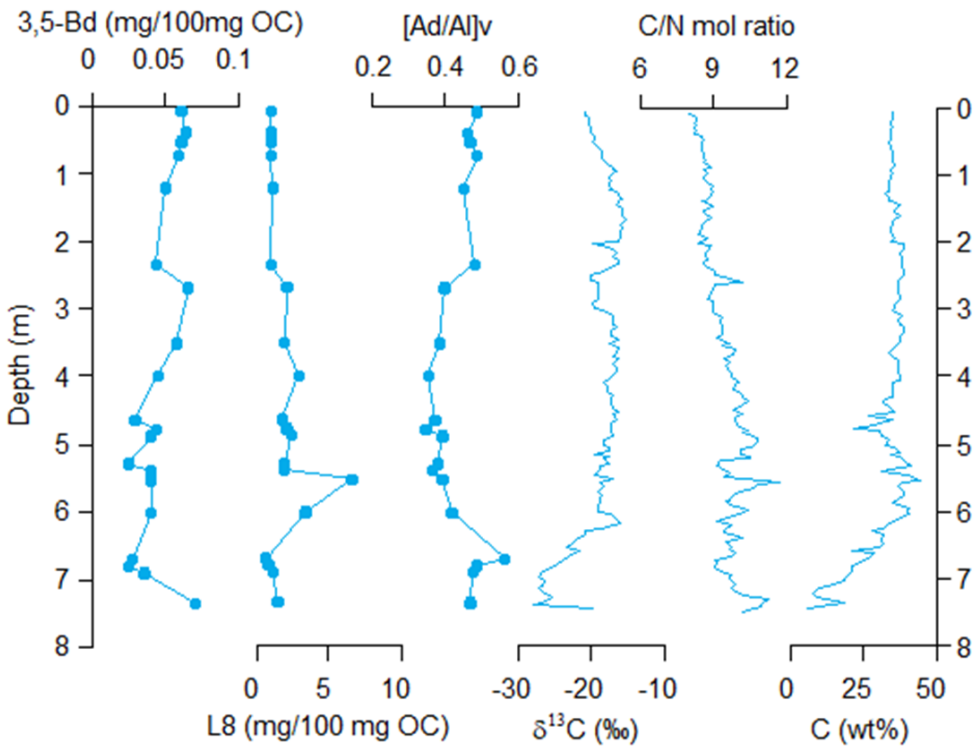

Figure 4. Summary of results from bulk proxy and biomarker analysis

Stable carbon isotope ratios ($\delta^{13}C$)

The lowest depth sampled for organic matter characterization was 7.46 m. Here values for $\delta^{13}C$ are -19 ‰. In the sample directly above this (7.4 m), the value is a much lower at -28‰ (Figure 4). Average values increase from about -28‰ to -18‰ between depths 7.4 through 6 m. Through depths 6 to 3.2 m concentrations vary between -19‰ to -16‰ overall, but averages increase from approximately -18‰ to -17‰ over this interval. Values remain at approximately -16‰ through depths 3.9 to 3.2 m. Through depths 3.2 to 2.3 m, there is a distinct flat topped negative excursion, where values decrease from -18‰ at 3.9 m, to -19‰ at 3.0 m, remain within the range of -20 to -19‰ through depths 3.0 to 2.5 m, then decrease to -16‰ at 2.3 m. Average values through depths 2.3 to 1.0 m vary between -17‰ to -16‰, with one negative excursion centered on 2.04 m with a value of -19‰. The values through the remaining upper portion of the core decrease from -16‰ to -20‰ through depths 1.0 to 0 m.

Ratios of carbon to nitrogen (C/N)

The ratio of carbon to nitrogen in the lowermost depths (7.5-5.0 m) varies between 9 and 12 (Figure 4). Beginning at 4.49 m, the ratio decreases from 10.80 to 8.94 at 2.86 m. The average ratio decreases from 11 to 8 through depths 5 to 0 m, with a positive excursion centered on 2.58 m that reaches a value of 10.

Lignin content (Λ8)

Values for Λ8 (Figure 4) vary between 0.6 to 6.5 mg/100mg OC overall, with one principal positive excursion centered at 5.5 m that reaches a value twice as high as the other values through the core. The lowermost values of Λ8 (depths 7.3 to 6.8 m) vary between 1.4 to 0.5 mg/100mg OC. There is an increase in lignin content through depths 6.7 m to 5.52 m, where values increase from 0.6 to 6.5 mg/100mg OC. Samples through depths 5.4 to 2.7 m vary between 1.5 to 3 mg/100mg OC. Average values of Λ8 decrease to approximately 1.0 mg/100mg OC through depths 2.3 to 0 m.

Acid to aldehyde ratio of vanillyl ([Ad/Al]v)

The ratio of acid: aldehyde in vanillyl varies between 0.4 to 0.6 through depths 7.3 to 6.7 m (Figure 4). The values decrease and vary between 0.3 and 0.4 through depths 6.0 to 2.5 m. Values decrease to an average of 0.5 through the remaining upper portions of the core.

3,5-dihydroxybenzoic acid (3,5-Bd)

The lowermost depth, 7.35 m, has a value of 0.07 mg/100mg OC. Then values decrease to a minimum of 0.02 at 6.7 m (Figure 4). The values through depths 6.0 to 4.6 m vary between 0.04 and 0.02 mg/100mg OC. Values increase

from 0.02 to 0.06 mg/100mg OC through depths 4.5 to 2.5 m, then decrease to an average of 0.04 through depths 2.5 to 1.2 m. The samples in the uppermost section of the core (depths 0.7 to 0 m) are an average of 0.06 mg/100mg OC.

Background

Loss on ignition

Loss on ignition (LOI) is commonly applied to lake sediment to determine the relative percentage abundance of carbonate, organic matter, and residual mineral matter in a given sample (Pompeani et al. 2013; Luly et al. 2006; Nelson et al. 2011; Henne and Hu 2010; Rasmussen et al. 1998). LOI is measured as the percent difference between the weight of dried sediment and the weight after it has been combusted at various temperatures. Combustion at 550˚ C will indicate the abundance of organic matter. At 1000˚ C carbonate minerals will combust allowing calculations of relative abundance of carbonates to be made for a given sample. The remaining residual matter is assumed to be lithogenic (Dean 1974). This proxy can give a preliminary indication of changes in lake environment relating to productivity and organic inputs as well as morphological changes in the catchment that influence sediment delivery to the lake basin (Shuman 2003). Values of LOI in deep lake environments varied by 2-5%, so changes in lake sediment with depth that exceed this margin of error can be interpreted as significant changes in lake conditions through time (Shuman 2003). LOI was used on sediment cores from Hurleg Lake in China to determine changes in delivery of organic matter through time, which can served as an indication of climate variation (Zhao et al. 2007). High resolution LOI analysis of lake sediment cores from southern Norway recorded a pronounced climatic event, inferred from changes in sediment organic matter, that correlated with climate interpretations made using oxygen isotope analysis of Greenland ice cores (Nesje and Dahl 2001). Loss on ignition can also be used to determine changes in lake level through time by analyzing adjacent sediment cores that

span multiple depositional environments within the same lake (Shuman 2003). Values of lithogenic material determined through LOI are typically higher in near shore environments because of the erosional processes, whereas deep lake environments exhibit higher percentages of organic material or carbonates depending on the type of lake (Dean 1999; Shuman 2003). This allows determinations to be made about the spatial migration of the boundaries between erosional and depositional environments through time.

Organic matter analysis

Organic matter bulk proxies such as C/N and $\delta^{13}C$, and biomarkers, such as lignin, have been applied to multiple aquatic systems to determine source and type of organic matter inputs (Mays et al. 2017; Talbot and Johannessen 1992; Tareq et al. 2006; Schreiner et al. 2013). The amount of organic matter in lake sediment can affect the sorption and cycling of other elements such as heavy metals, therefore, can impact their concentrations in the sediment (Santschi et al. 1999). In addition, climate and hydrologic conditions can be inferred from changes in type of vegetation depending on what kind of environment the plants are comfortable in (Gong et al. 2017; Tareq et al. 2011; McFadden et al. 2005).

Carbon to nitrogen ratios

The ratio of carbon to nitrogen (C/N) can be used to identify the source of organic matter to lakes and the abundance of the organisms that produced it (Mays et al. 2017; McFadden et al. 2005; Sampei and Matsumoto 2001). Terrestrially derived organic matter (allochthonous) is primarily composed of vascular plants, such as trees, shrubs, and grasses, which contain N-poor woody tissue and cellulose, lignin, and waxy hydrocarbons. Organic matter that is produced within the lake (autochthonous), such as by algae or macrophytes, contains N-rich protein material and little to no lignin or cellulose (Meyers 1997; Talbot and Johannessen 1992). Therefore, values of C/N ratios of terrestrial

organic matter are typically greater than 20, and the ratios measured in aquatic material are approximately 4-10 (Figure 5) (Meyers 1997).

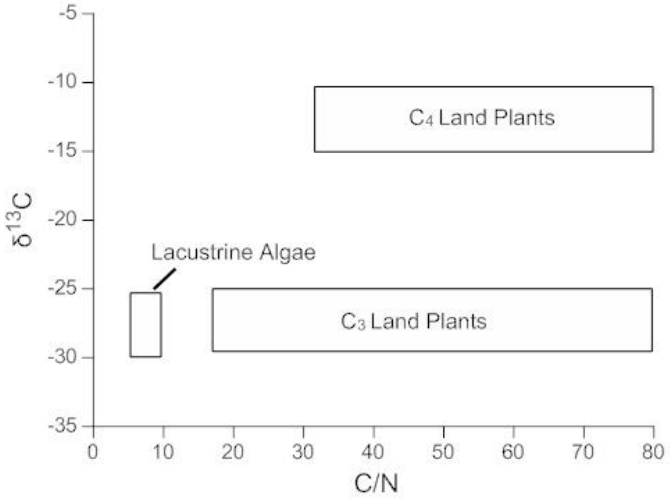

Figure 5. Generalized values for C3 and C4 terrestrial plants and C3 lacustrine algae. Adapted from Meyers (1997).

Ratios of C/N have been used in many studies to determine past changes in source and type of vegetation as well as a proxy for background environmental conditions (Sampei and Matsumoto 2001; Pompeani et al. 2014; Mays et al. 2017) . Increases in abundance of organic matter and the ratio of C/N were interpreted to be the result of higher inputs of C-rich terrestrial material and increased production or preservation of organic matter in the lake (Pompeani et al. 2014). Concurrent increases in C/N ratio, total organic carbon (TOC), and total nitrogen (TN) indicated short term oscillations towards warmer, more humid climate conditions in Quinghai lake in China (Ji et al. 2005). However, high C/N values in sediment records from Lake Bosumtwi in Ghana, were associated with dry climate conditions (Talbot and Johannessen 1992). Because of the complexities and dissimilarities between each depositional environment, interpreting results of autochthonous vs. allochthonous sources of organic matter using C/N ratios alone can be problematic. Therefore, it is necessary to employ additional proxies, such as stable isotope ratios.

Stable carbon isotope ratios ($\delta^{13}C$)

Measurements of $\delta^{13}C$ can help validate C/N interpretations because they reflect the relative abundance of C3 and C4 plants in the lake and catchment (Meyers 1997). $\delta^{13}C$ is the ratio of $^{13}C/^{12}C$ relative to a standard ratio such as

that of Vienna Pee Dee Belemnite (Eqn. 1). The fractionation of C isotopes occurs during plant respiration due to differences between the carbon fixation pathways of C3 and C4 plants.

$$\delta^{13}\mathrm{C} = \left(\frac{\left(\frac{^{13}\mathrm{C}}{^{12}\mathrm{C}}\right)_{sample}}{\left(\frac{^{13}\mathrm{C}}{^{12}\mathrm{C}}\right)_{standard}} - 1 \right) * 1000\ ‰$$

Equation 1. Delta notation for stable carbon isotope ratios of ^{12}C and ^{13}C.

Both types of plants incorporate carbon into their biomass through a photosynthetic carbon reduction cycle (PCR) that takes place in their mesophyll cells. In C3 plants, during this process 25% of the assimilated CO_2 is lost to photorespiration and leaks out through their cell walls. Because most plants prefer to fix the lighter isotope, this process results in depleted ^{13}C (Lara and Andreo 2011). This fractionation is expressed as more negative $\delta^{13}C$ values, which generally range between –25 to –35‰ (Figure 5) (Talbot and Laerdal 2000). The CO_2 fixation pathway of C4 plants is more efficient than that of C3 plants due to the cooperation between mesophyll and sheath bundle cells. The mesophyll cells assimilate incoming CO_2 and the bundle sheath cells convert 100% of it to organic carbon (Talbot and Laerdal 2000), resulting in less negative $\delta^{13}C$ values (-10 to -16‰) (Figure 5) (Talbot & Laerdal 2000). Because of the overall higher efficiency of carbon fixation in C4 plants they are able to thrive in drier, warmer climates than C3 plants (Lara and Andreo 2011). Therefore, shifts in catchment vegetation from C3 to C4 dominant can be interpreted as a general warming trend.

Interpretations of this proxy can be complicated during times of enhanced algal productivity. This is because of the presence of algae, which fractionate the dissolved inorganic carbon (DIC) pool in the lake through photosynthesis. As the remaining fraction of dissolved inorganic carbon becomes more enriched, so does the subsequently produced algal biomass (Meyers 1997). In addition, if dissolved CO_2 becomes scarce in the water column, algae will begin to fix carbon

from HCO_3^-, which contains heavier C isotopes than CO_2 and may cause the $\delta^{13}C$ value of algae to fall within the range of C4 plants (Meyers 1997). For these reasons, it is useful to compare results of $\delta^{13}C$ to C/N ratios (Figure 5), because it can help identify the source of organic matter when isotope fractionation processes in a lake are not fully understood.

Stable carbon isotopes have been used in multiple studies to detect changes in catchment vegetation (Mays et al. 2017; Talbot and Johannessen 1992), changes in depositional environment (Hassan et al. 1997) and lake level fluctuation (Fan et al. 2017; Finkenbinder et al. 2014). $\delta^{13}C$ was used in tandem with C/N ratios and pollen data on lake sediment cores from Guatemala, and there were higher values of $\delta^{13}C$ during times of aridity indicating a greater abundance of C4 terrestrial plants (Mays et al. 2017). These interpretations were supported by pollen abundance data that showed a dominance of C4 plant pollen during this time (Mays et al. 2017). $\delta^{13}C$ was used to detect seasonal variation in primary productivity in Lake Lugano, where results showed an increase in $\delta^{13}C$ values of particulate organic matter in the spring (Lehmann et al. 2004) because the DIC in the lake was depleted. The paleoclimate record produced by Finkenbinder et al. (2014) of an Alaskan lake showed $\delta^{13}C$ values of -27‰ and C/N ratio of 10-12 during tundra conditions. After vegetation was established, values for $\delta^{13}C$ decreased to -30‰ and C/N values stayed within a range similar to what was measured during tundra conditions. These changes were interpreted to be the result of increased algal productivity and higher inputs of depleted C from the lake catchment (Finkenbinder et al. 2014).

Lignin-phenol analysis

Characterization of catchment vegetation can be refined with the use of biomarkers, which can be used as an indicator of vegetation taxonomy when identifiable plant remains are no longer available (Gardner and Menzel 1974; Goñi and Hedges 1992). Lignin phenol analysis is commonly used in making determinations about past climate based on the evidence of vegetation change

preserved in various depositional environments (Hedges et al. 1982; Tareq et al. 2006; Schreiner et al. 2013; Tareq et al. 2007).

Lignin is a biopolymer found only in vascular plants and can be broken down into phenols. The three main types of lignin phenols used in the characterization of organic matter are vanillyls, syringyls, and cinnamyls. The vanillyl and syringyl phenol groups each contain three specific phenols, including an acid, an aldehyde, and a ketone (Figure 6) (Thevenot et al. 2010; Bianchi 2010). The cinnamyl group contains only two specific phenols, both of which are acids (Figure 6) (Bianchi 2010; Thevenot et al. 2010). Vanillyl phenols are produced by all plants that contain lignin, whereas syringyl phenols are unique to

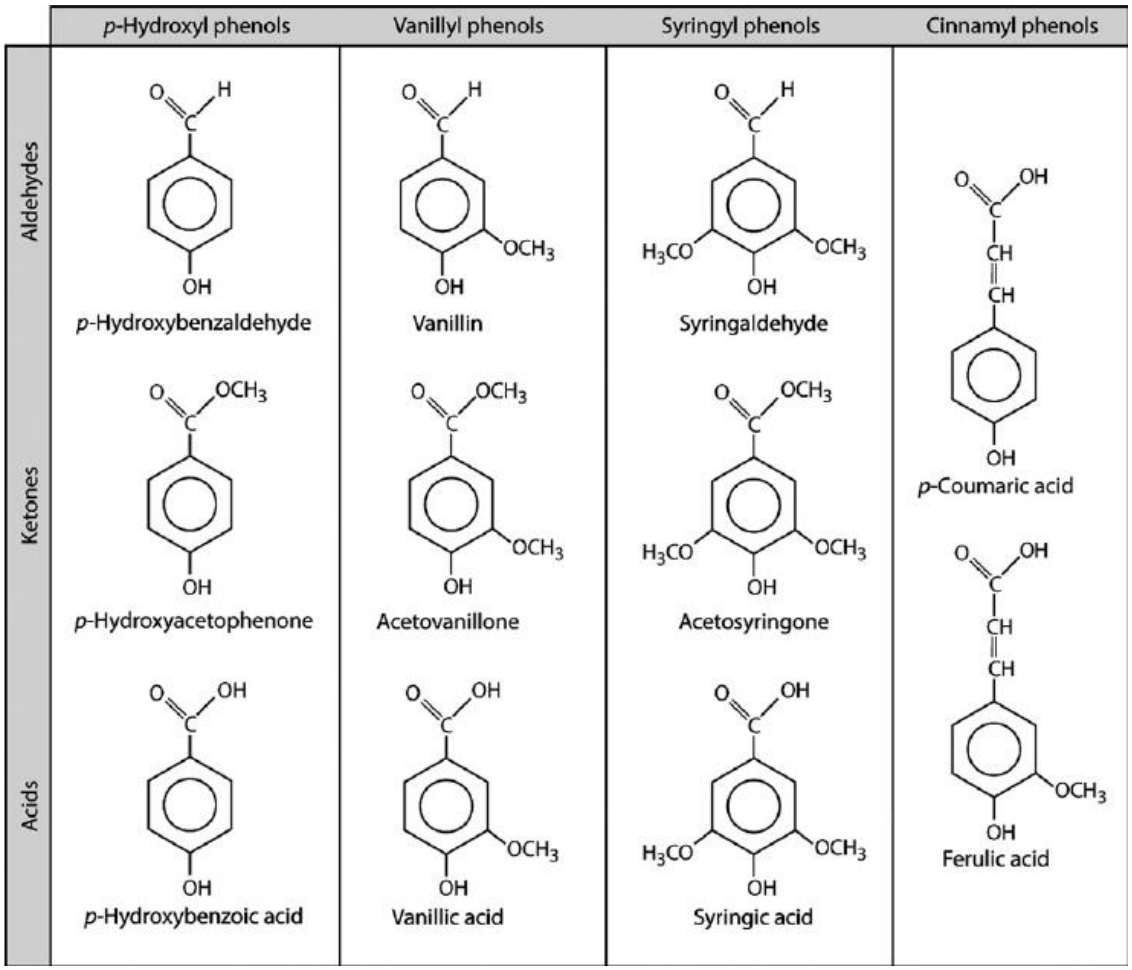

Figure 6. Groups of lignin-derived phenols (Thevenot et al. 2010)

angiosperms, and cinnamyl phenols are more common in non-woody plant

tissues (Hedges and Mann 1979). To determine the relative importance of angiosperm versus gymnosperms in samples of extracted lignin phenols, the sum of syringyl phenols are each presented as a ratio normalized to vanillyl (S/V), while the ratio of cinnamyl to vanillyl phenols (C/V) can indicate the relative amount of woody tissue preserved (Bianchi 2010; Gong et al. 2017; Hyodo et al. 2016).

Interpretations of ratios of S/V to C/V can be further improved through comparison with pollen analysis, which also gives an indication of relative abundance of angiosperms vs. gymnosperms. Comparing lignin biomarker results to pollen analysis is useful because lignin phenol composition varies between different types of pollen. For example, ratios of S/V agreed with the vegetation abundances inferred from pollen counts from Wein Lake, Alaska (Hu et al. 1999). However, the ratios of C/V were higher than expected because of the high C/V ratio in *Picea* pollen, which was the dominant vegetation type through that interval (Hu et al. 1999). Therefore, it is important to characterize lignin phenol profiles for pollen types in addition to woody and soft tissue, leaves and needles (Hu et al. 1999). To produce accurate interpretations, it is important to determine specific lignin signatures for local plants when analyzing ratios of lignin phenol, as there can be significant differences between regional vegetation assemblages (Moingt et al. 2016).

However, there are several factors to take into consideration when interpreting pollen abundance data. For example, the differences in transport distance depending on the pollen type affects the amount of pollen that is deposited in the lake, therefore may not reflect the actual catchment vegetation assemblage. Differences in transport are also important to consider when comparing results from pollen and lignin phenol analysis. Records of pollen were inconsistent with lignin in a study from Lake Washington due to differences in transport mechanisms (Leopold et al. 1982). Eolian transport was primarily responsible for pollen delivery to the lake as opposed to fluvial transport, which was the dominant mechanism for delivery of lignin (Leopold et al. 1982). Pollen grains are also typically the most resistant type of plant matter to degradation, so

the lignin signatures in preserved pollen can throw off the rest of the analysis (Tareq and Ohta 2015).

Additional information regarding soil development can be acquired from lignin phenol extraction (Otto and Simpson 2006; Otto et al. 2005). Measurements of benzene carboxylic acids (BCAs), such as 3,5-dihydroxybenzoic acid (3,5-Bd), can be used as a tracer to determine source of organic carbon in aquatic systems (Dickens et al. 2007). 3,5-Bd is a non-lignin phenol, so it has a similar chemical structure, but is not produced by vascular plants. The exact mechanism of this compound's formation is uncertain, but it is associated with degradation of lignin and development of humic matter in soil (Dickens et al. 2007). The presence of high amounts of 3,5-Bd can be an indicator of soil formation or establishment because there are more developed soil horizons and therefore more humic matter (Prahl et al. 1994). 3,5-Bd has a similar hexagonal structure as a lignin phenol, but it is not produced by any type of plant. Rather, it is a secondary product that occurs from the degradation of lignin in soil, therefore is considered a non-lignin phenol.

Organic matter degradation

Rate of degradation of organic matter (OM) is dependent on conditions such as physical processes within the lake, the oxygen environment and the type of organic matter (Aller 1998; Pellerin et al. 2010). Increases in benthic activity, either through biological or physical processes, can cause resuspension and increase the availability of OM for microbial degradation (Aller 1998). Lignin degrades more easily in surface environments, where oxygen is readily available, than in anaerobic environments because oxygen is an important requirement for the enzymes that degrade lignin (Pellerin et al. 2010; Ward et al. 2013). The rate of degradation can also depend on the type of organic matter. Typically, in lake sediments, the autochthonous fraction of organic matter is more labile than C-rich allochthonous material, thus is more readily degraded by microbial processes (Pellerin et al. 2010). These factors contribute to generally high

preservation potential of lignin in anaerobic environments (Dittmar and Lara 2001).

One method of determining the extent of lignin degradation in sediment is to evaluate changes in the radio of the acid to aldehyde of vanillyl ($[Ad/Al]_v$) (Hedges and Ertel 1982; Meyers and Ishiwatari 1993; Otto and Simpson 2006). Degradation results in the formation of acids through the oxidation of lignin moieties so measurements of the acid to aldehyde ratio can identify the degree of degradation of lignin (Ertel and Hedges 1985). Typically the acid:aldehyde ratio for fresh plants is between 0.1-0.3 and up to 0.6 for degraded material (Tareq et al. 2011; Hu et al. 1999).

Holocene climate change

Pollen maps show that there was a northward retreat of boreal forest across the upper Midwest during the Mid-Holocene Transition and an eastward migration of prairie grasslands indicating warmer summer temperatures and less precipitation in previously forested areas in this region (Bartlein et al. 1984). To date, only two studies on vegetation have been conducted on Isle Royale, and both used pollen abundance as a proxy (Flakne 2003; Potzger 1954). Results reported from the study conducted by Potzger et al. (1954) were focused on forest development and paleo- lake level change and few detailed interpretations were made of climate conditions through the Holocene. The study conducted by Flakne (2003) was more direct in comparing the pollen abundances to modern analogs to make inferences about climate conditions. Results and interpretations from the study conducted by Flakne (2003) were similar to those from other lakes in the Upper Midwest, which showed high abundances of spruce pollen in sediment from the early Holocene, indicating a cool climate, and a high percentage of pine pollen in sediment from the mid-Holocene, indicating a dry climate (Davis et al. 2000; Kirby et al. 2002).

Trace metal analysis

Analysis of trace metal concentrations in lake sediment can be used to determine changes in erosional processes, human activity, and atmospheric circulation (Anderson et al. 2000; Cooke et al. 2007; Rasmussen 1998). Metal cations from anthropogenic inputs weakly sorb to organic matter and organic coatings on lake sediment. Measurements of this easily exchangeable fraction of metals are used to identify modern contamination in sediments (Bain et al. 2012; Mahler et al. 2006).

Erosional processes transfer metals into various Earth systems including the atmosphere and hydrosphere. The Earth's crust hosts metals in varying quantities depending on the rock type. Lead is present in quantities between 7 to 9 ppm in sedimentary rock, and 15 to 20 ppm in granitic and basaltic igneous rocks (Turekian and Wedepohl 1961). Trace metals enter the atmosphere as airborne particulates or as aerosols, which are clouds of fine (<10 μm) particulates that are produced through evaporation, volatilization, combustion (Matthias-Maser et al. 2000; Murozumi, Chow, Tsaihwa, and Patterson 1969; Pachon et al. 2013). The largest contributors of trace metals to the atmosphere include wind-blown particles, (Nriagu 1979, 1989; Settle and Patterson 1982; Patterson 1965) which are estimated at 0.3 - 7.5 x 10^9 g/yr for lead (Nriagu 1989) and biogenic processes, which emit lead into the atmosphere at a rate of 0.05-3.33 x 10^9 g/yr (Nriagu 1989). Volcanic emissions, forest fires and sea spray also contribute to atmospheric trace metals (Nriagu 1979, 1989; Settle and Patterson 1982; Patterson 1965), ranging from 0.06-3.8 x10^9 and 0.02–2.8 x 10^9 g/yr, respectively. Volcanic emissions are difficult to quantify on a global scale because of the high variability of both volcanic events and the composition of emissive gasses, so estimates have a large range of 0.54 to 6.0 x 10^9 g/yr (Nriagu 1989). Mercury is delivered to the atmosphere through the aforementioned natural processes in lower quantities than Pb (Nriagu 1989), but analysis of Hg concentrations in various archives can indicate changes in the prevalence of each natural contributor. For example, high levels of mercury in Copper Falls lake sediment during the Holocene were interpreted to be the result

of increased forest fire frequency due to climate dryness (Pompeani et al. 2018). Based on an assessment of natural sources, estimates for the total global emissions of lead and mercury from natural contributors range from 0.97-23 x 10^9 g/yr and 0.1-4.9 x 10^9 g/yr, respectively (Nriagu 1989).

Trace metal pollution transport mechanisms

Human activity can accelerate the release of trace metals into the atmosphere and hydrosphere, which is referred to as pollution. Tailing piles, which consist of crushed waste rock left over from mining, provide large surface areas for weathering reactions that dissolve and mobilize trace metals (Smuda et al. 2008). Exposing fresh rock surfaces accelerate physical and chemical weathering processes which allow metals to be transported through fluvial processes as fine particulates or as dissolved ions (Spliethoff and Hemond 1996; Vermillion et al. 2005).

Energy demands in the form of combustion of wood and fossil fuels also impact the rate at which metals are emitted into the atmosphere as aerosols. Smoke is a combination of aerosols and airborne particulates and contain salts, metals, tar, and organic particles in varying quantities depending on what is burned (Li et al. 2003; Urban et al. 2012). Potassium is a major constituent of wood smoke, and is emitted into the atmosphere as potassium salts such as KCl (Li et al. 2003; Pio et al. 2008; Urban et al. 2012) Biomass burning produces trace amounts of metals (Fine et al. 2001), but combustion of fossil fuels results in much higher emissions of harmful metals such as Pb, As and Cd (Charlesworth and Foster 1999; Pacyna and Pacyna 2001). Metals such as Pb, K, and Hg can be mobilized through exposure to heat which volatilizes the metals and releases them into the air as gas (Carpi 1997; Urban et al. 2012). Metals can also enter the atmosphere through physical weathering processes and volcanic emissions that generate airborne particulates. The size of the particle influences the type of deposition (wet or dry), the amount of time it stays suspended, and the distance a particle will travel (Galloway et al. 1982). Airborne particulates are

coarser and do not travel as far as aerosols, though ash from volcanic emissions has been known to travel several thousand kilometers especially if the ash plumes permeate upper layers of atmospheric circulation (McGimsey et al. 2001; Sarna-Wojcicki et al. 1981).

Examples of lead and silver mining in Central Europe during the Greek and Roman era demonstrate that pollution was transported as atmospheric aerosols distances greater than 4,000 km (Hong et al. 1994; Renberg et al. 1994). The presence of anthropogenic trace metal signature in ice layers on the summit of the Greenland ice sheet 3238 m above sea level, indicates that aerosols reached the middle troposphere resulting in hemisphere scale dispersion of mining and smelting related pollution (Hong et al. 1994). Investigations of the transport of K aerosols from human activity in Brazil, found that pollution from the burning of sugar cane fields was able to travel more than 1200 km (Urban et al. 2012)

Modern trace metal emissions

Human activity is well known to disrupt the cycling of trace metals in the environment, in particular through mining and the combustion of fossil fuels (Pacyna and Pacyna 2001; Settle and Patterson 1982; Patterson 1965; Chow and Earl 2014). Early work to quantify Pb contamination identified enrichments in water, soil, and air well beyond the levels considered healthy for human exposure, and concluded that human activity, primarily the use of leaded gasoline, was the cause (Patterson 1965; Settle and Patterson 1982). Since this work, several efforts have been made to model the amount and transport behavior of several types of metals in the atmosphere and hydrosphere from anthropogenic sources (Rauch and Pacyna 2009; Nriagu 1979; Pacyna and Pacyna 2001; Nriagu et al. 1988; Nriagu 1989). Many of these studies have focused on elements such as silver, aluminum, chromium, copper, iron, nickel, lead, and zinc which account for 98% of the mass of metals mobilized by human activity (Rauch and Pacyna 2009). Nriagu and Pacyna (1988) produced a

quantitative assessment of the flux of harmful trace metals into the air, water, and soil. Rauch and Pacyna (2009) improved these estimates by taking the full cycle of each metal into account to illustrate the differences in magnitude between natural and anthropogenic stocks and flows (Rauch and Pacyna 2009). This research has consistently shown that emissions from the burning of fossil fuels continues to be the largest contributor of atmospheric trace metals such as Pb, As, Hg, Cd (Pacyna and Pacyna 2001). This research has also identified significant contribution of metals from anthropogenic sources that far outweighs contributions from natural sources (Pacyna and Pacyna 2001; Pacyna and Pacyna 2016). Through evaluation of metals enrichments in various natural archives, including peat deposits, lake sediment, and ice fields, it has been estimated that current emissions of lead are 6 to 35 times greater than natural background levels (Marx et al. 2016).

Analysis of trace metal concentrations has been conducted on various environmental archives such as peat deposits (Bindler 2006; Weiss et al. 1999), lake sediment (Cooke and Bindler 2015), ice cores (Murozumi et al. 1969), and plant matter (Weiss et al. 1999) to determine changes in natural and anthropogenic inputs of trace metals through time. In these systems, lead and other metals are weakly sorbed to reactive sites on the surfaces of organic coated particles and deposited as sediment (Bloom 1981; Bowen 1979). Lacustrine sediments are a mixture of organic matter from in lake (autochthonous) and delivered from the catchment (allochthonous) and lithogenic material which can be produced both in the lake (authigenic) and be delivered from the catchment (allogenic). Minerals are produced in the lake when ions in the dissolved fraction of the water column form a bond and precipitate out as a solid (Verschuren 1999). Iron and manganese oxides and carbonates occur as nodules and concretions that sequester trace metals (Tessier et al. 1979). Metal cations bind to the surfaces of organic matter, clays, and carbonate minerals. Of the three, organic matter has the highest cation exchange capacity, and contains proton reactive sites composed of functional groups such as -COOH and -OH that can bind (chelate) trace metals in the water column (Santschi et al. 1999)

and in soils that are then transported to the lake as particulate matter (Lützow et al. 2006). The bound metals and organic matter settle out and form sedimentary layers through time.

Methods for the analysis of trace metal concentrations in sediment employ weak acid digestion to selectively extract the fraction of trace metals that are weakly sorbed to the surfaces of organic matter, clays, and carbonate minerals (Tessier et al. 1979b). This exchangeable fraction is the most sensitive to anthropogenic inputs as determined through Pb isotope analysis of modern pollution sources in sediment (Graney et al. 1995; Rasmussen 1998). A strong acid digestion is used to evaluate the concentrations of trace metals that are bound within the matrices of minerals. The residual material that is left over after this process include the lithogenic or mineral fractions of the sediment that are not released into the lake system easily and are considered relatively inert (Tessier et al. 1979). Nitric acid (HNO_3) has a low pH and dissociates into hydrogen (H^+) and nitrate (NO_3) in aqueous solution. When this solution is combined with lake sediment, the H^+ exchanges with the metal cations that are electrostatically bound to the proton reactive surfaces and ligands in the sediment (Tessier and Campbell 1987). The metal cations are then available to bond with the NO_3 and are suspended in the solution as salts (Horowitz 1985).

Weak nitric acid digestion yields a suite of metals concentrations, and several of these can be used as proxies for anthropogenic inputs and a variety of natural catchment processes. Lead is the most ubiquitous proxy used to identify human activity because it is widely and easily distributed from mining and combustion of leaded gasoline (Cooke and Bindler 2015; Settle and Patterson 1982; Weiss et al. 1999). Pb is often found in ores that contain other precious metals such as gold, copper or silver (Cooke and Bindler 2015) , and is released during mining through physical and chemical weathering processes, as well as through volatilization (Meza-figueroa et al. 2009; Smuda et al. 2008). Lead is easily mobilized into the atmosphere as an aerosol and deposition has been traced as far as 150 km from the source of pollution (Gallon et al. 2006). The ease with which lead pollution is aerosolized and deposited results in higher

enrichments of lead in the sediment in areas where mining has occurred than in areas where there was none.

Records of changed in pollution can be developed by analyzing layers of sediment to produce a record of deposition through time. Analysis of concentrations of weakly bound metals at each sediment depth yield results which show elevated concentrations of trace metals during periods of mining activity (Gallon et al. 2006). Lead is also stable in lake sediment and does not migrate vertically in the sediment column, making interpretations of changes in deposition through time fairly straightforward (Gallon et al. 2006). Also, the ratio of stable Pb isotopes (^{206}[Pb]/^{207}[Pb]) can be used to track source of pollution as the lead isotope composition of ore bodies and bedrock varies based on geologic location, such that, for example, atmospheric aerosols from combustion of gasoline have a different isotopic composition than natural sources (Cooke and Bindler 2015; Renberg et al. 2002; Bränvall et al. 2001). Studying the changes in concentration of trace metals through time gives insight into large scale natural variation and anthropogenic activity.

In most cases, Cu is not a commonly used proxy to indicate anthropogenic inputs because it is not easily mobilized as an aerosol (Galloway et al. 1982). Copper may be present in lithogenic dust, but these types of airborne particles are heavy and are typically do not travel as far as the finer fraction of aerosols (Galloway et al. 1982). In some cases, Cu toxicity can be a problem if a lake receives direct inputs from surficial runoff, such as in the case of Lake Orta in Northern Italy, where point source pollution from a rayon factory resulted in elevated Cu concentrations and acidification of the water column (Smol 2009).

To more accurately determine the extent of anthropogenic inputs of proxy trace metals such as lead or mercury, the concentrations are evaluated based on enrichment factors. These calculations account for the variation in other metals that reflect changes in natural catchment weathering processes. The metals used to calculate enrichment factors for a given study are chosen based on their concentrations in the surrounding bedrock. Ti and Mg are used to determine

catchment weathering rates when these elements are present in high concentrations in the surrounding ore bodies, so changes in concentrations through time will reflect natural delivery of metals to the lake basin (Pompeani et al. 2013; Boës et al. 2011; Kerfoot and Robbins 1999). Typically, elements used in these calculations are less sensitive to anthropogenic inputs because they are not readily mobilized as aerosols and are associated with minerals that are resistant to weathering processes (Boës et al. 2011; Bowen 1979). Enrichment factor of metals associated with pollution from anthropogenic activity, are calculated by normalizing the ratios of individual samples to samples with ratios that represent natural, background conditions in the record using the following equation:

$$EF\ X = \frac{\left(\frac{X}{Y}\right)_{sample}}{\left(\frac{X}{Y}\right)_{background}}$$

Where EF is the enrichment factor, X is the concentration of an anthropogenic proxy metal, such as Pb, and Y is the concentration of a less sensitive element such as Al or Ti (Weiss et al. 1999). This analysis provides an estimate of background variability in the deposition rates of Pb, and other pollution proxy metals, unrelated to potential large scale atmospheric deposition events and/or ancient mining related activities. Therefore, values of enrichment factors provide a context for evaluating extent of pollution associated with periods of mining.

Results from trace metal analysis conducted on sediment cores from Isle Royale and McCargoe Cove were evaluated based enrichment factors, where Ti, Mg, Fe and organic matter were used as proxies for background conditions (Pompeani et al. 2013). Iron was used as a proxy for redox changes because it is readily mobile under reducing conditions (Boyle 2001; Hamilton-Taylor and Davison 1995). Background conditions were evaluated based on the concentration of organic matter, because the amount of organic matter present in the sediment reflects the sorption surfaces available for trace metals (Bloom 1981; Bowen 1979; Boyle 2001).

Europe and Asia

Concentrations of lead and other toxic metals have been measured in lake sediment records in quantities significantly exceeding background conditions in many regions around the world, even before the beginning of the industrial revolution (Hong et al. 1994; McConnell et al. 2018; Lee et al. 2008; Cooke et al. 2007; Pompeani et al. 2013). Mining history in Europe and Asia has been tracked through analysis of ice cores and lake sediment cores (Hong et al. 1994; McConnell et al. 2018; Renberg et al. 1994; Bränvall et al. 2001; Murozumi et al. 1969; Lee et al. 2008). The Greenland ice cores show that during the Greek and Roman era, 2,500 to 1,700 BP (500 BCE to 300 CE) there were increases in concentrations of lead that exceeded four times the natural levels as a result of lead and silver mining activities in Central Europe (Hong et al. 1994). More precise analysis of Greenland ice cores identified decreased emissions of lead during times of war and increases during times of prosperity and stability when mining operations could continue unimpeded (McConnell et al. 2018). Elevated concentrations of lead from Greek and Roman mining activities more than 2,600 BP was also detected in lake sediment records from Sweden (Renberg et al. 1994). Analysis of trace metal concentration in lake sediment records from Asia has also uncovered evidence of metal pollution deposited 2,200 yr BP (200 BCE) (Dearing et al. 2008), and in 5,000 BP (3,000 BCE) (Lee et al. 2008).

South America

In South America, Abbott and Wolfe (2003) used Pb, Sb, Bi, Ag, and Sn to evaluate the history of metallurgy in the Bolivian Andes, and identified time periods of mining intensity consistent with the Tiwanaku culture 950 to 750 BP (1000 to 1200 CE) and early colonial times 550 to 300 BP (1400 to 1650 CE). Similar dates for the onset of mining activity were determined through analysis of Pb, Sn, Cu, Ag, Sb, Bi, and Ti concentrations in lake sediment cores from the Peruvian Andes, where metal pollution was deposited as early as 950 BP (1000

CE) (Cooke et al. 2007). The Incan empire mined with an emphasis on acquiring silver, as indicated by increases in Pb, Sb, and Bi (Cooke et al. 2007). Increases in these same three elements were also identified in sediments deposited during later colonial metal extraction that also targeted silver. Mining for silver involved a smelting technique that used galena, a mineral which contains lead (Cooke et al. 2007). In the Cerro de Pasco another period of intensive mining occurred following colonial control after 350 BP (1600 CE), which was characterized by higher mercury emissions as a result of the switch to an extraction method that used mercury amalgamation (Cooke et al. 2009).

North America

Some of the oldest evidence of metalworking in the world, dating to 8,000 BP, can be found in North America on the Keweenaw Peninsula of Michigan (Pompeani et al. 2013; Reardon 2014; Beukens et al. 2006). This determination was made using the combined evidence of archaeological artifacts and concentrations of metals in lake sediment. The Keweenaw Peninsula and Isle Royale host extensive deposits of native copper in the form of fissure veins (Rosenmeyer 2009). These copper deposits were exploited by Archaic North Americans, and shaped into tools such as needles, blades, scrapers, fish hooks and spear points (Ehrhardt 2013; Pleger and Stoltman 2009). Artifacts were traded across hundreds of miles (Ehrhardt 2013), and many of them have been traced back to their source in the Great Lakes region through analysis of relative concentrations of trace elements such as Ag, As, Au, Cr, Fe, Hg, La, Sb, W, and Zn (Rapp et al. 2000).

Ages of copper artifacts cannot be determined from the copper artifacts themselves, but rather must be inferred through radiocarbon dates of organic material directly associated with the artifacts, such as the wood from mounted spear points or sinew bindings. The archaeological record on Isle Royale is limited because no long-term habitation sites or burial sites, the locations that copper artifacts are most commonly found (Pleger and Stoltman 2009), have

been discovered. Therefore, there is a lack of radiocarbon dates from in situ copper artifacts on Isle Royale that can be used to constrain the timing of mining intensity through archaeological methods alone.

Mining operations were heavily concentrated along the Minong ridge on the northeastern side of Isle Royale (Gallagher and Josephs 2008). This feature is the surface expression of tilted beds of the Portage Lake Volcanic group, which hosts numerous copper deposits (Rosenmeyer 2009). Pit mines have also been identified along the southern shore of Isle Royale near Siskiwit Bay; however archaeological excavations of these sites have not yet been conducted (personal communication with Seth Depasqual).

Ancient mining sites in Isle Royale and the Keweenaw Peninsula are characterized by large pits or trenches and piles of rock left over after the copper has been extracted, as well as hammer stones used in the process of extracting the copper (Holmes 1901; Lathrop 1901). Determining the age of the pits using archaeological techniques has been the focus of many studies, but has proven difficult because there is often a lack of material suitable for dating within the pit mines (Campetti 2016; Pompeani et al. 2014). Paleolimnological methods have therefore been applied to investigate the timing of ancient mining activities that may have produced air and water borne pollution that was deposited and preserved in lake sediment (Pompeani et al. 2013b, 2014). Analysis of weakly bound metal concentrations in sediment from lakes near pit mines has revealed that the ages of increases in metal concentration are consistent with the ages of copper bearing artifacts found in this region, thus providing insight into the timing, duration and intensity of ancient mining activities.

The exact method of copper extraction used by archaic people is unclear. However, archaeologists have identified the use of fires in the mining and annealing process based on charcoal found in and near the pit mines (Holmes 1901; Lathrop 1901) as well as crystallographic evidence of heat treatment in copper artifacts (LaRonge 2001; Schroeder and Ruhl 1968). Ancient people used the fires in the hammering and annealing process to soften the metal using heat,

so it could be more easily shaped (LaRonge 2001). However, there is no archaeological evidence from this region that copper was cast. The process of casting differs from annealing in that the metal must be heated to temperatures above 1080˚C in order to be melted to a liquid and poured into a mold (LaRonge 2001; Schroeder and Ruhl 1968).

It is unclear to what extent the anthropogenically sensitive concentrations of metals are dependent on atmospheric transportation versus surficial runoff. Pollution from ancient mining activity is delivered to the lake sediment through atmospheric deposition of aerosols that are produced during the extraction process. The two metals most commonly associated with pollution aerosols are K, which is released during the burning of wood fuel (Calloway et al. 1989; Fine et al. 2001), and Pb, which is present in the copper ore (Rapp et al. 2000) and is volatilized through exposure to heat during the annealing process (LaRonge 2001). Additionally, metals may reach the lakes through surficial runoff from tailing piles located within the lake catchment (Kerfoot and Robbins 1999). In the case of McCargoe Cove on Isle Royale, there were a large number of Minong Ridge pit mines and tailing piles located directly within the catchment (Pompeani et al. 2014). It is necessary to evaluate metal concentrations in sediment from lakes that do not contain pit mines in their catchment, and therefore receive no inputs of trace metals through surficial runoff, to make determinations about the relative importance of atmospheric vs. terrestrial loading of metal contaminants.

Analysis of dune formation during the mid-Holocene shows that the prevailing wind direction during the time of archaic mining was from the northwest (Dean et al. 1996), which places Lily Lake upwind of McCargoe cove and the pit mines adjacent Siskiwit Bay during that time, and suggests that a shift in wind direct would be required for eolian transport of pollution from these sites to Lily Lake. Nevertheless, recent research shows that wind direction in the Lake Superior region can change on decadal time scales (Waples and Klump 2002). Additionally, lakes are extremely sensitive recorders of pollution, especially when background concentrations of a contaminant are low (Blais et al. 2015; Graney et al. 1995). Therefore, easterly winds (a common occurrence over Lake

Superior) sustained over a short duration of perhaps a few days or weeks during peak mining could potentially have produced a significant metal signal in the sediment of Lily Lake. Considering that the range of deposition of contaminants produced by mining processes can exceed hundreds of kilometers (Gallon et al. 2006), it is likely that extensive burning and mining activity near McCargoe cove (as well as the pit mines near Siskiwit Bay) could have distributed atmospheric pollution across most of Isle Royale.

Pompeani et al. (2014) suggest that mining activities were halted due to the onset of dry conditions during the mid-Holocene (Pompeani et al. 2014). This dry period, known as the Mid-Holocene transition, has been identified through analysis of sediment from several lakes located in the Midwest, northeastern United States, and southern Canada (Kirby et al. 2002; Dean et al. 1996; Bartlein et al. 1984; Flakne 2003). Pollen derived estimates indicate that, beginning 9,000 BP, precipitation decreased across the Midwest by 10-25% and temperatures increased 1-2˚C by 6,000 BP (Bartlein et al. 1984). The cause of this dry period has been widely attributed to changes in atmospheric circulation that reduced the delivery of moist air from the Gulf of Mexico and increased prevalence of drier cross-continental air masses (Kirby et al. 2002). A study of more recent paleoenvironmental change by Bird et al. (2017) found that between 1350-1450 CE a climatic shift produced widespread, sustained summer drought across the Midwest, resulting in increased migration, decreased social stability, and more frequent conflict among the Mississippian people.

Discussion

Trace metals

Significant increases in concentrations of lead (Figure 7) have been measured in lake sediment cores from Isle Royale and the Keweenaw Peninsula (Figure 8) (Pompeani et al. 2014, 2013a). These increases predate modern industrialization, and evaluation of enrichment factors has identified these early peaks as likely anthropogenic in origin (Pompeani et al. 2013a, 2014). Pb

deposition occurred in multiple lakes at rates greater than background levels during three principal time periods over the last 10,000 years. The oldest of these events occurred during the Early Archaic from 10,000 to 9,000 BP and has been detected in all sediment records that extend far enough to capture this time period (Pompeani 2015; Pompeani et al. 2013a). This event has not been identified in sediment from Lake Medora and McCargoe Cove, because these records are not old enough, extending to 7,500 and 9,000 BP, respectively (Pompeani et al. 2013a, 2014). The next Pb enrichment event occurred during the Middle Archaic from 7,000 to 6,500 BP and is identifiable in sediment from Lake Manganese, Lily Lake and Copper Falls Lake. The third occurrence of increased Pb deposition occurred from 6,500 to 5,400 BP and is detectable in sediment from McCargoe Cove, Copper Falls, and Lake Medora (Figure 7). Based on the data summarized above, the most intensive prehistoric period of Pb deposition occurred during the Middle Archaic from 6,500 to 5,400 BP based on the magnitude of the Pb concentration anomalies at this time in most of the lake records.

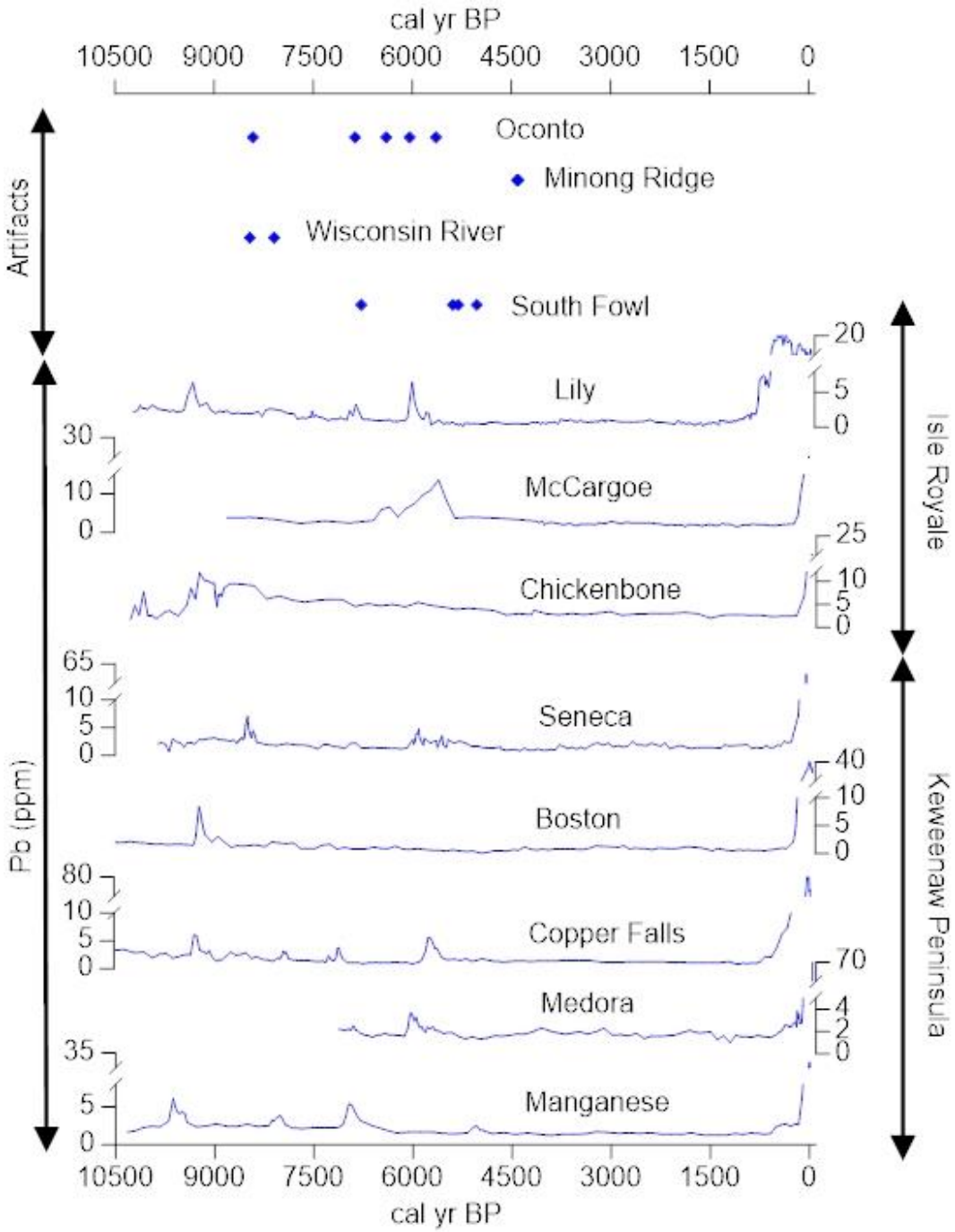

Figure 7. Records of lead concentration from lakes located on the Keweenaw Peninsula and Isle Royale (Pompeani et al. 2013; 2014; Pompeani 2015) compared to radiocarbon dates associated with copper artifacts (Beukens et al. 2006; Crane and Griffin 1965; Reardon 2014; Pleger 2009).

Pb is used as a proxy for anthropogenic inputs in this study because it is associated with the geologic formation that hosts the copper fissure veins; the Portage Lake Volcanics. Pb is often found in association with sulfide and chalcophilic deposits, which are prevalent in the Portage Lake Volcanics (Rapp et al. 2000). To determine whether the increases in Pb concentrations in lake sediment were the result of catchment weathering and enhanced clastic deposition or anthropogenic inputs, enrichment factor analysis was conducted on records from Copper Falls, McCargoe Cove, Lake Medora, and Lake Manganese. Results from this assessment demonstrate that Pb increases during the enrichment periods described above far exceed the magnitude of background natural variability (Pompeani et al. 2013a, 2014). Similar

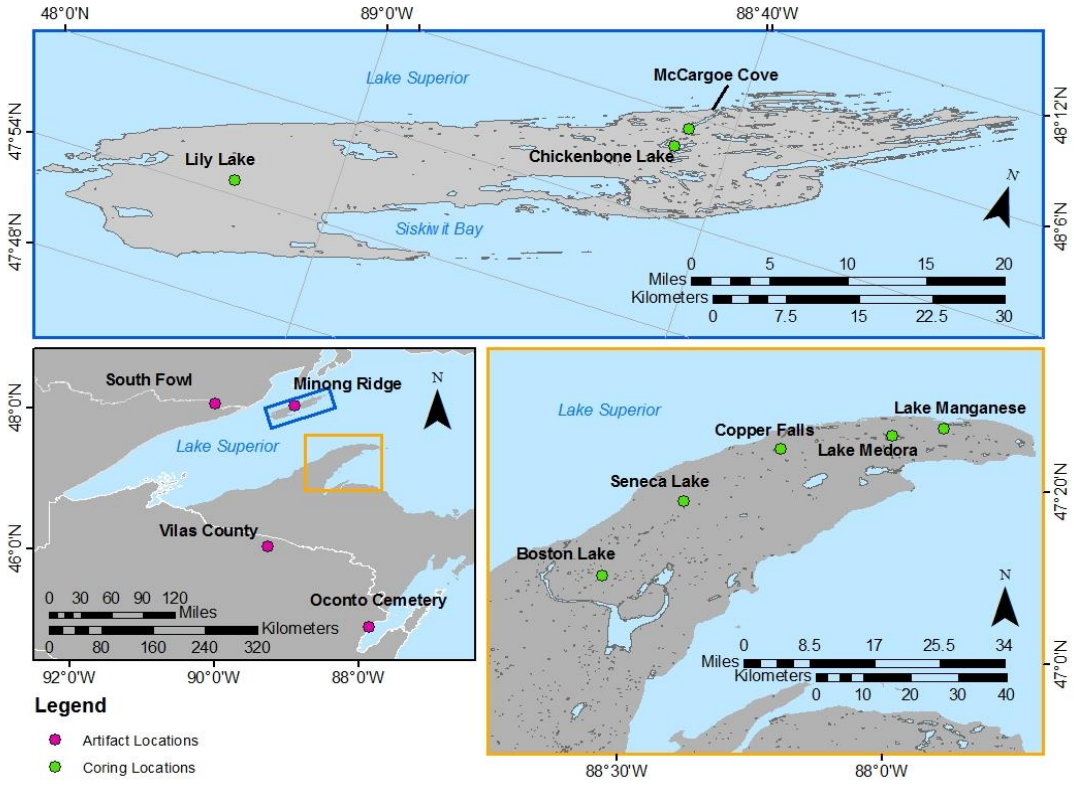

Figure 8. Map showing locations of copper extraction, archaeological sites, and lakes previously evaluated for trace metal contamination from ancient mining.

occurrences of high Pb concentrations have been identified in other regions of the world, such as Europe and South America, and have been determined to be

of anthropogenic origin (Bränvall et al. 2001; Cooke et al. 2007). Each of these records exhibit pronounced increases in Pb at concentrations that considerably exceed background variability. Therefore, we conclude that the increases present in Pb in the Lily Lake record also reflect pollution associated with mining activity.

There are two mechanisms that can potentially explain how Pb was transported from the mining sites to the lakes: through surficial runoff at sites located within lake catchments, and aerosolization. The former mechanism is especially applicable to explain the presence of metal pollution in lake sediments for catchments containing large tailing piles that resulted from the excavation of copper. However, Lily Lake does not contain any tailing piles or pit mines in its catchment. Furthermore, the parent material is predominantly glacial overburden, meaning that surficial runoff is an unlikely explanation for the enrichments of Pb that appear in the sediment record. We therefore conclude that atmospheric deposition of pollution from smelting and annealing elsewhere on the island is primarily responsible for producing this signal.

The fires used by ancient groups could easily have produced the signal seen in the Lily Lake record. Aerosolization of trace metals occurred during the annealing of copper and its host rock, purportedly as part of a fire-fracture process wherein copper bearing bedrock was repeatedly heated via wood fire and then rapidly cooled through water quenching. The minimum temperature required for annealing copper is 200-225˚C, and average campfire temperatures of between 865-920° C are easily maintained as determined through measurements of experimental archaeological methods (LaRonge 2001). Pb is volatilized at a temperature of 285˚ C, therefore, the campfires used in the annealing process would have been sufficient to release Pb present in the copper ore into the atmosphere as an aerosol.

Pollution from modern smelting has been recorded as far as 300 km away from the source in lakes in Canada. In Europe, the signal from Pb smelting in the Greek and Roman era times was identified in ice cores and lake sediment several thousand kilometers from the source of pollution (Hong et al. 1994;

Renberg et al. 1994) These cases demonstrate the likelihood that a strong signal could occur in lake sediments that are less than 10 km from the source of pollution, as is the case with Lily Lake. The wind direction on Isle Royale at the time was predominantly from the northeast (Dean et al. 1996). However, if the pit mines were active for centuries at a time, with fires burning semiregularly, Lily Lake is in a good position to be sensitive to the inputs on other parts of the island. Lakes in such pristine condition are extremely sensitive to anthropogenic inputs. With the amount of burning taking place during mining, a change in wind direction for even a short amount of time would be enough to elevate the signal in the lake sediments.

McCargoe Cove and Chickenbone Lake, Isle Royale, have pit mines directly in their catchments, thus received direct inputs via surficial runoff. The signal is recorded clearly in McCargoe, however there is no evidence of a Middle Archaic lead peak in the Chickenbone record (Pompeani et al. 2014). This could be because of poor preservation of the sediment, as this core was collected in a shallow part of the lake, making it likely that there was post depositional mixing of the sediment. Despite the lack of a distinct peak, the Chickenbone record exhibits considerably higher concentrations of lead through the Holocene than what would be considered background levels in other lake sediment cores, indicating that this lake received inputs of lead from non-natural sources. In the case of Copper Falls Lake, most of the exposed fissure veins and pit mine locations are located outside of the Copper Falls catchment; however, the sediment record exhibits distinct peaks, suggesting that atmospheric deposition is a major contributor of pollution to the sediments. The catchments of Lake Medora and Lake Manganese have not been fully surveyed, but there is little recorded evidence suggesting that ancient pit mines exist within their catchments (Pompeani et al. 2013a). This suggests that all the lakes with detectable increases in Pb concentrations, received at least part of their inputs from atmospheric deposition.

Increases in Pb and K are coupled in the Archaic period, but do not appear to increase simultaneously in the modern signal. In the Lily Lake record,

increases in K appear approximately 400-700 years later than the Pb enrichments. This decoupling is evident in records from McCargoe Cove as well (Pompeani et al. 2014). The cause of this is uncertain, but one possible explanation is that it is because of differences in the mining process, where wood was used to a lesser extent during modern mining, resulting in lower inputs of K into the atmosphere, and coal was used more frequently, resulting in higher inputs of Pb.

The Pb and K increases in the Lily Lake record are consistent with known ages of organic materials associated with copper artifacts (Figure 7) (Beukens et al. 2006). The oldest known dates associated with archaic copper culture on Isle Royale and the Keweenaw come from two pieces of organic matter taken from inside projectile points from Eagle River Wisconsin, and were dated to 8478 ±40 cal yr BP and 8110 ±60 cal yr BP (Reardon 2014). Consistent with these ages, a date of 8412 ±600 cal yr BP was obtained from artifacts found in the Oconto Cemetery in Wisconsin (Pleger and Stoltman 2009). There are several artifacts that have been found in association with the Middle Archaic mining periods between 6,500 to 5,400 BP (Beukens et al. 2006; Pleger and Stoltman 2009). The radiocarbon dates that provide age constraint for the Minong Ridge sites (4420± 150 cal yr BP, 4400 ± 150 cal yr BP) were acquired from pieces of charcoal found in the pit mines tailing piles and in association with hammerstones (Crane and Griffin 1965), thus indicating time periods of mining activity. These and other artifacts and features in the Lake Superior region help provide a temporal context for mining activities that are evident in lake sediment cores.

Provenance of copper artifacts associated with Pb peaks has been determined through analysis of Pb isotopes and trace element profiles (Beukens et al. 2006; Rapp et al. 2000). The isotopic composition of Pb in copper artifacts from the South Fowl site (Figure 8) was analyzed, and results confirmed that the material was sourced from the deposits on Isle Royale and the Keweenaw Peninsula (Beukens et al. 2006). Patterns of trace element concentrations of regional copper deposits are statistically compared to the profiles of copper from

archaeological artifacts (Rapp et al. 2000). There is interest in the sources and distribution of native copper and how it may inform on past human behavior and societal structure. Determining the provenance of the raw materials used in the production of ancient artifacts provides insight into patterns of trade between groups and the spatial patterns of human migration.

The metal pollution records from Isle Royale and the Keweenaw can potentially provide insight on the complexity and structure of archaic civilization, given that mining operations of the scale conducted on Minong Ridge and near Island Mine, Isle Royale were likely difficult to sustain, requiring stable infrastructure for transporting goods and extracted mineral resources to and from the island. Such records have provided insight on human society in other locations. For example, sediment records from lakes in Europe exhibit Pb enrichment increases that correspond to times of economic prosperity throughout the Greek and Roman Empires (McConnell et al. 2018). During known times of war and political unrest, when economies were destabilized, Pb enrichment values are lower in these records, presumably because there was less infrastructure to support large scale mining operations (McConnell et al. 2018).

Alternative hypotheses

Forest fires release K, Pb, and other elements as smoke, which are then available to be deposited onto lake surfaces (Pio et al. 2008). Isle Royale does not have an extensive record of forest fire history. Historic records begin at 1848 CE (Hansen et al. 1973), but there is otherwise a lack of research of charcoal in sediment cores with which to build a history of forest fires. However, in general, forest fires occur more frequently during dry climate periods (Pompeani et al. 2018). Written records of forest fires occurrence from the last century show increased frequency during historic mining periods (Hansen et al. 1973). During this time, the people mining copper built large fires to power their smelters and were also utilizing fires for habitation (Lankton 2010). It may be that during times of prehistoric mining, similar increases in forest fire frequency occurred, causing

higher amounts of Pb, K, and other elements to be entrained as smoke particles and deposited in distant lakes.

Lily Lake was also not exposed to any recorded land use changes such as logging, habitation, or agriculture. Therefore, changes in soil retention are not responsible for increases in metals. Lily Lake also does not have any pit mines in its catchment, so it will not receive pollution from direct runoff. The pollution that was delivered through aerosols was produced through the burning of wood and rock near the pit mine sites. The known locations of mining sites are the Minong ridge, and on the south shore of the island near Siskiwit Bay. These mining pits have not been radiocarbon dated, but preliminary evidence suggests they are Middle Archaic (Dustin 1957).

It is important to consider the range of variability associated with human behavior, and how this may impact the length of time raw materials and tools may have been in circulation (Hill et al. 2017). Little is understood about the Archaic period of archaeology on Isle Royale, because until only recently, archaeological sites were focused on the recent shoreline, which is several meters below the location of the Nipissing shoreline during the Archaic period. Radiocarbon dates associated with archaeological features also have a large range of uncertainty. For example, the radiocarbon dates acquired from Minong Ridge were dated to be approximately 1,500 years younger than the Pb peaks at McCargoe Cove. While there is some overlap in the analytical uncertainties, it is also likely that the dates are younger, because the pieces of charcoal that were analyzed reflect the infilling of the pit mines after mining had ceased and are not an accurate representation of when they were exploited (Crane and Griffin 1965; Pompeani et al. 2014).

Vegetation and climate

Using the combination of lignin phenol analysis, stable carbon isotope ratios ($\delta^{13}C$) and the ratio of carbon to nitrogen (C/N) we have made interpretations pertaining to sources of organic matter to Lily Lake (Meyers 1997;

Talbot and Laerdal 2000), as well as changes in catchment vegetation taxonomy throughout the Holocene (Lara and Andreo 2011; Mays et al. 2017; Tareq et al. 2011). Lignin content can provide evidence of post-glacial vegetation establishment and can be used in tandem with bulk proxies such as C/N and $\delta^{13}C$, which reflect changes in aquatic productivity in the lake. The changes in abundant taxonomic types of terrestrial vegetation can be indicated by ratios of S/V to C/V in the sediment record (Bianchi 2010; Tareq et al. 2011). Using these data we can infer climate trends through the Holocene, and these interpretations support previous paleoclimate research conducted on Isle Royale based on pollen abundance analysis (Flakne 2003).

The ratios of lignin phenol groups show that there is a shift from more gymnosperm dominance in lower sections of the core to more angiosperm dominance in upper sections of the core (Figure 9), which indicates an overall warming trend through the Holocene (Tareq et al. 2004). The C/N ratio (Figure

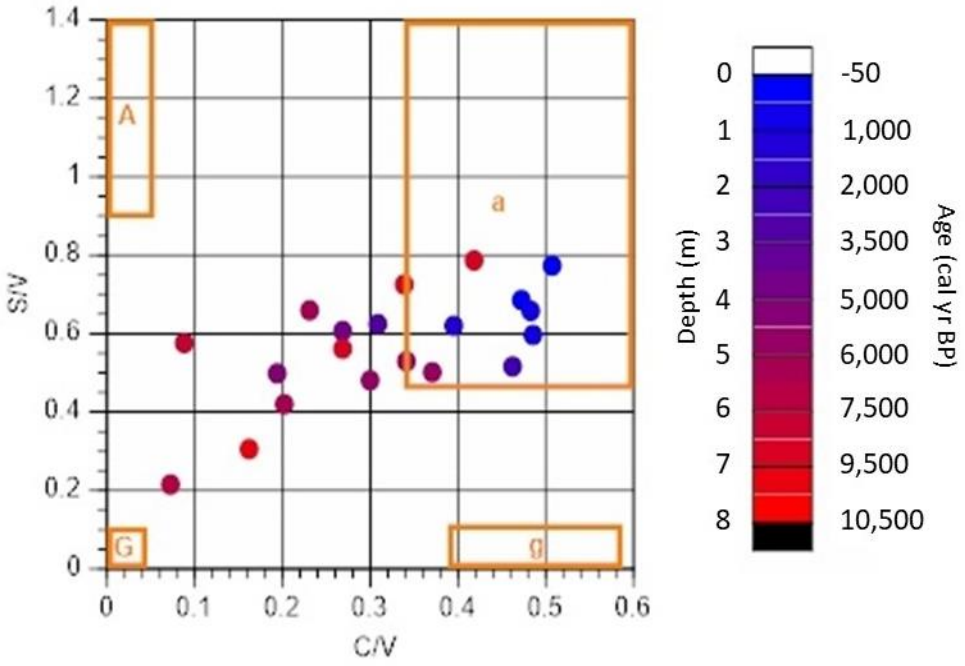

Figure 9. Cross plot diagram showing ratios of cinnamyl phenols and syringyl phenols normalized to vanillyl phenols with depth indicated by color. A= woody angiosperms, a= non-woody angiosperms, G= woody gymnosperms, g= non-woody gymnosperms (Goñi and Hedges 1992).

10) decreases steadily and $\delta^{13}C$ (Figure 10, 11) becomes generally more negative over the course of the Holocene, because of the progressive increase in primary productivity as a result of the transition from cool to warm climate (Meyers 1997).

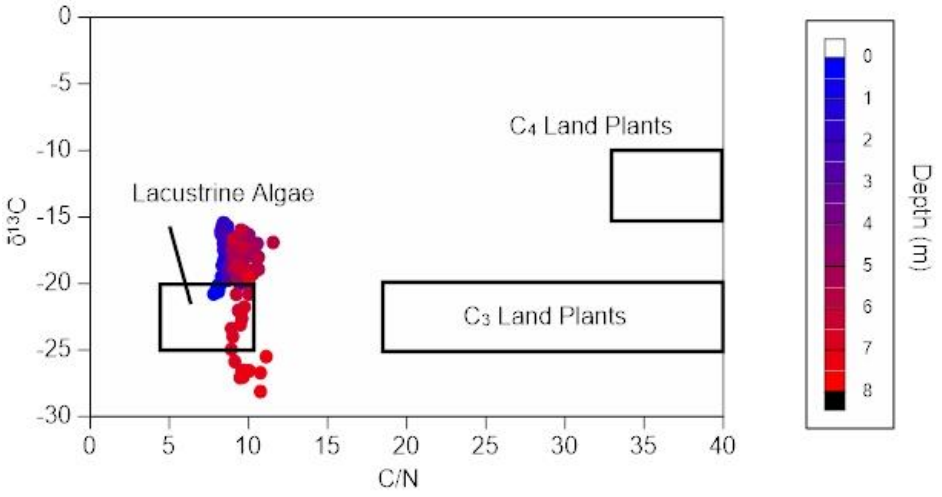

Figure 10. Cross plot of C/N and $\delta^{13}C$ with depth indicated by color. Adapted from Meyers (1997).

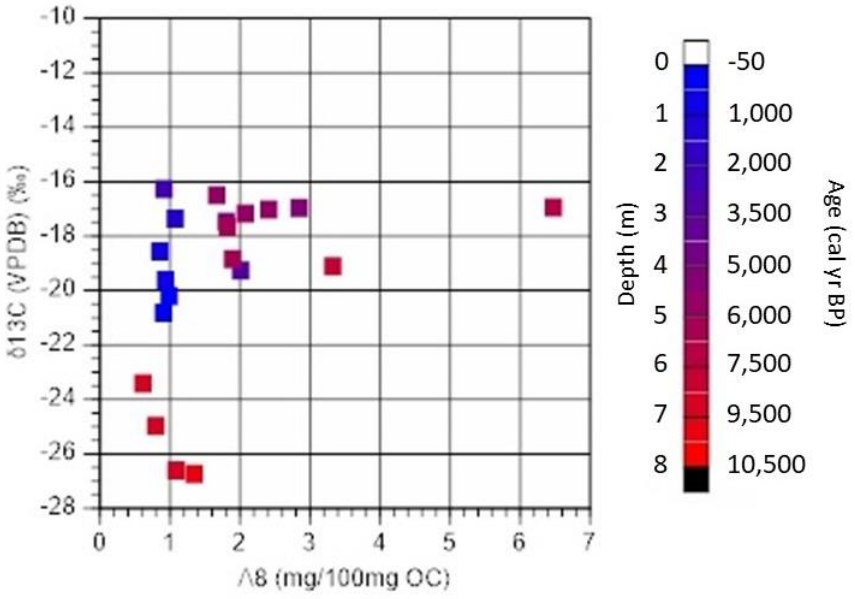

Figure 11. Cross plot of $\delta^{13}C$ and Λ8 with depth and approximate age indicated by color.

10,000 to 10,500 BP (7-8 m)

The Lily Lake sediment record begins soon after deglaciation, which occurred approximately 11,000 BP (Flakne 2003; Huber 1973; Lewis and Anderson 1989; Saarnisto 1974). The climate on Isle Royale at this time was cool because of the proximity to the Laurentide ice sheet (Kirby et al. 2002). This time period is characterized by low values of $\delta^{13}C$ of approximately -23 to -27‰, which indicates low productivity (Brenner et al. 1999), and by low Λ8, indicating that there were low amounts of fresh lignin reaching the lake basin (Figure 11; 12) (Thevenot et al. 2010). This is likely because early post glacial vegetation was typically composed of shrubs and grasses, which contain lower amounts of lignin than the trees and forests that developed later (Goñi and Hedges 1992; Schwark et al. 2002).

Ratios of S/V and C/V show that non-woody angiosperms were dominant between 10,000 to 10,500 BP (Figure 9). The pollen abundance analysis conducted by Flakne (2003) shows a high abundance of shrubs and grasses in the earliest part of the record, as well as high abundances of spruce and pine, and low abundances of birch (Figure 13). The Abundance of spruce is higher during this time than any other point in the record, indicating that climate during the Early Holocene was cooler than the mid-Holocene or Late Holocene (Flakne 2003).

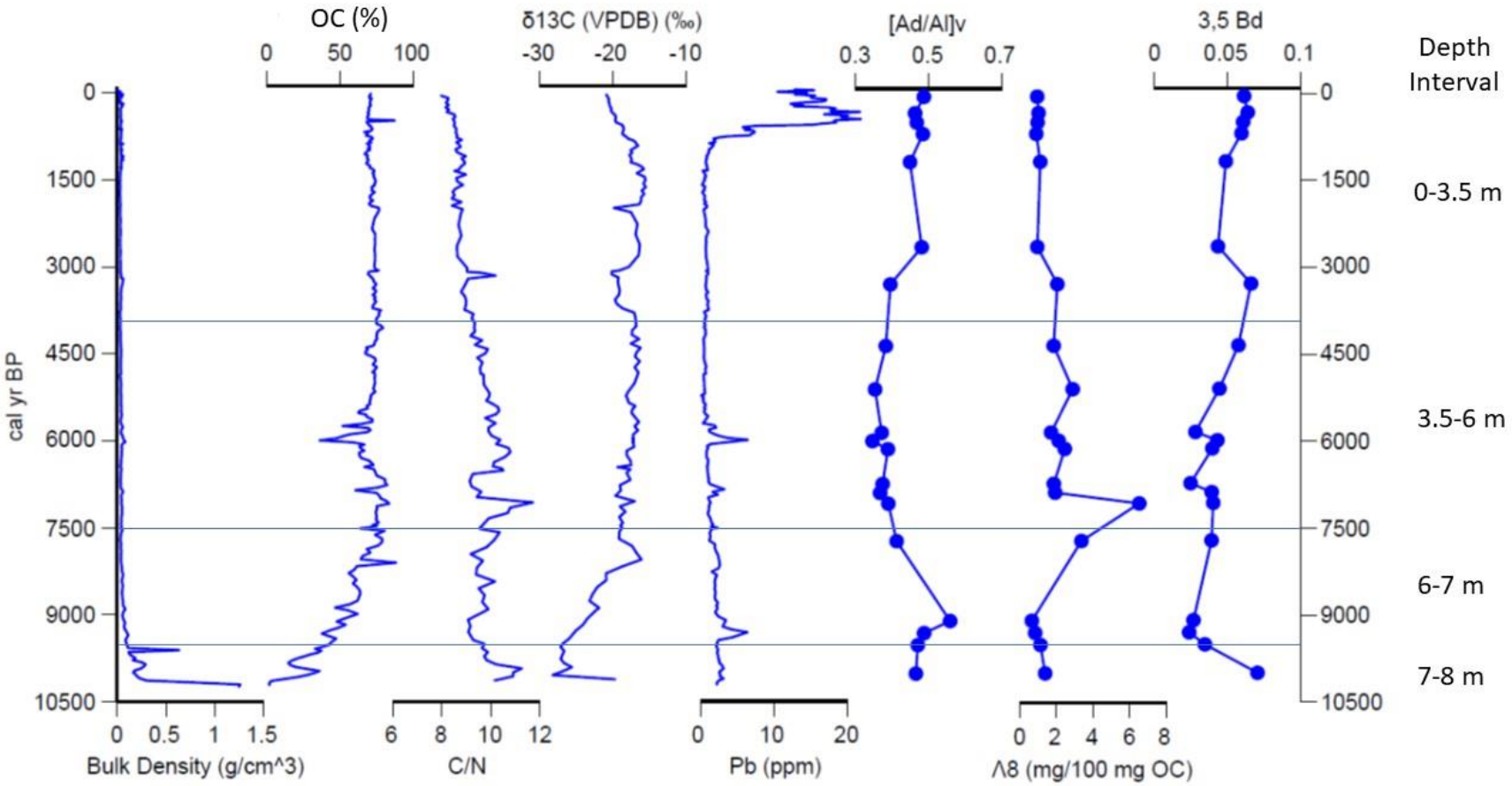

Figure 12. Summary of acquired geochemical proxy data. Horizontal lines indicate the depth intervals described in text.

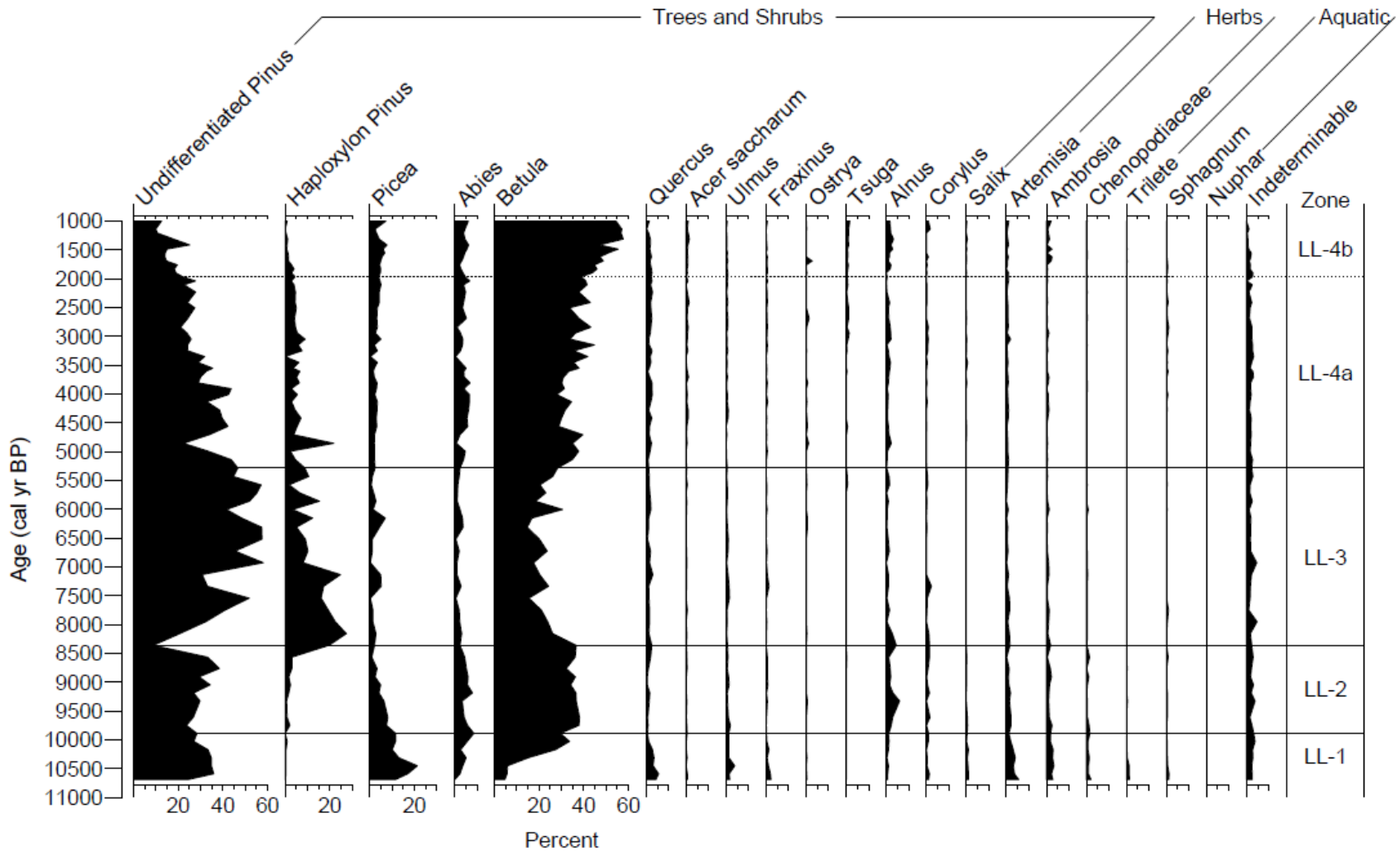

Figure 13. Percentage pollen abundance from dominant taxa based on data from Flakne, 2003.

7,500 to 9,500 BP (6-7 m)

From 7,500 to 9,500 BP lake productivity increased as the climate warmed following the recession of the Laurentide ice sheet. This interpretation is supported by the increasing OC% in the sediment, a decrease in the C/N values from 11 to ~9, and a $\delta^{13}C$ excursion from -27‰ to -22‰ (Figure 12). The increase in Λ8 indicates that terrestrial vegetation and forests were becoming established. These changes signify the gradual maturation of the post glacial forest ecosystem.

The ratios of S/V to C/V show that woody gymnosperms were dominant through the interval from 7,500 to 9,500 yr BP, which is supported by high abundance of birch and pine in the pollen record and a low abundance of spruce (Figure 13). This shift in dominant vegetation indicates climate warming and a decrease in precipitation (Flakne 2003). During this interval, preservation of lignin is higher than at any other point in the record, and it corresponds to relatively low amounts of 3,5 Bd, (Figure 12) which indicates low soil development (Otto and Simpson 2006). Additionally, because there was likely less precipitation during this time (Flakne 2003), the low amounts of 3,5-Bd and lignin may be attributed to diminished transport of humic matter via surficial runoff.

4,000 to 7,500 BP (3.5-6 m)

The ratios of S/V to C/V shows a transition from woody gymnosperms to non-woody angiosperms during the interval from 4,000 to 7,500 BP. During this time, $\delta^{13}C$ is enriched and Λ8 is stable at about 1 mg/100 mg OC, which is consistent because of the stable forest stands present during this time (Flakne 2003). Soil and roots were developing, as indicated by the increase in 3,5-Bd and low values of [Ad/Al]v (Figure 12). By this time, the soil had a sufficient amount of time to develop, leading to higher inputs of degraded terrestrial material in the sediment (Hedges and Ertel 1982; Otto and Simpson 2005, 2006).

During this interval, lignin content reaches the highest values of the record and then decreases rapidly (Figure 9, 12). Initially, C/N ratios are within a range of 9 to 10. At about 7000 BP, approximately the same time as the peak in lignin, there is an increase in C/N ratio to about 12, which indicates higher inputs of carbon rich material (Kaushal and Binford 1999).

Pollen abundance data from Isle Royale show that between 5,300 to 2,000 BP pines gradually declined, and birch increased (Figure 13) (Flakne 2003). This trend indicates the onset of dry conditions associated with the mid-Holocene transition, a climatic event which has been recorded in multiple lakes across the Midwest, Canada, and northeastern United States (Davis et al. 2000; Flakne 2003; Kirby et al. 2002). However, the onset of the mid-Holocene transition is more subtle in records from Isle Royale, where temperatures were lower and precipitation was higher relative to inland locations, such as lakes in Minnesota, because of the ameliorating thermal effects of Lake Superior (Davis et al. 2000).

0 to 4,000 BP (0-3.5 m)

The ratios of syringyl to cinnamyl show that non-woody angiosperms predominated during this interval (Figure 9). Values for $\delta^{13}C$ decline, suggesting a decrease in productivity (Meyers 1997). Λ8 is low, and values of 3,5-Bd and [Ad/Al]v are high, suggested increased delivery of degraded, soil-sourced terrestrial material as the soil horizons continue to mature in the catchment (Dickens et al. 2007; Otto and Simpson 2007; Prahl et al. 1994).

$\delta^{13}C$ becomes more depleted after approximately 1,000 BP. This change could be partly because of the Suess effect, which refers to the dilution of ^{13}C in the atmosphere from the combustion of fossil fuels, which impacts the isotopic composition of plants (Tans et al. 1979; Verburg 2007). Discrepancies in measurements of $\delta^{13}C$ from the Suess effect are usually estimated to be about 1‰ (Gruber et al. 1999; Verburg 2007). However, this interval shows a change in values of about 4‰, indicating that the positive trend occurring after 1,500 BP is

quantitatively significant, and that productivity during this time is lower than it was during the mid-Holocene transition (Meyers 1997).

Climate and human civilization

The onset of the mid-Holocene transition around 5200 BP corresponds to the cessation of mining activity as indicated by the absence of prehistoric Pb and K peaks after 5200 BP (Figure 12). It is reasonable to assume that the establishment of dry conditions during mid-Holocene transition would contribute to the halting of mining activities in the upper Midwest region. Studies of climate/human relationships in central north America reached similar conclusions. For example, from 1350-1450 CE in North America, a shift toward drier conditions during the growing season likely caused reductions in agricultural output that led to social stress and increased warfare between tribes (Bird et al. 2017).

Conclusions

Analyses of multiple paleolimnological proxies relating to ancient mining pollution and vegetation on Isle Royale have yielded multiple results that improve our understanding of the temporal patterns of mining and paleoenvironmental changes related to climate. Trace metal analysis of sediment from Lily Lake demonstrates evidence of periods of mining spanning 9,500 to 9,000 BP, 7,000 to 6,700 BP, and 6,100 to 5,700 BP where Pb concentrations are two to three times higher than the values of background concentrations and reach values that are approximately 25-30% of the magnitude of the maximum value of the modern Pb signal. These ages are approximately consistent with trace metal records from other lakes on Isle Royale and the Keweenaw Peninsula, though a more thorough assessment of age model uncertainty is necessary to validate temporal consistency (see Future Work, below). Analysis of K concentrations revealed

temporal patterns and magnitudes similar to those of Pb, with increases centered at 9,200 BP, 6,800 BP, and 5,900 BP.

The signals of Pb and K are likely to be anthropogenic based on variations in concentrations in metals such as Ti, Mg, and Fe that are predominantly controlled by changes in redox conditions and catchment weathering and erosion (Boës et al. 2011). Concentrations of these metals are high immediately following deglaciation approximately 11,000 BP because of the accelerated weathering processes associated with glacial retreat (Anderson et al. 2000). In response to a reduction in available weathering surfaces, concentrations of Ti, Mg, and Fe decrease between 10,000 to 7,000 BP, after which no other major changes in redox and weather/erosion conditions occur in the Lily Lake record.

The Pb peaks in the Lily Lake record as well as those of Copper Falls Lake, McCargoe Cove, Lake Medora, and Lake Manganese are consistent with radiocarbon ages acquired from organic matter associated with copper artifacts from the greater Lake Superior region (Figure 7; 8). The oldest radiocarbon dates associated with artifacts sourced from deposits on Isle Royale and the Keweenaw are 8,405 to 8,551 BP, and the uncertainty of these dates overlap with the dates of the Pb peak at 9,500 to 9,000 BP in the Lily Lake sediment. Artifacts from South Fowl Lake and Oconto cemetery have been dated to roughly 7,000 to 6,500 BP, which is consistent with Pb concentrations exceeding background levels in the Lily Lake sediment from 7,030 to 6,750 BP. The youngest Pb peak, from 6,130 to 5,700 BP is associated with ages of artifacts from Oconto cemetery, South Fowl Lake, and Minong Ridge. These data indicate that there is a strong relationship between the ages of copper artifacts discovered in the region and the occurrence of pollution signal in multiple lake sediment records.

The lack of evidence for mining activity in the Lily Lake catchment suggests that the metal pollution recorded in the sediment record is likely the result of atmospheric deposition of aerosols produced through the burning of wood and heating of rock as part of the mining and annealing processes.

Research on wind direction and strength as it relates to pollution signals in modern sediments demonstrates that atmospheric pollution can travel more than 10 km from active mining locations and produce signals discernable from background levels (Gallon et al. 2006; Waples and Klump 2002). The correspondence between the ages of distinct peaks in Pb and K in the Lily Lake Record with ages of inferred mining determined from previous research in Isle Royale and the Keweenaw, as well as the lack of evidence for past human activity in the Lily Lake catchment suggests that atmospheric deposition was the primary source of Pb and K in the trace metal record. This indicates that atmospheric deposition may have contributed significantly to Pb signals in other lake sediment records from the region.

Results of biogeochemical analyses of Lily Lake sediment are consistent with paleoclimate inferences based on the analysis of pollen. The pollen abundance study conducted by Flakne (2003) indicates a cool climate during the early Holocene, dry climate during the mid-Holocene, then an increase in precipitation and slight cooling during the Late Holocene. A high abundance of spruce and pine in the early Holocene demonstrate that climate was cool. This interpretation is supported by the bulk proxy and biomarker data which show higher percentages of gymnosperms and lower primary productivity during this time, which are also indications of a cool climate. The transition to dryer, warmer conditions during the mid-Holocene is inferred from the shift to birch in the pollen data (Flakne 2003), a conclusion that is supported by lignin phenol data that indicate the predominance of angiosperms. The continued increase in the abundance of birch trees through the late Holocene indicates that climate gradually became warmer and wetter than during the mid-Holocene. In general, the organic geochemical data acquired through this study are characterized by a shift from gymnosperms to angiosperms as well as an increase in aquatic productivity through the Holocene, demonstrating an overall warming trend,

The Lily Lake trace metal record expands our knowledge of the timing, spatial extent, and transport mechanisms of pollution presumably having resulted from mining activities during prehistoric times on Isle Royale. Results from this

study can be synthesized with other records to better constrain the history of mining practices associated with the Ancient Copper Culture. In addition, the information on changes in catchment vegetation and climate on Isle Royale through the Holocene not only provides environmental context for understanding past human behavior, but also contributes information that can aid in the projection of future vegetation responses to climate and anthropogenic stressors.

Suggestions for future work

The collection and analysis of additional sediment cores from lakes on Isle Royale and the Keweenaw Peninsula would likely help to better constrain the timing, magnitude, and spatial extent of mining related pollution and provide additional insight on the transport mechanisms (i.e. atmospheric deposition and catchment runoff). Complimentary biogeochemical analyses, such as those applied herein, would, furthermore, provide perspective on how lake/catchment ecological systems may have been impacted by ancient mining activities.

A more detailed statistical evaluation of the timing of the pollution signals in the Lily Lake record relative to that of lakes on the Keweenaw Peninsula (e.g. Copper Falls Lake) would help define the temporal boundaries of periods of mining. Hence, we propose using the already acquired data from the lakes on Isle Royale and the Keweenaw to conduct a series of statistical tests to determine the extent to which the ages of the Pb and K peaks are temporally consistent. These tests should account for age model uncertainty through the application of multiple age model iterations sampled from the probability distribution of age model control points for each record. More specifically, mean ages for the maximum pollution concentration (e.g. K or Pb) across several hundred (or thousand) iterations of each record along with accompanying standard deviations could be calculated, and an assessment of the similarity of the timing between records assessed using two sample t-tests.

The amount of organic matter is important in evaluating trace metal records of anthropogenic pollution. Therefore, it would be useful to compare the productivity, sedimentation rates, depths, and other sedimentary characteristics that may impact the creation, deposition, and degradation of organic matter. This would potentially help with interpretations of the timing of paleoenvironmental signals in records from Lily Lake and other from the region and may also allow for more informed selection of sampling locations, to optimize the likelihood of producing a record from sediment containing a well-preserved signal.

Comparison of Pb isotope signatures of sediment from McCargoe Cove, Chickenbone Lake, and Lily Lake would be helpful in determining any differences in fractionation processes or Pb source that may be responsible for the differences in the expression of the Pb signal in lake sediment cores. The analysis of isotopic signatures can be used to identify the provenance of Pb pollution (Graney et al 1995), and may prove useful in refining our understanding of the source and transport mechanisms of ancient pollution on Isle Royale.

Given that K and Pb increases in recently deposited sediment appear to be decoupled in both the Lily Lake and Copper Falls Lake records (as well as others), further investigation of the differences between the timing and magnitude of shifts in K and Pb concentrations in prehistoric and modern sediments is warranted. This may provide a useful context for determining the procedures used by ancient cultures in their mining activities and how these processes differ from modern human activities in terms of pollution production and transport. It would also likely be useful to assess the timing of recent and ancient changes in records of other trace metals. For example, assessing the magnitude and timing of peaks in cadmium, antimony, and arsenic elements that are associated with coal burning, may help to distinguish the differences between long range atmospheric transport and deposition and that from more localized sources, as well as differences in natural and anthropogenic inputs.

Works cited

Abbott, M. B. and T. W. Stafford. 1996. “Radiocarbon Geochemistry of Modern and Ancient Arctic Lake Systems, Baffin Island, Canada.” *Quaternary Research* 45(3):300–311.

Abbott, Mark B. and Alexander P. Wolfe. 2003. “Intensive Pre-Incan Metallurgy Recorded by Lake Sediments from the Bolivian Andes.” *Science* 301(5641):1893–95.

Aller, Robert C. 1998. “Mobile Deltaic and Continental Shelf Muds as Suboxic, Fluidized Bed Reactors.” *Marine Chemistry* 61(3–4):143–55.

Anderson, S. P., J. I. Drever, C. D. Frost, and P. Holden. 2000. “Chemical Weathering in the Forefield of a Retreating Glacier.” *Geochim. Cosmochim. Acta* 64(7):1173–1189.

Bain, Daniel J., Ian D. Yesilonis, and Richard V. Pouyat. 2012. “Metal Concentrations in Urban Riparian Sediments along an Urbanization Gradient.” *Biogeochemistry* 107(1–3):67–79.

Bartlein, P. J., T. Webb, and E. Fleri. 1984. “Holocene Climate Change in the Northern Midwest: Pollen-Derived Estimates.” *Quaternary Research* 22:361–74.

Beukens, R. P. et al. 2006. “Radiocarbon Dating of Copper-Preserved Organics.” *Radiocarbon* 34(3):890–97.

Bianchi. 2010. *Lignins, Cutins, and Suberins*.

Bindler, Richard. 2006. “Mired in the Past - Looking to the Future: Geochemistry of Peat and the Analysis of Past Environmental Changes.” *Global and Planetary Change* 53(4):209–21.

Binford, Michael W. et al. 1997. “Climate Variation and the Rise and Fall of an Andean Civilization.” *Quaternary Research* 47(2):235–48.

Bird, Broxton W., Jeremy J. Wilson, William P. Gilhooly III, Byron A. Steinman, and Lucas Stamps. 2017. “Midcontinental Native American Population Dynamics and Late Holocene Hydroclimate Extremes.” *Scientific Reports* 7(September 2016):41628.

Blais, Jules M., Michael R. Rosen, and John P. Smol. 2015. *Environmental Contaminants*. Vol. 18.

Bloom. 1981. “Metal-Organic Matter Interactions in Soil.” *Chemistry in the Soil Environment: Proceedings of a Symposium Sponsored by Division S-2 of the American Society OfAgronomy and the Soil Science Society OfAmerica : Papers Were Presented during the Annual Meetings in Fort Collins,*

Colorado, August 5-10, 19 129–50.

Boës, Xavier, J. Rydberg, A. Martinez-Cortizas, R. Bindler, and I. Renberg. 2011. "Evaluation of Conservative Lithogenic Elements (Ti, Zr, Al, and Rb) to Study Anthropogenic Element Enrichments in Lake Sediments." *Journal of Paleolimnology* 46(1):75–87.

Bornhorst, Theodore J. and Robert J. Barron. 2011. "Copper Deposits of the Western Upper Peninsula of Michigan." *GSA Field Guides* 0024(05):83–99.

Bowen, H. J. M. 1979. *Environmental Chemistry of the Elements.* London: Academic Press.

Boyle, J. F. 2001. "Inorganic Geochemical Methods in Palaeolimnology." *Tracking Environmental Change Using Lake Sediments* 2:83–141.

Bränvall, M. L., R. Bindler, O. Emteryd, and I. Renberg. 2001. "Four Thousand Years of Atmospheric Lead Pollution in Northern Europe: A Summary from Swedish Lake Sediments." *Journal of Paleolimnology* 25(4):421–35.

Brenner, Mark, Thomas J. Whitmore, Jason H. Curtis, David A. Hodell, and Claire L. Schelske. 1999. "Stable Isotope (Δ13C and Δ15N) Signatures of Sedimented Organic Matter as Indicators of Historic Lake Trophic State." *Journal of Paleolimnology* 22(2):205–21.

Calloway, C. P., S. Li, J. W. Buchanan, and R. K. Stevens. 1989. "A Refinement of the Potassium Tracer Method for Residential Wood Smoke." *Atmospheric Environment (1967)* 23(1):67–69.

Campetti, Leigh Casey. 2016. "A Predictive Model for the Archaic/Woodland Transition on Isle Royale National Park, Michigan." *ProQuest Dissertations and Theses* 145.

Carpi, Anthony. 1997. "Mercury from Combustion Sources: A Review of the Chemical Species Emitted and Their Transport in the Atmosphere." *Water, Air, and Soil Pollution* 98(3–4):241–54.

Charles Kerfoot, W. and John a. Robbins. 1999. "Nearshore Regions of Lake Superior: Multi-Element Signatures of Mining Discharges and a Test of Pb-210 Deposition under Conditions of Variable Sediment Mass Flux." *Journal of Great Lakes Research* 25(4):697–720.

Charlesworth, S. M. and I. D. L. Foster. 1999. "Sediment Budgets and Metal Fluxes in Two Contrasting Urban Lake Catchments in Coventry, UK." *Applied Geography* 19(3):199–210.

Chow, Tsaihwa J. and John L. Earl. 2014. "Lead Aerosols in the Atmosphere : Increasing Concentrations." *Science* 169(3945):577–80.

Cooke, Colin A., Mark B. Abbott, Alexander P. Wolfe, and John L. Kittleson. 2007. "A Millennium of Metallurgy Recorded by Lake Sediments from Morococha, Peruvian Andes." *Environmental Science and Technology*

41(10):3469–74.

Cooke, Colin A. and Richard Bindler. 2015. “Environmental Contaminants.” 18.

Cooke, Colin A., Alexander P. Wolfe, and William O. Hobbs. 2009. “Lake-Sediment Geochemistry Reveals 1400 Years of Evolving Extractive Metallurgy at Cerro de Pasco, Peruvian Andes.” *Geology* 37(11):1019–22.

Crane, H. R. and James B. Griffin. 1965. “University of Michigan Radiocarbon Dates X.” *Radiocarbon* 7:123–52.

Davis, Margaret et al. 2000. “Holocene Climate in the Western Great Lakes National Parks and Lakeshores : Implications for Future Climate Change.” *Conservation Biology* 14(4):968–83.

Dean, Walter E. 1974. “Determination of Carbonate and Organic Matter in Calcareous Sediments and Sedimentary Rocks by Loss on Ignition: Comparison with Other Methods.” *Journal of Sedimentary Petrology* 44(1):242–48.

Dean, Walter E., Thomas S. Ahlbrandt, Roger Y. Anderson, and J. Platt Bradbury. 1996. “Regional Aridity in North American during the Middle Holocene.” *The Holocene* 6:145–55.

Dean, WE. 1999. “The Carbon Cycle and Biogeochemical Dynamics in Lake Sediments.” *Journal of Paleolimnology* (1997):375–93.

Dearing, J. A. et al. 2008. “Using Multiple Archives to Understand Past and Present Climate-Human- Environment Interactions: The Lake Erhai Catchment, Yunnan Province, China.” *Journal of Paleolimnology* 40(1):3–31.

Dickens, Angela F. et al. 2007. “Sources and Distribution of CuO-Derived Benzene Carboxylic Acids in Soils and Sediments.” *Organic Geochemistry* 38(8):1256–76.

Dittmar, Thorsten and Rubén José Lara. 2001. “Molecular Evidence for Lignin Degradation in Sulfate-Reducing Mangrove Sediments (Amazõnia, Brazil).” *Geochimica et Cosmochimica Acta* 65(9):1417–28.

Dustin, Fred. 1957. “Archaeological Reconnaissance of Isle Royale.” *Michigan HIstory* 41(1).

Ehrhardt, Kathleen L. 2013. “Copper Working Technologies, Contexts of Use, and Social Complexity in the Eastern Woodlands of Native North America.” *Archaeometallurgy in Global Perspective: Methods and Syntheses* 303–28.

Ertel, John R. and John I. Hedges. 1985. “Sources of Sedimentary Humic Substances: Vascular Plant Debris.” *Geochimica et Cosmochimica Acta* 49(10):2097–2107.

Fan, Jiawei et al. 2017. “Carbon and Nitrogen Signatures of Sedimentary Organic Matter from Dali Lake in Inner Mongolia: Implications for Holocene

Hydrological and Ecological Variations in the East Asian Summer Monsoon Margin." *Quaternary International* 452:65–78.

Fine, Philip M., Glen R. Cass, and Bernd R. T. Simoneit. 2001. "Chemical Characterization of Fine Particle Emissions from Fireplace Combustion of Woods Grown in the Northeastern United States." *Environmental Science and Technology* 35(13):2665–75.

Finkenbinder, Matthew S. et al. 2014. "A 31,000 Year Record of Paleoenvironmental and Lake-Level Change from Harding Lake, Alaska, USA." *Quaternary Science Reviews* 87:98–113.

Flakne, Robyn. 2003. "The Holocene Vegetation History of Isle Royale National Park, Michigan, U.S.A." *Canadian Journal of Forest Research* 33.

Gallagher, Julie M. and Richard L. Josephs. 2008. "Using LiDAR to Detect Cultural Resources in a Forested Environment: An Example from Isle Royale National Park, Michigan, USA." *Archaeological Prospection* 15(3):187–206.

Gallon, Céline, André Tessier, Charles Gobeil, and Richard Carignan. 2006. "Historical Perspective of Industrial Lead Emissions to the Atmosphere from a Canadian Smelter." *Environmental Science and Technology* 40(3):741–47.

Galloway, James N., J. David Thornton, Stephen A. Norton, Herbert L. Volchok, and Roland A. N. McLean. 1982. "Trace Metals in Atmospheric Deposition: A Review and Assessment." *Atmospheric Environment* 16(7):1677–1700.

Gardner, Wayne S. and David W. Menzel. 1974. "Phenolic Aldehydes as Indicators of Terrestrially Derived Organic Matter in the Sea." *Geochimica et Cosmochimica Acta* 38(6):813–22.

Gong, Fei et al. 2017. "Evidence for Paleoclimate Changes from Lignin Records of Sediment Core A02 in the Southern Yellow Sea since ~ 9.5 Cal. Kyr B.P." *Palaeogeography, Palaeoclimatology, Palaeoecology* 479:173–84.

Goñi, Miguel A. and John I. Hedges. 1992. "Lignin Dimers: Structures, Distribution, and Potential Geochemical Applications." *Geochimica et Cosmochimica Acta* 56(11):4025–43.

Graney, J. R., A. N. Halliday, et al. 1995. "Isotopic Record of Lead Pollution in Lake Sediments from the Northeastern United States." *Geochemica et Cosmochimica Acta.* 59(9):1715–28.

Graney, J. R., A. N. Halliday, et al. 1995. "Isotopic Record of Lead Pollution in Lake Sediments Fromthe Northeastern United States." *Geochemica et Cosmochimica Acta.* 59(9):1715–28.

Grimm, Eric C., Louis J. Maher, and David M. Nelson. 2009. "The Magnitude of Error in Conventional Bulk-Sediment Radiocarbon Dates from Central North America." *Quaternary Research* 72(2):301–8.

Gruber, Nicolas et al. 1999. "Spatiotemporal Patterns of Carbon-13 in the Global

Surface Oceans and the Oceanic Suess Effect." *Global Biogeochemical Cycles* 13(2):307–35.

Hamilton-Taylor, J. and W. Davison. 1995. "Redox-Driven Cycling of Trace Elements in Lakes." *Physics and Chemistry of Lakes* 217–63.

Hansen, HL, LW Krefting, and V. Kurmis. 1973. "The Forest of Isle Royale in Relation to Fire History and Wildlife."

Harris, David, William R. Horwáth, and Chris van Kessel. 2001. "Acid Fumigation of Soils to Remove Carbonates Prior to Total Organic Carbon or CARBON-13 Isotopic Analysis." *Soil Science Society of America Journal* 65(6):1853.

Hassan, Kameleldin M., James B. Swinehart, and Roy F. Spalding. 1997. "Evidence for Holocene Environmental Change from C/N Ratios, and Δ13C and Δ15N Values in Swan Lake Sediments, Western Sand Hills, Nebraska." *Journal of Paleolimnology* 18(2):121–30.

Hedges, John I. and John R. Ertel. 1982. "Characterization of Lignin by Gas Capillary Chromatography of Cupric Oxide Oxidation Products." *Anal. Chem* 5(4):174–78.

Hedges, John I., John R. Ertel, and Estella B. Leopold. 1982. "Lignin Geochemistry of a Late Quaternary Sediment Core from Lake Washington." *Geochimica et Cosmochimica Acta* 46(10):1869–77.

Hedges, John I. and Dale C. Mann. 1979. "The Characterization of Plant Tissues by Their Lignin Oxidation Products." *Geochimica et Cosmochimica Acta* 43(11):1803–7.

Henne, Paul D. and Feng Sheng Hu. 2010. "Holocene Climatic Change and the Development of the Lake-Effect Snowbelt in Michigan, USA." *Quaternary Science Reviews* 29(7–8):940–51.

Hill, Mark A., Mark F. Seeman, Kevin C. Nolan, and Laure Dussubieux. 2017. "An Empirical Evaluation of Copper Procurement and Distribution." *Archaeological and Anthropological Science* 1–13.

Holmes, William. 1901. "Aboriginal Copper Mines of Isle Royale, Lake Superior." *American Anthropologist* 3(4):684–96.

Hong, S., J. P. Candelone, C. C. Patterson, and C. F. Boutron. 1994. "Greenland Ice Evidence of Hemispheric Lead Pollution Two Millenia Ago by Greek and Roman Civilisations." *Science* 265:1841–43.

Horowitz, A. 1985. "A Primer on Trace Metal- Sediment Chemistry." *U.S. Geological Survey Water-Supply Paper* 72.

Hu, Feng Sheng, John I. Hedges, Elizabeth S. Gordon, and Linda B. Brubaker. 1999. "Lignin Biomarkers and Pollen in Postglacial Sediments of an Alaskan Lake." *Geochimica et Cosmochimica Acta* 63(9):1421–30.

Huber, N. King. 1973. “Glacial and Postglacial Geologic History of Isle Royale National Park, Michigan.” A1–15.

Hyodo, Fujio et al. 2016. “Variations in Lignin-Derived Phenols in Sediments of Japanese Lakes over the Last Century and Their Relation to Watershed Vegetation.” *Organic Geochemistry* 103:125–35.

Ji, Shen, Liu Xingqi, Wang Sumin, and Ryo Matsumoto. 2005. “Palaeoclimatic Changes in the Qinghai Lake Area during the Last 18,000 Years.” *Quaternary International* 136(1 SPEC. ISS.):131–40.

Kaushal, Sujay and Michael W. Binford. 1999. “Relationship between C:N Ratios of Lake Sediments, Organic Matter Sources, and Historical Deforestation in Lake Pleasant, Massachusetts, USA.” *Journal of Paleolimnology* 22(4):439–42.

Kirby, Matthew E., Henry T. Mullins, William P. Patterson, and Adam W. Burnett. 2002. “Late Glacial-Holocene Atmospheric Circulation and Precipitation in the Northeast United States Inferred from Modern Calibrated Stable Oxygen and Carbon Isotopes.” *Bulletin of the Geological Society of America* 114(10):1326–40.

Lankton, Larry D. 2010. *Hollowed Ground: Copper Mining and Community Building on Lake Superior, 1840s-1990s. Wayne State University Press*.

Lara, Maria V. and Carlos S. Andreo. 2011. *C4 Plants Adaptation to High Levels of CO2 and to Drought Environments*.

LaRonge, Michael. 2001. “An Experimental Analysis of Great Lakes Archaic Copper Smithing.”

Lathrop, H. 1901. “Prehistoric Mines of Lake Superior.” *The American Antiquarian and Oriental Journal (1880-1914)* 24(4):248.

Lee, C. S. L. et al. 2008. “Seven Thousand Years of Records on the Minincg and Utilization of Metals from Lake Sediments in Central China.” *Environmental Science & Technology* 42(13):4732–38.

Lehmann, Moritz F. et al. 2004. “Seasonal Variation of the D13C and D15N of Particulate and Dissolved Carbon and Nitrogen in Lake Lugano: Constraints on Biogeochemical Cycling in a Eutrophic Lake.” *Limnology and Oceanography* 49(2):415–29.

Leopold, Estella B., Rudy Nickmann, John I. Hedges, and John R. Ertel. 1982. “Pollen and Lignin Records of Late Quaternary Vegetation, Lake Washington.” *Science* 218(4579):1305–7.

Lewis, C. F. M. and T. W. Anderson. 1989. “Oscillations of Levels and Cool Phases of the Laurentian Great Lakes Caused by Inflows from Glacial Lakes Agassiz and Barlow-Ojibway.” *Journal of Paleolimnology* 2(2):99–146.

Li, Jia, Mihály Pósfai, Peter V. Hobbs, and Peter R. Buseck. 2003. “Individual

Aerosol Particles from Biomass Burning in Southern Africa: 2, Compositions and Aging of Inorganic Particles." *Journal of Geophysical Research: Atmospheres* 108(D13):n/a-n/a.

Luly, J. G., J. F. Grindrod, and D. Penny. 2006. "Holocene Palaeoenvironments and Change at Three-Quarter Mile Lake, Silver Plains Station, Cape York Peninsula, Australia." *The Holocene* 16(8):1085–94.

Lützow, M. V. et al. 2006. "Stabilization of Organic Matter in Temperate Soils: Mechanisms and Their Relevance under Different Soil Conditions - A Review." *European Journal of Soil Science* 57(4):426–45.

Mahler, Barbara J., Peter C. Van Metre, and Edward Callender. 2006. "Trends in Metals in Urban and Reference Lake Sediments across the United States, 1970 to 2001." *Environmental Toxicology and Chemistry* 25(7):1698–1709.

Marx, Samuel K., Shaqer Rashid, and Nicola Stromsoe. 2016. "Global-Scale Patterns in Anthropogenic Pb Contamination Reconstructed from Natural Archives." *Environmental Pollution* 213:283–98.

Matthias-Maser, S., V. Obolkin, T. Khodzer, and R. Jaenicke. 2000. "Seasonal Variation of Primary Biological Aerosol Particles in the Remote Continental Region of Lake Baikal/Siberia." *Atmospheric Environment* 34(22):3805–11.

Mays, Jennifer et al. 2017. "Stable Carbon Isotopes (d 13 C) of Total Organic Carbon and Long-Chain n-Alkanes as Proxies for Climate and Environmental Change in a Sediment Core from Lake Petén-Itzá, Guatemala." *Journal of Paleolimnology* 57:307–19.

McConnell, Joseph R. et al. 2018. "Lead Pollution Recorded in Greenland Ice Indicates European Emissions Tracked Plagues, Wars, and Imperial Expansion during Antiquity." *Proceedings of the National Academy of Sciences of the United States of America* 201721818.

McFadden, Melany A., William P. Patterson, Henry T. Mullins, and William T. Anderson. 2005. "Multi-Proxy Approach to Long- and Short-Term Holocene Climate-Change: Evidence from Eastern Lake Ontario." *Journal of Paleolimnology* 33(3):371–91.

McGimsey, R. G., C. A. Neal, and C. M. Riley. 2001. "Areal Distribution, Thickness, Mass, Volume, and Grain Size of Tephra-Fall Deposits from the 1992 Eruptions of Crater Peak Vent, Mt. Spurr Volcano, Alaska." *USGS Open-File Report 01–370*.

Meyers, Philip A. 1997. "Organic Geochemical Proxies of Paleoceanographic, Paleolimnologic, and Paleoclimatic Processes." *Organic Geochemistry* 27(5/6):213–50.

Meyers, Philip A. and Ryoshi Ishiwatari. 1993. "Lacustrine Organic Geochemistry-an Overview of Indicators of Organic Matter Sources and Diagenesis in Lake Sediments." *Organic Geochemistry* 20(7):867–900.

Meza-figueroa, Diana et al. 2009. “The Impact of Unconfined Mine Tailings in Residential Areas from a Mining Town in a Semi-Arid Environment: Nacozari, Sonora, Mexico.” *Chemosphere* 77(1):140–47.

Moingt, Matthieu, Marc Lucotte, and Serge Paquet. 2016. “Lignin Biomarkers Signatures of Common Plants and Soils of Eastern Canada.” *Biogeochemistry* 129(1–2):133–48.

Murozumi, M., J. Chow, Tsaihwa, and Clair Patterson. 1969. “Chemical Concentrations of Pollutant Lead Aerosols, Terrestrial Dusts, and Sea Salts in Greenland and Antarctic Snow Strata.” *Geochimica et Cosmochimica Acta* 33(10):1247–94.

Nelson, Daniel B. et al. 2011. “Drought Variability in the Pacific Northwest from a 6 ,000-Yr Lake Sediment Record.” *PNAS* 108(10):3870–75.

Nesje, Atle and Svein Olaf Dahl. 2001. “The Greenland 8200 Cal. Yr BP Event Detected in Loss-on-Ignition Profiles in Norwegian Lacustrine Sediment Sequences.” *Journal of Quaternary Science* 16(2):155–66.

Nriagu, J. O. et al. 1988. “Quantitative Assessment of Worldwide Contamination of Air, Water and Soils by Trace Metals.” *Nature* 333(6169):134–39.

Nriagu, Jerome O. 1989. “A Global Assessment of Natural Sources of Atmospheric Trace Metals.” *Nature* 338(6210):47–49.

Nriagu, Jerome O. 1979. “Global Inventory of Natural and Anthropogenic Emissions of Trace Metals to the Atmosphere [7].” *Nature* 279(5712):409–11.

Nriagu, Jerome O., Henry K. T. Wong, Gregory Lawson, and Peter Daniel. 1998. “Saturation of Ecosystems with Toxic Metals in Sudbury Basin, Ontario, Canada.” *Science of the Total Environment* 223(2–3):99–117.

Otto, Angelika, Chubashini Shunthirasingham, and Myrna J. Simpson. 2005. “A Comparison of Plant and Microbial Biomarkers in Grassland Soils from the Prairie Ecozone of Canada.” *Organic Geochemistry* 36(3):425–48.

Otto, Angelika and Myrna J. Simpson. 2007. “Analysis of Soil Organic Matter Biomarkers by Sequential Chemical Degradation and Gas Chromatography - Mass Spectrometry.” *Journal of Separation Science* 30(2):272–82.

Otto, Angelika and Myrna J. Simpson. 2005. “Degradation and Preservation of Vascular Plant-Derived Biomarkers in Grassland and Forest Soils from Western Canada.” *Biogeochemistry* 74(3):377–409.

Otto, Angelika and Myrna J. Simpson. 2006. “Evaluation of CuO Oxidation Parameters for Determining the Source and Stage of Lignin Degradation in Soil.” *Biogeochemistry* 80(2):121–42.

Pachon, Jorge E., Rodney J. Weber, Xiaolu Zhang, James A. Mulholland, and Armistead G. Russell. 2013. “Revising the Use of Potassium (K) in the

Source Apportionment of PM2.5." *Atmospheric Pollution Research* 4(1):14–21.

Pacyna, J. M. and E. G. Pacyna. 2001. "An Assessment of Global and Regional Emissions of Trace Metals to the Atmosphere from Anthropogenic Sources Worldwide." *Environmental Reviews* 9(4):269–98.

Pacyna, Jozef M. and Elisabeth G. Pacyna Editors. 2016. *Environmental Determinants of Human Health*.

Parnell, A. C., J. Haslett, J. R. M. Allen, C. E. Buck, and B. Huntley. 2008. "A Flexible Approach to Assessing Synchroneity of Past Events Using Bayesian Reconstructions of Sedimentation History." *Quaternary Science Reviews* 27(19–20):1872–85.

Parnell, Andrew C., Caitlin E. Buck, and Thinh K. Doan. 2011. "A Review of Statistical Chronology Models for High-Resolution, Proxy-Based Holocene Palaeoenvironmental Reconstruction." *Quaternary Science Reviews* 30(21–22):2948–60.

Patterson, Clair. 1965. "Contaminated and Natural Lead Environments of Man." *Arch Environ Health* 11:344–60.

Pellerin, Brian A., Peter J. Hernes, JohnFranco Saraceno, Robert G. M. Spencer, and Brian A. Bergamaschi. 2010. "Microbial Degradation of Plant Leachate Alters Lignin Phenols and Trihalomethane Precursors." *Journal of Environment Quality* 39(3):946.

Pio, C. A. et al. 2008. "Chemical Composition of Atmospheric Aerosols during the 2003 Summer Intense Forest Fire Period." *Atmospheric Environment* 42(32):7530–43.

Pleger, Thomas C. and James B. Stoltman. 2009. "The Archaic Tradition in Wisconsin." *Archaic Societies: Diversity and Complexity across the Midcontinent* 697–724.

Pompeani, David. 2015. "Human Impacts on the Environment over the Holocene in Michigan and Illinois Using Lake Sediment Geochemistry." *Doctoral Dissertation, University of Pittsburgh. (Unpublished)*.

Pompeani, David, M. B. Abbott, D. J. Bain, S. DePasqual, and M. S. Finkenbinder. 2014. "Copper Mining on Isle Royale 6500-5400 Years Ago Identified Using Sediment Geochemistry from McCargoe Cove, Lake Superior." *The Holocene* 25(2):253–62.

Pompeani, David P., Mark B. Abbott, Byron A. Steinman, and Daniel J. Bain. 2013a. "Lake Sediments Record Prehistoric Lead Pollution Related to Early Copper Production in North America." *Environmental Science and Technology* 47(11):5545–52.

Pompeani, David P., Mark B. Abbott, Byron A. Steinman, and Daniel J. Bain. 2013b. "Lake Sediments Record Prehistoric Lead Pollution Related to Early

Copper Production in North America." *Environmental Science and Technology* 47(11):5545–52.

Pompeani, David P., Colin A. Cooke, Mark B. Abbott, and Paul E. Drevnick. 2018. "Climate, Fire, and Vegetation Mediate Mercury Delivery to Mid-Latitude Lakes over the Holocene." *Environmental Science & Technology* acs.est.8b01523.

Potzger, J. E. 1954. "Post-Algonquin and Post-Nipissing Forest History of Isle Royale , Michigan Botanical Studies." 11(22).

Prahl, F. G., J. R. Ertel, M. A. Goni, M. A. Sparrow, and B. Eversmeyer. 1994. "Terrestrial Organic Carbon Contributions to Sediments on the Washington Margin." *Geochimica et Cosmochimica Acta* 58(14):3035–48.

Rapp, G., J. Allert, V. Vitali, Z. Jing, and E. Henrickson. 2000. *Determining Geologic Sources of Artifact Copper. Source Characterization Using Trace Element Patterns*.

Rasmussen, P. E. 1998. "Long-Range Atmospheric Transport of Trace Metals: The Need for Geoscience Perspectives." *Environmental Geology* 33(2–3):96–108.

Rasmussen, P. E. et al. 1998. "Mercury in Lake Sediments of the Precambrian Shield near Huntsville, Ontario, Canada." *Environmental Geology* 33(2–3):170–82.

Rauch, Jason N. and Jozef M. Pacyna. 2009. "Earth's Global Ag, Al, Cr, Cu, Fe, Ni, Pb, and Zn Cycles." *Global Biogeochemical Cycles* 23(2):1–16.

Raymond, Randall E., Ronald O. Kapp, and Robert A. Janke. 1975. "Postglacial and Recent Sediments of Inland Lakes of Isle Royale National Park, Michigan." *The Mighigan Academician*.

Reardon, Bill. 2014. "Oldest Carbon-14 Dated Copper Projectile Points from Wisconsin.Pdf."

Reimer, Paula. 2013. "IntCal13 and Marine13 Radiocarbon Age Calibration Curves 0–50,000 Years Cal BP." *Radiocarbon* 55(4):1869–87.

Renberg, I., M. L. Brännvall, R. Bindler, and O. Emteryd. 2002. "Stable Lead Isotopes and Lake Sediments - A Useful Combination for the Study of Atmospheric Lead Pollution History." *Science of the Total Environment* 292(1–2):45–54.

Renberg, Ingemar, Maria Wlk Persson, and Ove Emteryd. 1994. "Pre-Industrial Atmospheric Lead Contamination Detected in Swedish Lake Sediments." *Nature* 368.

Rosenmeyer, Tom. 2009. "Copper - Bearing Fissure Veins: Keweenaw County, Michigan." *Rocks and Minerals* 84:298–323.

Saarnisto, Matti. 1974. “The Deglaciation History of the Lake Superior Region and Its Climatic Implications.” *Quaternary Research* 4(3):316–39.

Sampei, Y. and E. Matsumoto. 2001. “C/N Ratios in a Sediment Core from Nakaumi Lagoon, Southwest Japan - Usefulness as an Organic Source Indicator -.” *Geochemical Journal* 35(3):189–205.

Santschi, P. H., Guo, L., Means, J. C., and Ravichandran, M. 1999. “NOM Binding with Trace Metal and Organic Material.Pdf.” *John Wiley & Sons, Inc* 347–80.

Sarna-Wojcicki, Andrea. M., Susan Shipley, Richard B. Jr. Waitt, Daniel Dzurisin, and Spencer H. Wood. 1981. “Areal Distribution, Thickness, Mass, Volume, and Grain Size of Air-Fall Ash from Six Major Eruptions of 1980.” *The 1980 Eruptions of Mount St. Helens, Washington* 577–600.

Schreiner, Kathryn M., Thomas S. Bianchi, Timothy I. Eglinton, Mead A. Allison, and Andrea J. M. Hanna. 2013. “Sources of Terrigenous Inputs to Surface Sediments of the Colville River Delta and Simpson’s Lagoon, Beaufort Sea, Alaska.” *Geophys. Res. Biogeosci* 118:808–24.

Schroeder, David L. and Katharine C. Ruhl. 1968. “Metallurgical Characteristics of North American Prehistoric Copper Work.” *American Antiquity* 33(2):162–69.

Schwark, L., K. Zink, and J. Lechterbeck. 2002. “Reconstruction of Postglacial to Early Holocene Vegetation History in Terrestrial Central Europe via Cuticular Lipid Biomarkers and Pollen Records from Lake Sediments.” *Geology* 30(5):463–66.

Settle, D. M. and C. C. Patterson. 1982. “Magnitudes and Sources of Precipitation and Dry Deposition Fluxes of Industrial and Natural Leads to the North Pacific at Enewatak.” *Journal of Geophysical Research* 87(C11):8857–69.

Shuman, Bryan. 2003. “Controls on Loss-on-Ignition Variation in Cores from Two Shallow Lakes in the Northeastern United States.” *Journal of Paleolimnology* 30(4):371–85.

Smol, John P. 2009. *Pollution of Lakes and Rivers: A Paleoenvironmental Perspective, 2nd Edition*.

Smuda, Jochen, Bernhard Dold, Jorge E. Spangenberg, and Hans Rudolf Pfeifer. 2008. “Geochemistry and Stable Isotope Composition of Fresh Alkaline Porphyry Copper Tailings: Implications on Sources and Mobility of Elements during Transport and Early Stages of Deposition.” *Chemical Geology* 256(1–2):62–76.

Spliethoff, H. M. and H. F. Hemond. 1996. “History of Toxic Metal Discharge to Surface Waters of the Aberjona Watershed.” *Environmental Science and Technology* 30(1):121–28.

Talbot, Michael R. and Truls Johannessen. 1992. “A High Resolution Palaeoclimatic Record for the Last 27,500 Years in Tropical West Africa from the Carbon and Nitrogen Isotopic Composition of Lacustrine Organic Matter.” *Earth and Planetary Science Letters* 110:23–37.

Talbot, Michael R. and Tine Laerdal. 2000. “The Late Pleistocene - Holocene Palaeolimnology of Lake Victoria, East Africa, Based upon Elemental and Isotopic Analyses of Sedimentary Organic Matter.” *Journal of Paleolimnology* 23(2):141–64.

Tans, P. P., A. F. M. De Jong, and W. G. Mook. 1979. “Natural Atmospheric 14C Variation and the Suess Effect [5].” *Nature* 280(5725):826–28.

Tareq, Shafi M., Nobuhiko Handa, and Eiichiro Tanoue. 2006. “A Lignin Phenol Proxy Record of Mid Holocene Paleovegetation Changes at Lake DaBuSu, Northeast China.” *Journal of Geochemical Exploration* 88(1–3 SPEC. ISS.):445–49.

Tareq, Shafi M., Hiroyuki Kitagawa, and Keiichi Ohta. 2011. “Lignin Biomarker and Isotopic Records of Paleovegetation and Climate Changes from Lake Erhai, Southwest China, since 18.5kaBP.” *Quaternary International* 229(1–2):47–56.

Tareq, Shafi M. and Keiichi Ohta. 2015. “Lignin and Isotope Signatures in Pollen: A Caveat of Lignin Phenol Biomarker for Reconstructing Paleovegetation.” *Asian Journal of Water, Environment and Pollution* 12(1):1–9.

Tareq, Shafi M., Noriyuki Tanaka, and Keiichi Ohta. 2004. “Biomarker Signature in Tropical Wetland: Lignin Phenol Vegetation Index (LPVI) and Its Implications for Reconstructing the Paleoenvironment.” *Science of the Total Environment* 324(1–3):91–103.

Tareq, Shafi M., Noriyuki Tanaka, and Keiichi Ohta. 2007. “Isotope and Lignin Signatures in Tropical Peat Core (Rawa Danau, Indonesia): An Approach to Reconstruct Past Vegetation and Climate Changes.” *Tropics* 16(2):131–40.

Tessier, A., P. G. C. Campbell, and M. Bisson. 1979a. “Sequential Extraction Procedure for the Speciation of Particulate Trace Metals.” *Analytical Chemistry* 51(7):844–51.

Tessier, A., P. G. C. Campbell, and M. Bisson. 1979b. “Sequential Extraction Procedure for the Speciation of Particulate Trace Metals.” *Analytical Chemistry* 51(7):844–51.

Tessier and Campbell. 1987. “Partitioning of Trace Metals in Sediments: Relationships with Bioavailability.” in *Ecological Effects of In Situ Sediment Contaminants*.

Thevenot, Mathieu, Marie France Dignac, and Cornelia Rumpel. 2010. “Fate of Lignins in Soils: A Review.” *Soil Biology and Biochemistry* 42(8):1200–1211.

Turekian, Karl K. and Karl H. Wedepohl. 1961. “Distribution of the Elements in

Some Major Units of the Earth's Crust." *Geological Society of America Bulletin* 72(February):175–92.

Urban, Roberta Cerasi et al. 2012. "Use of Levoglucosan, Potassium, and Water-Soluble Organic Carbon to Characterize the Origins of Biomass-Burning Aerosols." *Atmospheric Environment* 61:562–69.

Verburg, Piet. 2007. "The Need to Correct for the Suess Effect in the Application of Δ13C in Sediment of Autotrophic Lake Tanganyika, as a Productivity Proxy in the Anthropocene." *Journal of Paleolimnology* 37(4):591–602.

Vermillion, B., R. Brugam, W. Retzlaff, and I. Bala. 2005. "The Sedimentary Record of Environmental Lead Contamination at St. Louis, Missouri (USA) Area Smelters." *Journal of Paleolimnology* 33(2):189–203.

Verschuren, Dirk. 1999. "Sedimentation Controls on the Preservation and Time Resolution of Climate-Proxy Records from Shallow Fluctuating Lakes." *Quaternary Science Reviews* 18(6):821–37.

Waples, James T. and J. Val Klump. 2002. "Biophysical Effects of a Decadal Shift in Summer Wind Direction over the Laurentian Great Lakes." *Geophysical Research Letters* 29(8):43-1-43–44.

Ward, Nicholas D. et al. 2013. "Degradation of Terrestrially Derived Macromolecules in the Amazon River." *Nature Geoscience* 6(7):530–33.

Weiss, Dominik, William Shotyk, Peter G. Appleby, Jan D. Kramers, and Andriy K. Cheburkin. 1999. "Atmospheric Pb Deposition since the Industrial Revolution Recorded by Five Swiss Peat Profiles: Enrichment Factors, Fluxes, Isotopic Composition, and Sources." *Environmental Science and Technology* 33(9):1340–52.

Weiss, Dominik, William Shotyk, and Oliver Kempf. 1999. "Archives of Atmospheric Lead Pollution." *Naturwissenschaften* 86(6):262–75.

Wright, H. E., D. H. Mann, and P. H. Glaser. 1984. "Piston Corers for Peat and Lake Sediments." *Ecology* 65(2):657–59.

Zhao, Yan, Zicheng Yu, Fahu Chen, Emi Ito, and Cheng Zhao. 2007. "Holocene Vegetation and Climate History at Hurleg Lake in the Qaidam Basin, Northwest China." *Review of Palaeobotany and Palynology* 145(3–4):275–88.

Appendix

Table 1. Accelerator Mass Spectrometry radiocarbon dates

Sample Number									Core position	Sediment depth (cm)	14C age (BP)	Calibrated Median Age	2 sigma low	2 sigma high
194225	85.5 cm wood	0.73579321	0.00142105	-264.206788	1.42104943	2465	20	1	85.5	210.5	2465	2595	2384	2711
194226	NS225;Lily Lake B16 D1 115.5 cm .22mgC	0.6928345	0.00131537	-307.165502	1.31536805	2950	20	1	115.5	240.5	2950	3112	3026	3174
194227	NS226;Lily Lake B16 D2 1.5 cm	0.69572219	0.00114776	-304.27781	1.14776063	2915	15	2	1.5	256.5	2915	3050	2985	3143
194229	NS228;Lily Lake B16 D2 122 cm .1mgC	0.59598878	0.00185372	-404.011216	1.85371643	4155	25	2	122	377	4155	4701	4583	4825
194230	NS229;Lily Lake B16 D2 130.5-132.5 cm .081mgC	0.58672464	0.00309798	-413.275361	3.09798485	4285	45	2	131.5	386.5	4285	4855	4659	4972
194311	NS230;Lily Lake B16 D3 7.5-9.5 cm .16mgC	0.58549344	0.00159121	-414.506556	1.5912075	4300	25	3	8.5	393.5	4300	4856	4830	4957
194312	NS231;Lily Lake B16 D3 15.5 cm	0.57253019	0.00125027	-427.469808	1.25026625	4480	20	3	15.5	400.5	4480	5188	5039	5286
194313	NS232;Lily Lake B16 D3 61.5 cm	0.54433964	0.00113871	-455.660359	1.13870919	4885	20	3	61.5	446.5	4885	5615	5592	5647
194314	NS233;Lily Lake B16 D3 115.5-117.5 cm .12mgC	0.50412798	0.00193885	-495.87202	1.93884502	5500	35	3	116.5	501.5	5500	6299	6214	6397
194315	NS234;Lily Lake B16 D3 136.5-138.5 cm .094mgC	0.48761898	0.00303444	-512.381018	3.03443696	5770	50	3	137.5	522.5	5770	6571	6443	6674
194316	NS235;Lily Lake B16 D4 61.5-63.5 cm .10mgC	0.43868836	0.00171646	-561.311642	1.71646266	6620	35	4	62.5	577.5	6620	7511	7441	7570
194317	NS236;Lily Lake B16 D4 76.5-78.5 cm	0.43936196	0.00088954	-560.638042	0.88954235	6605	20	4	77.5	592.5	6605	7497	7439	7563
194318	NS237;Lily Lake B16 D5 10.5 cm	0.3642218	0.00090471	-635.778201	0.90471297	8115	20	5	10.5	665.5	8115	9030	9003	9112
194319	NS238;Lily Lake B16 D5 28.5 cm .18mgC	0.35294956	0.00135921	-647.050438	1.35921011	8365	35	5	28.5	683.5	8365	9402	9298	9471

Table 2. Trace metal concentrations in parts per million (ppm) and corresponding age model outputs for core subsamples.

Sample Name	Drive	Depth in drive (cm)	Sediment Depth (m)	2σ low	Median	2σ high	Pb	K	Mg	Ti	Fe	Cu	Mn
LL-M227	S1	1	0.005	-64	-52	84	12.83	460.1	551.3	61.49	1712	15.373	21.89
LL-M228	S2	2	0.015	-62	-39	138	15.51	426.2	490.7	68.23	1752	16.917	22.85
LL-M229	S4	4	0.035	-58	-13.5	208.02	10.52	70.52	338.9	52.39	1100	11.041	16.32
LL-M230	S6	6	0.055	-55	10	260	14.54	417.8	546.5	67.43	1402	15.867	25.65
LL-M231	S8	8	0.075	-51	32	306.02	12.88	112.2	492.7	63.41	1107	13.268	21.37
LL-M232	S10	10	0.095	-48	53	348	15.65	96.17	531.1	68.42	1196	14.497	24.31
LL-M233	S12	12	0.115	-44	75	392	15.02	319.7	511.7	65.32	1165	15.313	24.2
LL-M234	S14	14	0.135	-40	96	430	15.29	79.04	531.2	70.4	1214	17.103	24.23
LL-M235	S16	16	0.155	-35	116	470	17.16	65.32	515.3	70.19	1185	18.338	23.45
LL-M236	S18	18	0.175	-30	136	502.02	17.12	50.83	523.1	71.55	1169	19.146	22.99
LL-M237	S20	20	0.195	-24.02	155	537.02	16.53	68.5	510.8	70.05	1118	18.46	22.02
LL-M238	S22	22	0.215	-19	176	566	13.67	40.97	452.8	61.42	945.9	14.749	18.6
LL-M239	S24	24	0.235	-13	195.5	600	12.3	13.74	394.9	56.96	794.6	13.116	16.04
LL-M240	S26	26	0.255	-8	215	632	14.01	35.34	449.8	56.62	879.4	15.501	18.31
LL-M241	S28	28	0.275	-2	235	659.02	12.76	35.69	387.6	54.48	819.1	14.187	15.39
LL-M242	S30	30	0.295	5	256	686	17.47	48.74	542.6	75.41	1154	19.129	23.59
LL-M243	S32	32	0.315	13	275	711.02	18.44	62.65	567.9	77.53	1253	19.697	24.34
LL-M244	S34	34	0.335	20	295	732.02	17.97	28.35	528.3	76.42	1208	19.294	23.45
LL-M245	S36	36	0.355	29	316	759.02	17.74	65.4	576.4	71.13	1165	19.744	24.89
LL-M246	S38	38	0.375	38	334	795	21.77	61.83	692.5	90.03	1415	23.101	28.64
LL-M247	S40	40	0.395	48.98	356	815.02	18.77	33.15	607	78.44	1233	20.124	25.21
LL-M248	S42	42	0.415	58	376	842	16.88	17.72	514	68.9	1163	18.774	22.97
LL-M249	S44	44	0.435	68	398	865.02	20.14	13.94	590.4	81.24	1487	22.069	26
LL-M250	S46	46	0.455	77	419	892.02	19.2	0	566.8	81.6	1412	21.159	24.87
LL-M251	S48	48	0.475	88	438	919	19.42	0	564	78.13	1378	21.913	24.87
LL-M252	S50	50	0.495	100	458.5	948	21.87	6.42	650.8	88.55	1558	24.882	29.44
LL-M253	S52	52	0.515	112	479	972.02	18.46	16.05	553.7	77.03	1308	21.305	24.31
LL-M254	S54	54	0.535	126	497	995.02	18.16	3.434	562.3	75.55	1236	20.176	23.61
LL-M255	S56	56	0.555	139	517	1015	18.52	1.468	572.9	78.27	1299	21.178	23.22
LL-M256	S58	58	0.575	152	537	1037	16.48	0	571.4	79.33	1284	22.005	23.42
LL-M257	S60	60	0.595	165	556	1055	15.29	0	559.3	79.69	1312	20.888	21.83
LL-M258	S62	62	0.615	179	575	1080	7.526	0	568.1	77.69	1020	21.948	22.58
LL-M259	S64	64	0.635	191	597	1099	5.776	0	556	63.16	1047	19.487	22.67
LL-M260	S66	66	0.655	205	617	1119	6.197	0	565.5	62.36	1042	19.521	24.25
LL-M261	S67	67	0.665	210	626	1129	6.749	0	540.7	55.99	1089	18.905	20.9
LL-M262	S68	69	0.68	224	646	1153	6.066	0	494.6	68.13	965.9	18.338	18.29
LL-M263	S69	70	0.695	232	656	1168	7.164	0	560.7	54.9	1145	19.157	21.65
LL-M264	S71	72	0.715	248	677	1188	7.412	0	573.4	75.52	1161	21.35	19.95
LL-M265	S73	74	0.735	264	696	1215	7.259	0	571	76.94	1161	21.292	19.74
LL-M266	S75	76	0.755	282	716	1235	6.915	0	571.5	74.43	1138	21.081	19.5
LL-M267	S77	78	0.775	296	737	1255	6.783	0	594.2	74.14	1167	21.296	19.46
LL-M268	S79	80	0.795	310	757.5	1273	3.605	0	618.2	69.1	1133	21.664	20.83
LL-M269	S81	82	0.815	325	776.5	1288	2.455	0	588.1	93.58	1002	26.591	19.53
LL-M270	S83	84	0.835	342	796	1305	1.771	0	612.3	73.85	1089	25.474	19.4
LL-M271	S85	86	0.855	355	816	1329	2.044	0	587.9	66.81	1060	24.585	19.33
LL-M272	S87	88	0.875	372	836	1352	1.851	0	615.3	75.58	1110	27.277	19.77
LL-M273	S89	90	0.895	385	855	1374	2.017	0	605.4	71.72	1066	25.428	18.49
LL-M274	S91	92	0.915	401	876	1393	1.191	0	424	72.83	738.7	19.767	12.8
LL-M275	S93	94	0.935	419	896	1409	1.803	0	620.9	89.08	1107	31.908	19.27
LL-M276	S95	96	0.955	438	918	1427	1.743	0	611	84.64	986.6	28.046	17.93

Sample Name	Drive	Depth in drive (cm)	Sediment Depth (m)	2σ low	Median	2σ high	Pb	K	Mg	Ti	Fe	Cu	Mn
LL-M277	S97	98	0.975	456	939	1446	1.541	0	593.2	90.04	1139	27.596	17.8
LL-M278	S99	100	0.995	474	959	1465	1.505	0	609.5	93.81	1230	27.771	18.6
LL-M279	S101	102	1.015	485	978	1485	1.165	0	506	79.55	990.5	23.506	15.09
LL-M280	S103	104	1.035	504	999	1506	1.216	0	625.9	113.9	1339	28.318	18.01
LL-M281	S105	106	1.055	530	1019	1526	1.138	0	618.2	95.54	1264	26.834	17.98
LL-M282	S107	108	1.075	549	1038	1545	1.144	0	618.8	92.08	1297	30.742	17.92
LL-M283	S109	110	1.095	569	1057	1563	1.023	0	592.5	110.2	1454	33.422	17.87
LL-M284	S111	112	1.115	586	1077	1580	1.014	0	599.5	92.73	1259	29.802	17.68
LL-M285	S113	114	1.135	601	1097	1595	0.82	0	497.9	89	1071	30.755	14.5
LL-M286	S115	116	1.155	621	1116	1612	0.916	0	664.2	91.64	1358	33.551	18.96
LL-M287	S117	118	1.175	637	1137	1624	0.877	0	658.8	93.13	1392	36.359	18.92
LL-M288	S119	120	1.195	662	1159	1640	0.764	0	630.8	92.49	1243	35.195	17.93
LL-M289	S121	122	1.215	684	1179.5	1650	0.779	0	650.3	87.51	1325	29.36	18.7
LL-M290	S123	124	1.235	704	1201	1668	0.763	0	676.4	99.57	1310	29.708	18.51
LL-M291	S125	126	1.255	720	1222	1682	0.77	0	712.2	89.38	1367	29.826	18.02
LL-M292	S127	128	1.275	738.9	1242	1696	0.825	0	698	94.77	1483	31.947	18.5
LL-M293	S129	130	1.295	757	1262	1710	0.854	0	688.1	100.9	1407	34.508	17.95
LL-M294	S131	132	1.315	780	1282	1724.1	0.937	0	705	117.4	1483	37.701	18.53
LL-M295	S133	134	1.335	795	1302	1743	0.889	0	729.7	112.3	1595	31.619	20.16
LL-M296	S135	136	1.355	816	1322	1755	0.975	0	714.9	100.4	1558	33.425	18.8
LL-M297	S137	138	1.375	835	1342	1773	0.992	0	718.5	92.09	1548	31.525	18.52
LL-M5	D1	14	1.39	850	1351	1781	0.301	88.02	808.8	92.18	1398	34.197	18.5
LL-M6	D1	17	1.42	882	1384	1801	0.566	60.96	816.5	91.99	1453	33.911	17.15
LL-M7	D1	20	1.45	909	1415	1819	0.632	78.61	818.9	114.6	1821	36.554	15.2
LL-M8	D1	23	1.48	940	1444	1839	0.766	73.24	871.1	103.8	1554	32.901	21.14
LL-M9	D1	26	1.51	976	1476	1859	0.528	67.51	896.3	101.5	1418	31.598	18.66
LL-M10	D1	29	1.54	1012	1506	1884	0.641	73.46	872.7	111	1966	32.976	18.95
LL-M11	D1	32	1.57	1045	1533	1905	0.431	78.78	920	83.01	1269	29.452	18.35
LL-M12	D1	35	1.6	1082	1564	1922	0.383	60.15	886.2	92.38	1418	27.875	18.74
LL-M13	D1	38	1.63	1116	1594	1938	0.216	0	730.6	65.06	1031	22.52	15.51
LL-M14	D1	41	1.66	1158	1624	1952	0.644	81.86	916.5	96.79	2121	32.076	20.34
LL-M15	D1	44	1.69	1192	1655	1967	0.511	66.8	906.5	84.82	1675	29.476	21.42
LL-M16	D1	47	1.72	1227	1685	1981	0.561	66.69	922.6	76.69	1684	422.38	21.62
LL-M17	D1	50	1.75	1267	1712	1994	0.266	80.07	904.9	76.78	1629	28.958	22.49
LL-M18	D1	53	1.78	1300	1742	2008	0.377	72.92	928	92.8	1795	29.057	20.94
LL-M19	D1	56	1.81	1343	1770	2023	0.545	69.94	917.4	77.66	1608	28.52	22.53
LL-M20	D1	59	1.84	1383	1799	2035	0.618	91.7	949	87.97	1386	30.495	22.18
LL-M21	D1	62	1.87	1426	1828	2046	0.547	44.31	920.5	86.34	1327	32.762	20.7
LL-M22	D1	65	1.9	1471	1859	2054	0.517	81.06	943.7	95.58	1772	34.662	20.33
LL-M23	D1	68	1.93	1521	1889	2063	0.777	76.73	924.5	77.2	1263	32.358	19.68
LL-M24	D1	71	1.96	1575	1920	2073	0.518	59.13	863.7	86.37	1200	35.535	19.36
LL-M25	D1	74	1.99	1631	1951	2082	0.911	72.06	998.5	106.5	1807	39.066	20.64
LL-M26	D1	77	2.02	1692	1981	2090	0.864	80.1	1028	111.3	2284	37.949	24.31
LL-M27	D1	80	2.05	1774	2012	2099	0.495	69.06	1052	105.8	2344	35.162	25.66
LL-M28	D1	83	2.08	1860	2046	2109	0.477	98.94	1149	79.89	1696	30.91	26.55
LL-M29	D1	86	2.11	2037	2114	2329	0.6	82.89	1020	87.67	1466	31.985	22
LL-M30	D1	89	2.14	2089	2212	2630	0.733	78.18	1081	122.8	1875	35.914	24.68
LL-M31	D1	92	2.17	2119	2308	2751	0.706	73.04	978.8	87.94	1361	28.619	27.77
LL-M32	D1	95	2.2	2147	2399	2839	1.105	77.56	1105	131.7	1997	38.993	26.14
LL-M33	D1	98	2.23	2178	2489	2895	0.799	88.09	1101	113	1786	37.628	25.56

Sample Name	Drive	Depth in drive (cm)	Sediment Depth (m)	2σ low	Median	2σ high	Pb	K	Mg	Ti	Fe	Cu	Mn
LL-M34	D1	101	2.26	2217	2577	2939	0.805	84.84	1089	119.5	1644	40.878	25.07
LL-M35	D1	104	2.29	2268	2667	2974	0.745	61.26	1033	84.58	1289	36.118	24.28
LL-M37	D1	110	2.35	2412	2850	3039	0.792	83.57	1090	123	2670	41.784	23.68
LL-M38	D1	113	2.38	2529	2950	3069	0.94	76.57	1090	98.21	1818	35.163	23.59
LL-M39	D1	116	2.41	2781	3066	3119	1.049	76.93	1094	110.7	1934	37.265	26.24
LL-M40	D1	119	2.44	2829	3077	3139	0.776	56.98	1086	104.6	1645	37.527	26.18
LL-M41	D1	122	2.47	2873	3085	3156	0.86	73.22	1133	107.6	2056	37.478	30.69
LL-M42	D1	125	2.5	2917	3093	3174	0.912	68.93	1284	112.3	1944	44.164	28.07
LL-M43	D1	128	2.53	2965	3103	3199	1.041	83.06	1645	122	1767	42.949	29.54
LL-M44	D1	131	2.56	3009	3119	3230	1.064	74.02	1640	127.4	3062	41.686	26.49
LL-M45	D1	134	2.59	3054	3161	3422	0.863	59.28	1173	139.1	2982	42.936	25.76
LL-M48	D2	5	2.6	3062	3175	3461	0.793	57.1	988	110.4	1604	40.196	20.25
LL-M49	D2	8	2.63	3080	3215	3550	0.831	53.01	1041	104.1	1549	40.6	19.21
LL-M50	D2	11	2.66	3097	3253	3618	0.774	52.99	1072	102.2	1607	41.34	19.26
LL-M51	D2	14	2.69	3113	3291	3681	0.794	55.26	1075	105.7	1601	40.92	20.35
LL-M52	D2	17	2.72	3129	3329	3749	0.689	62.55	1139	104.6	1510	39.438	24.78
LL-M53	D2	20	2.75	3144	3368	3800	0.776	60.57	1116	94.17	2506	39.495	23.48
LL-M54	D2	23	2.78	3158	3405	3856	0.785	63.4	1169	28.38	1661	37.136	21.39
LL-M55	D2	26	2.81	3173	3443	3899	1.059	68.57	1190	100.9	1673	41.528	22.22
LL-M56	D2	29	2.84	3189	3480	3952	0.795	69.26	1164	84.56	1700	37.01	20.86
LL-M57	D2	32	2.87	3208	3518	3998	0.813	78.69	1194	87.09	1980	34.702	24.53
LL-M58	D2	35	2.9	3226	3556	4036	0.842	89.04	1210	86.14	1936	34.987	25.26
LL-M59	D2	38	2.93	3244	3595	4086	1.118	81.67	1188	88.66	2197	33.236	25.42
LL-M60	D2	41	2.96	3268	3633	4119	0.99	90.73	1232	89.18	2036	35.364	29.08
LL-M61	D2	44	2.99	3288	3672	4162	0.979	81.97	1224	87.66	1878	37.91	24.42
LL-M62	D2	47	3.02	3311	3711	4200	1.059	101.8	1307	96.26	1910	37.389	26.45
LL-M63	D2	50	3.05	3336	3747.5	4242	1.138	98.32	1299	107.6	1982	38.033	29.08
LL-M64	D2	53	3.08	3359	3784	4274	0.512	52.07	1323	118	2868	44.704	28.11
LL-M65	D2	56	3.11	3383	3822	4302	0.644	62	1206	107.3	1654	48.68	24.94
LL-M66	D2	59	3.14	3412	3862	4332	0.801	60.31	1277	79.06	1536	40.189	28.43
LL-M67	D2	62	3.17	3445	3900	4360	0.624	72.46	1295	114.6	2007	40.209	31.06
LL-M68	D2	65	3.2	3476	3937	4388	0.634	51.56	1246	88.99	1596	37.933	30.81
LL-M69	D2	68	3.23	3510	3977	4418.1	0.521	77.72	1295	116.6	1912	45.153	27.51
LL-M70	D2	71	3.26	3544	4016	4448	0.664	52.01	1209	81.24	1570	40.225	27.2
LL-M71	D2	74	3.29	3577	4050	4474	0.478	50.44	1522	74.84	1692	39.981	29.99
LL-M72	D2	77	3.32	3613	4088	4499	0.707	68.53	1339	104.7	1711	45.526	30.55
LL-M73	D2	80	3.35	3650	4127	4520	0.668	43.16	1418	69.67	1582	39.092	31.74
LL-M74	D2	83	3.38	3686	4164	4539	0.736	64.66	1782	71.89	1663	41.772	28.59
LL-M75	D2	86	3.41	3727	4201	4560	0.626	40.29	1752	92.91	1728	43.566	26.28
LL-M76	D2	89	3.44	3766	4240	4579	0.453	44.05	1175	67.6	1610	37.971	28.9
LL-M77	D2	92	3.47	3811	4279	4595	0.44	31.65	1200	57.67	1440	38.987	17.44
LL-M78	D2	95	3.5	3858	4316	4619	0.485	52.3	1267	69.09	1636	37.184	30.76
LL-M79	D2	98	3.53	3907	4353	4635	0.493	51.37	1265	64.71	1704	36.358	28.5
LL-M80	D2	101	3.56	3958	4391	4650	0.508	52.5	1793	52.5	1938	41.016	27.57
LL-M81	D2	104	3.59	4015	4428	4668	0.515	28.17	1745	58	1898	41.809	28.07
LL-M82	D2	107	3.62	4073	4466	4683	0.5	58.36	1713	60.44	1580	37.473	27.01
LL-M83	D2	110	3.65	4138	4503	4702	0.518	58.32	1750	69.64	1502	39.344	26.03
LL-M84	D2	113	3.68	4205	4540	4724	0.479	48.85	1782	81.89	1540	37.222	25.87
LL-M85	D2	116	3.71	4279	4577	4744	0.469	38.03	1673	75.83	1332	35.707	27.36
LL-M86	D2	119	3.74	4377	4616	4768	0.534	54.7	1809	86.25	1422	40.307	30.42

Sample Name	Drive	Depth in drive (cm)	Sediment Depth (m)	2σ low	Median	2σ high	Pb	K	Mg	Ti	Fe	Cu	Mn
LL-M87	D2	122	3.77	4586	4674	4805	0.633	29.41	1841	89.37	1395	40.217	31.92
LL-M88	D2	125	3.8	4630	4721	4825	0.8	70.82	1886	86.74	1416	41.526	29.25
LL-M89	D2	128	3.83	4657	4768	4844	0.679	48.59	1906	106	1667	42.307	28.94
LL-M90	D2	131	3.86	4696	4822	4877	0.702	53.49	1836	90.66	1730	37.935	27.92
LL-M91	D2	134	3.89	4748	4846	4920	0.757	58.26	1805	74.16	1676	36.661	30
LL-M92	D2	137	3.92	4794	4858	4945	0.493	46.88	1752	57.98	1550	34.461	29.4
LL-M97	D3	8	3.93	4822	4866	4964	0.44	40.49	1575	32.79	1759	31.574	17.88
LL-M98	D3	11	3.96	4886	4973	5108	0.499	39.57	1614	55.95	1489	31.716	18.11
LL-M99	D3	14	3.99	4937	5053	5198	0.534	42.47	1735	56.52	1391	34.351	27.07
LL-M100	D3	17	4.02	5036	5144	5317	0.559	38.74	1914	75.55	2422	40.662	25.6
LL-M101	D3	20	4.05	5063	5193	5381	0.624	57.91	1839	76.67	2272	41.6	25.45
LL-M102	D3	23	4.08	5078	5226	5429	0.12	10.43	672.4	41.43	1447	21.396	10.94
LL-M103	D3	26	4.11	5091	5257	5464	0.463	38.32	1824	75.03	3429	41.029	21.56
LL-M104	D3	29	4.14	5106	5285	5487	0.317	17.54	1518	67.6	2277	34.255	22.31
LL-M105	D3	32	4.17	5122	5314	5510	0.447	29.89	1496	63.64	2092	35.433	16.67
LL-M106	D3	35	4.2	5143	5342	5532	0.397	31.49	1545	65.47	2008	33.62	20.27
LL-M107	D3	38	4.23	5163	5370	5549	0.674	41.13	1860	78.34	3102	43.869	34.35
LL-M108	D3	41	4.26	5187	5401	5564	0.7	37.63	1873	83.98	3059	49.401	23.75
LL-M109	D3	44	4.29	5212	5431	5577	0.504	46.83	1775	66	3354	43.616	20.02
LL-M110	D3	47	4.32	5242	5461	5589	0.68	38.46	1871	73.37	3314	50.228	25.31
LL-M111	D3	50	4.35	5275	5491	5600	0.507	47.08	1801	63.54	3191	46.626	23.45
LL-M112	D3	53	4.38	5316	5521	5611	0.545	47.75	1761	61.27	2135	54.51	24.42
LL-M113	D3	56	4.41	5364	5551	5620	0.722	53.27	1831	63.12	3116	45.969	22.77
LL-M114	D3	59	4.44	5431	5582	5631	1.057	62.52	1935	66.98	2162	55.818	27.2
LL-M115	D3	62	4.47	5598	5631	5733	0.798	54.35	1880	68.82	1705	48.655	25.82
LL-M116	D3	65	4.5	5612	5671	5878	0.591	38.84	1889	61.51	1511	39.373	26.68
LL-M117	D3	68	4.53	5623	5707	5947	0.344	0	922.9	35.64	1076	21.303	10.07
LL-M118	D3	71	4.56	5633	5744	6008	1.939	85.67	1932	91.79	2218	41.69	25.32
LL-M119	D3	74	4.59	5644	5780	6056	2.14	98.32	2013	99.59	2123	41.829	26.19
LL-M120	D3	77	4.62	5656	5816	6096	1.163	58.15	2049	91.77	3285	46.34	26.8
LL-M121	D3	80	4.65	5669	5851	6129	1.235	59.15	1889	77.8	3267	44.458	25.8
LL-M122	D3	83	4.68	5683	5885	6157	1.745	65.82	1971	84.19	2843	40.949	25.76
LL-M123	D3	86	4.71	5700	5921	6182	2.459	112.8	1950	87.14	2423	46.825	24.59
LL-M124	D3	89	4.74	5720	5958	6207	3.682	126.1	2039	90.48	2455	40.417	25.88
LL-M125	D3	92	4.77	5740	5993	6227	6.449	478.7	2398	93.77	2781	40.75	25.8
LL-M126	D3	95	4.8	5765	6028	6246	4.044	243.7	2047	87.61	2430	46.822	23.27
LL-M127	D3	98	4.83	5791	6064	6263	1.401	36.26	1906	77.56	2296	53.629	27.35
LL-M128	D3	101	4.86	5826	6100	6280	0.908	45.6	1956	70.8	5636	56.357	18.96
LL-M129	D3	104	4.89	5861	6134	6296	1.038	47.05	1939	68.16	2872	58.486	21.86
LL-M130	D3	107	4.92	5903	6170	6315	0.894	44.24	1955	77.86	3698	60.606	22.47
LL-M131	D3	110	4.95	5958	6206	6334	0.829	32.09	1918	80.12	6272	60.435	20.15
LL-M132	D3	113	4.98	6032	6244	6356	0.858	44.82	1816	64.2	5014	66.097	22.87
LL-M133	D3	116	5.01	6168	6290	6384	0.82	32.99	1866	63.48	2613	70.389	24.18
LL-M134	D3	119	5.04	6252	6339	6481	1.079	34.28	1906	64.09	2075	66.199	25.72
LL-M135	D3	122	5.07	6285	6380	6525	1.009	34.41	2037	66.08	2135	67.253	24.91
LL-M136	D3	125	5.1	6310	6417	6557	1.027	43.96	2001	60.39	2905	66.144	24.03
LL-M137	D3	128	5.13	6331	6451	6585	0.92	39.85	1971	63.03	2340	82.226	22.49
LL-M138	D3	131	5.16	6353	6485	6609	0.975	37.31	1971	69.35	2168	77.443	26.33
LL-M139	D3	134	5.19	6384	6521	6634	0.966	30.57	2058	65.63	2865	72.147	23.03
LL-M140	D3	137	5.22	6444	6571	6685	1.025	28.35	2113	69	1991	68.209	24.68

Sample Name	Drive	Depth in drive (cm)	Sediment Depth (m)	2σ low	Median	2σ high	Pb	K	Mg	Ti	Fe	Cu	Mn
LL-M141	D3	140	5.25	6509	6644	6890	1.08	28.27	2005	76.23	3450	75.041	21.28
LL-M148	D4	11	5.26	6518	6661	6936	1.161	21.53	2137	73.88	2649	58.048	28.87
LL-M149	D4	14	5.29	6543	6707	7036	1.087	27.6	2055	72.22	2266	60.601	24.16
LL-M150	D4	17	5.32	6563	6755	7099	1.282	10.06	2083	77.22	2359	69.589	24.07
LL-M151	D4	20	5.35	6586	6802	7151	2.27	39.35	2250	104.1	2874	58.475	24.83
LL-M152	D4	23	5.38	6606	6846	7195	3.266	106.3	2405	111.7	3105	61.02	26.88
LL-M153	D4	26	5.41	6628	6892	7242	1.655	45.75	2174	87.14	2971	63.965	27.39
LL-M154	D4	29	5.44	6652	6938	7281	2.38	73.11	2134	88.93	2981	66.081	26.29
LL-M155	D4	32	5.47	6677	6984	7316	1.067	30.63	2355	69.07	2870	71.31	27.58
LL-M156	D4	35	5.5	6706	7032	7346	1.178	45.81	2624	70.78	3215	81.399	28.67
LL-M157	D4	38	5.53	6734	7078	7370	1.399	48.53	2532	129.9	3406	100.13	27.72
LL-M158	D4	41	5.56	6772	7122	7388	1.167	44.68	2519	91.84	5502	105.49	27.34
LL-M159	D4	44	5.59	6813	7167	7409	1.172	28.23	2344	68.9	3851	102.39	25.41
LL-M160	D4	47	5.62	6858	7214	7427	1.144	42.94	2324	73.03	3624	95.531	20.12
LL-M161	D4	50	5.65	6910	7258	7441	1.01	52.12	2327	73.05	4186	98.906	19.12
LL-M162	D4	53	5.68	6966	7304	7455	1.163	21.6	2223	82.48	4713	107.62	20.78
LL-M163	D4	56	5.71	7036	7353	7471	1.384	43.32	2495	90.12	4745	99.696	26.21
LL-M164	D4	59	5.74	7132	7402	7488	1.465	41.62	2414	96.56	4620	103.22	25.68
LL-M165	D4	62	5.77	7299	7457	7514	1.725	40.65	2477	110	5969	99.166	28.57
LL-M166	D4	65	5.8	7442	7484	7534	1.456	39.24	2425	113.4	5085	112.56	27.9
LL-M167	D4	68	5.83	7449	7497	7541	1.885	46.25	2413	126.4	4895	111	25.78
LL-M168	D4	71	5.86	7456	7510	7546	2.333	68.28	2439	129.3	5310	88.001	23.14
LL-M169	D4	74	5.89	7466	7525	7551	1.452	50.64	2566	147.7	3849	93.263	26.04
LL-M170	D4	77	5.92	7480	7543	7593	1.468	49.7	2572	74.54	3548	99.851	25.35
LL-M171	D4	80	5.95	7512	7600	7933	1.284	42.6	2726	82.21	3995	101.44	28.89
LL-M172	D4	83	5.98	7533	7666	8088	1.372	42.41	2607	83.81	3661	102.23	27.08
LL-M173	D4	86	6.01	7554	7730	8216	1.199	36.08	2529	61.84	3133	98.261	21.2
LL-M174	D4	89	6.04	7572	7792	8298.1	1.978	59.4	2855	115	6371	125.98	29.08
LL-M175	D4	92	6.07	7589	7854	8385	1.956	67.16	2999	134.7	6321	128.79	35.56
LL-M176	D4	95	6.1	7610	7913	8453	2.114	61.01	2969	128.5	8078	139.21	33.56
LL-M177	D4	98	6.13	7631	7971	8513	2.374	68.74	3070	154.3	8813	137.89	35.59
LL-M178	D4	101	6.16	7653	8030	8572	2.476	74.54	3180	136.2	12056	140.35	36.67
LL-M179	D4	104	6.19	7680	8088	8632	2.585	66.75	3155	169.1	8499	128.15	34.53
LL-M180	D4	107	6.22	7709	8148	8677	2.645	73.53	2895	140.8	5932	145.39	32.09
LL-M181	D4	110	6.25	7742	8207	8726	2.488	92.06	3172	166.1	4925	145.96	36.62
LL-M182	D4	113	6.28	7779	8266	8773	1.544	47.2	2308	128.5	5961	92.337	27.53
LL-M183	D4	116	6.31	7820	8327	8809	2.252	53.42	3077	177.8	9403	177.37	36.5
LL-M184	D4	119	6.34	7865	8385	8844	2.03	75.94	3150	169.6	7819	200.14	36.68
LL-M185	D4	122	6.37	7908	8446	8875	1.945	59.81	2909	139.9	7763	174.9	34.13
LL-M186	D4	125	6.4	7959	8504.5	8900	2.012	61.42	3265	155.8	7873	175.19	37.18
LL-M187	D4	128	6.43	8026	8565	8926	1.936	43.04	3267	162.7	8089	198.59	39.22
LL-M188	D4	131	6.46	8087	8622	8949	2.065	67.38	3281	177	7775	193.77	37.92
LL-M189	D4	134	6.49	8147	8682	8969	1.975	48.14	3410	185.3	7693	205.59	40.67
LL-M190	D4	137	6.52	8226	8742	8986	2.001	37.6	3381	205.4	8464	192.2	37.78
LL-M191	D4	140	6.55	8307	8802	9005	2.376	55.2	3660	238.8	10257	178.12	47.76
LL-M192	D4	143	6.58	8405	8862.5	9024	2.2	47.28	3727	238.4	10058	167.49	47.28
LL-M194	D5	2	6.57	8369	8843	9018	2.218	44.82	3545	217.4	9815	177.47	44.5
LL-M195	D5	5	6.6	8484	8903	9037	2.332	46.11	3707	223.1	10628	178.3	48.75
LL-M196	D5	8	6.63	8636	8969	9058	2.003	39.5	3628	227.9	12059	197.75	39.09
LL-M197	D5	11	6.66	9015	9039	9161	2.448	51.44	3441	208.4	9977	206.19	38.76

Sample Name	Drive	Depth in drive (cm)	Sediment Depth (m)	2σ low	Median	2σ high	Pb	K	Mg	Ti	Fe	Cu	Mn
LL-M198	D5	14	6.69	9035	9105	9285	3.48	108.5	3636	213	9987	214.18	45.25
LL-M199	D5	17	6.72	9053	9161	9331	3.239	92.08	3558	210.5	9668	195.46	42.69
LL-M200	D5	20	6.75	9075	9214	9365	3.037	56.2	3617	224.8	8920	204.72	43.98
LL-M201	D5	23	6.78	9107	9264	9394	4.24	91.99	3754	220.4	11673	172.3	47.63
LL-M202	D5	26	6.81	9153	9312	9423	6.403	440.9	3637	190.1	10363	146.16	44.43
LL-M203	D5	29	6.84	9305	9398	9528	4.422	138.5	3615	219.7	13515	162.37	52.06
LL-M204	D5	32	6.87	9326	9447	9690	2.466	51.52	3621	246.1	14054	228.57	56.52
LL-M205	D5	35	6.9	9339	9482	9790	2.309	57.16	3735	269.9	13958	215.36	57.16
LL-M206	D5	38	6.93	9349	9516	9863	2.279	46.78	3536	262.2	12610	190.82	57.58
LL-M207	D5	41	6.96	9360	9551	9942	2.14	41.92	3482	263.2	12332	191.73	55.78
LL-M208	D5	44	6.99	9370	9586	10010	2.306	73.63	3650	262.2	12155	165.97	60.39
LL-M209	D5	47	7.02	9381	9622	10069	2.415	58.12	3647	291.9	14509	163.17	67.16
LL-M210	D5	50	7.05	9394	9656	10133	2.288	45.76	3608	287.8	14917	180.41	65.56
LL-M211	D5	53	7.08	9406	9691	10194	2.338	51.48	3731	271.6	11665	171.91	60.92
LL-M212	D5	56	7.11	9420	9727	10258	2.435	56.87	3923	281.3	10841	154.18	63.98
LL-M213	D5	59	7.14	9433	9762	10314	2.436	99.81	4195	302.9	11124	155.21	70.35
LL-M214	D5	62	7.17	9449	9795	10372	2.561	370.4	4368	313	12075	146.02	75.36
LL-M215	D5	65	7.2	9464	9833	10426	2.559	392.5	4674	317.5	12532	140.63	82.2
LL-M216	D5	68	7.23	9478	9867	10486	2.819	448.3	4887	345.7	13004	151.04	80.37
LL-M217	D5	71	7.26	9489	9902	10539	3.034	481.4	5043	393.5	14251	147.09	82.52
LL-M218	D5	74	7.29	9502	9938	10595	3.163	474.1	4877	451.3	18051	154.07	77.95
LL-M219	D5	77	7.32	9516	9973	10646	2.795	402.9	4311	384.8	19375	184.22	72.14
LL-M220	D5	80	7.35	9528	10006	10693	2.548	83.21	3880	312.8	11594	192.14	53.29
LL-M221	D5	83	7.38	9547	10040	10739	2.723	362.3	4089	341.5	15891	220.25	58.83
LL-M222	D5	86	7.41	9558	10075	10795	2.675	437.2	5530	360.4	16830	171.16	77.24
LL-M223	D5	89	7.44	9573	10111	10847	3.163	554	4188	308.4	9030	140.47	59.76
LL-M224	D5	92	7.47	9584	10146	10896	2.52	583.4	3831	306.9	7312	88.286	60.67
LL-M225	D5	95	7.5	9595	10180	10950	2.252	559.5	3824	242.2	7542	44.263	68.34
LL-M226	D5	98	7.53	9612	10217	11003	2.242	655.8	8041	231.3	7187	36.744	115

Table 3. Bulk organic proxy data

Sample name	Drive	Depth in Drive (cm)	Sediment Depth (m)	2sσ low	Median	2σ high	C (wt%)	C (mol)	N (wt%)	N (mol)	C/N mol ratio	δ13C (VPDB) (‰)
S9	Surface	9	0.085	-50	43	327	34.64	415.68	3.73	52.18	7.97	-20.89
S13	Surface	13	0.125	-42	86	411	34.64	415.71	3.59	50.29	8.27	-20.71
S17	Surface	17	0.165	-33	126	485	34.68	416.16	3.60	50.46	8.25	-20.53
S21	Surface	21	0.205	-21	166	553	34.37	412.47	3.61	50.50	8.17	-20.59
S25	Surface	25	0.245	-11	205	616	34.25	410.94	3.55	49.63	8.28	-20.44
S29	Surface	29	0.285	2	246	673	34.56	414.76	3.63	50.87	8.15	-20.43
S33	Surface	33	0.325	16	285	723	34.45	413.38	3.56	49.84	8.29	-20.19
S37	Surface	37	0.365	34	325	775	34.52	414.26	3.61	50.48	8.21	-20.27
S41	Surface	41	0.405	54	366	829	33.98	407.79	3.42	47.94	8.51	-19.98
S45	Surface	45	0.445	72	408	880	33.88	406.58	3.40	47.56	8.55	-19.63
S49	Surface	49	0.485	94	448	937	33.99	407.84	3.45	48.26	8.45	-19.58
S53	Surface	53	0.525	119	488	984	33.71	404.54	3.39	47.48	8.52	-19.67
S57	Surface	57	0.565	144	528	1023	33.96	407.47	3.41	47.81	8.52	-19.53
S61	Surface	61	0.605	174	567	1067	34.43	413.16	3.47	48.64	8.49	-18.75
S65	Surface	65	0.645	197	607	1111	35.00	419.95	3.49	48.90	8.59	-18.55
S68	Surface	69	0.68	224	646	1153	34.65	415.79	3.46	48.41	8.59	-18.53
S72	Surface	73	0.725	255	686	1200	34.82	417.79	3.48	48.73	8.57	-18.62
S76	Surface	77	0.765	290	726	1246	34.98	419.74	3.47	48.65	8.63	-18.70
S80	Surface	81	0.805	317	767	1281	35.15	421.83	3.50	49.02	8.61	-18.25
S84	Surface	85	0.845	348	806	1317	35.83	429.99	3.48	48.77	8.82	-17.89
S88	Surface	89	0.885	378	845	1364	34.80	417.58	3.47	48.57	8.60	-17.08
S92	Surface	93	0.925	411	885	1401	33.98	407.78	3.35	46.84	8.71	-16.83
S96	Surface	97	0.965	448	929	1435	34.73	416.71	3.39	47.52	8.77	-16.55
S100	Surface	101	1.005	480	968	1477	34.32	411.87	3.43	48.08	8.57	-17.07
S104	Surface	105	1.045	517	1009	1516	34.43	413.21	3.43	48.04	8.60	-17.58
S108	Surface	109	1.085	556	1048	1554	33.57	402.86	3.29	46.00	8.76	-17.35
S112	Surface	113	1.125	594	1087	1587	32.98	395.76	3.15	44.07	8.98	-17.72
S116	Surface	117	1.165	630	1126	1619	33.62	403.43	3.27	45.77	8.81	-17.56
S120	Surface	121	1.205	671	1169	1646	33.67	404.01	3.24	45.35	8.91	-17.42
S124	Surface	125	1.245	710	1212	1675	33.11	397.33	3.17	44.40	8.95	-17.57
S128	Surface	129	1.285	747	1252	1702	32.74	392.84	3.18	44.52	8.82	-16.65
S132	Surface	133	1.325	786	1291	1735	33.75	404.98	3.31	46.33	8.74	-16.05
S136	Surface	137	1.365	826	1331	1764	33.07	396.86	3.27	45.76	8.67	-15.76
C3	D1	13	1.38	835	1342	1773	34.40	412.85	3.46	48.46	8.52	-15.91
C4	D1	19	1.44	900	1404	1812	37.59	451.13	3.59	50.22	8.98	-16.73
C5	D1	25	1.5	962	1465	1852	36.03	432.31	3.59	50.33	8.59	-15.66
C6	D1	31	1.56	1033	1524	1896	35.76	429.12	3.55	49.70	8.64	-15.56
C7	D1	37	1.62	1105	1584	1933	37.61	451.36	3.64	50.90	8.87	-15.82
C8	D1	43	1.68	1180	1644	1962	34.76	417.16	3.48	48.66	8.57	-15.52
C9	D1	49	1.74	1254	1703	1990	35.11	421.37	3.56	49.91	8.44	-16.06
C10	D1	55	1.8	1327	1761	2019	34.54	414.46	3.47	48.64	8.52	-15.71
C11	D1	61	1.86	1413	1818	2043	33.85	406.15	3.45	48.30	8.41	-16.14
C12	D1	67	1.92	1507	1879	2060	36.08	433.01	3.51	49.18	8.81	-16.15
C13	D1	73	1.98	1610	1940	2079	34.02	408.25	3.47	48.52	8.41	-16.39
C14	D1	79	2.04	1746	2002	2096	39.09	469.12	3.79	52.99	8.85	-19.84
C15	D1	85	2.1	1972	2075	2118	38.55	462.54	3.76	52.67	8.78	-17.52
C16	D1	91	2.16	2110	2276	2712	37.31	447.76	3.68	51.55	8.69	-16.64
C17	D1	97	2.22	2167	2458	2877	37.94	455.30	3.70	51.75	8.80	-16.89
C18	D1	103	2.28	2247	2637	2964	38.00	456.02	3.78	52.92	8.62	-16.32

Sample name	Drive	Depth in Drive (cm)	Sediment Depth (m)	2sσ low	Median	2σ high	C (wt%)	C (mol)	N (wt%)	N (mol)	C/N mol ratio	δ13C (VPDB) (‰)
C19	D1	109	2.34	2380	2818	3028	38.36	460.27	3.81	53.28	8.64	-16.47
C20	D1	115	2.4	2682	3019	3100	38.85	466.21	3.68	51.57	9.04	-17.80
C21	D1	121	2.46	2857	3082	3151	38.90	466.83	3.69	51.67	9.03	-19.13
C22	D1	127	2.52	2950	3099	3192	37.83	453.94	3.38	47.28	9.60	-20.13
C23	D1	133	2.58	3046	3148	3374	36.64	439.65	3.08	43.11	10.20	-20.15
C26	D2	7	2.62	3074	3202	3523	36.59	439.02	3.46	48.38	9.07	-19.22
C27	D2	13	2.68	3109	3279	3662	36.36	436.28	3.47	48.56	8.98	-19.31
C28	D2	19	2.74	3139	3355	3784	36.86	442.36	3.55	49.76	8.89	-19.19
C29	D2	25	2.8	3167	3430	3885	37.02	444.24	3.61	50.54	8.79	-19.04
C30	D2	31	2.86	3202	3506	3985	37.44	449.31	3.59	50.24	8.94	-19.18
C31	D2	37	2.92	3237	3583	4071	35.76	429.13	3.41	47.68	9.00	-19.70
C32	D2	43	2.98	3280	3658	4149	35.68	428.14	3.40	47.65	8.99	-19.46
C33	D2	49	3.04	3328	3736	4231	34.99	419.90	3.36	47.03	8.93	-18.64
C34	D2	55	3.1	3373	3809	4291	38.37	460.41	3.54	49.54	9.29	-17.08
C35	D2	61	3.16	3435	3888	4352	36.46	437.54	3.39	47.43	9.23	-16.92
C36	D2	67	3.22	3498	3964	4410	37.33	447.96	3.42	47.89	9.35	-16.85
C37	D2	73	3.28	3565	4039	4465	39.10	469.18	3.59	50.31	9.33	-16.80
C38	D2	79	3.34	3636	4115	4513	38.89	466.65	3.57	49.91	9.35	-17.35
C39	D2	85	3.4	3712	4189	4553	37.48	449.80	3.50	49.01	9.18	-17.41
C40	D2	91	3.46	3793	4265	4591	37.50	449.94	3.33	46.63	9.65	-16.40
C41	D2	97	3.52	3892	4342	4631	36.36	436.32	3.33	46.63	9.36	-17.54
C42	D2	103	3.58	3991	4416	4662	35.45	425.37	3.07	43.03	9.89	-16.20
C43	D2	109	3.64	4117	4490	4695	33.15	397.83	2.90	40.67	9.78	-16.74
C44	D2	115	3.7	4256	4565	4736	35.02	420.28	3.18	44.46	9.45	-16.97
C45	D2	121	3.76	4478	4647	4788	36.68	440.17	3.25	45.56	9.66	-16.32
C46	D2	127	3.82	4649	4751	4837	36.91	442.92	3.31	46.34	9.56	-17.02
C47	D2	133	3.88	4732	4842	4910	36.48	437.70	3.26	45.61	9.60	-16.50
C51	D3	7	3.92	4794	4858	4945	36.91	442.88	3.26	45.63	9.71	-16.56
C52	D3	13	3.98	4918	5026	5166	37.08	444.93	3.27	45.79	9.72	-17.04
C53	D3	19	4.04	5058	5180	5365	37.69	452.32	3.24	45.42	9.96	-17.95
C54	D3	25	4.1	5086	5246	5452	35.26	423.13	3.05	42.63	9.93	-18.20
C55	D3	31	4.16	5116	5304	5504	34.80	417.65	3.04	42.53	9.82	-17.97
C56	D3	37	4.22	5158	5361	5544	34.98	419.81	2.98	41.67	10.08	-17.84
C57	D3	43	4.28	5204	5420	5573	35.01	420.13	2.91	40.78	10.30	-16.92
C58	D3	49	4.34	5263	5480	5597	32.64	391.68	2.70	37.85	10.35	-17.36
C59	D3	55	4.4	5350	5541	5617	31.48	377.74	2.64	36.97	10.22	-17.42
C60	D3	61	4.46	5523	5604	5642	34.20	410.39	3.00	41.98	9.77	-17.03
C61	D3	67	4.52	5619	5695	5927	36.12	433.49	3.04	42.50	10.20	-16.43
C62	D3	73	4.58	5640	5768	6041	26.12	313.45	2.26	31.61	9.92	-17.02
C63	D3	79	4.64	5664	5839	6119	35.20	422.38	3.04	42.59	9.92	-16.56
C64	D3	85	4.7	5693	5910	6174	28.34	340.09	2.42	33.89	10.03	-17.22
C65	D3	91	4.76	5734	5982	6220	21.38	256.56	1.76	24.68	10.39	-17.23
C66	D3	97	4.82	5782	6052	6256	29.86	358.34	2.50	35.05	10.22	-17.23
C67	D3	103	4.88	5850	6122	6290	31.24	374.83	2.50	34.93	10.73	-17.09
C68	D3	109	4.94	5941	6193	6327	33.30	399.62	2.64	36.99	10.80	-18.12
C69	D3	115	5	6112	6274	6371	32.54	390.45	2.63	36.86	10.59	-18.09
C70	D3	121	5.06	6274	6367	6513	35.46	425.46	3.00	41.97	10.14	-17.57
C71	D3	127	5.12	6323	6439	6577	37.38	448.58	3.18	44.45	10.09	-17.51
C72	D3	130	5.15	6345	6474	6601	34.02	408.20	2.79	39.09	10.44	-19.36

Sample name	Drive	Depth in Drive (cm)	Sediment Depth (m)	2sσ low	Median	2σ high	C (wt%)	C (mol)	N (wt%)	N (mol)	C/N mol ratio	δ13C (VPDB) (‰)
C73	D3	133	5.18	6373	6509	6626	36.96	443.48	3.01	42.14	10.52	-17.60
C77	D4	7	5.22	6444	6571	6685	38.49	461.92	3.56	49.85	9.27	-18.13
C78	D4	13	5.28	6535	6692	7008	39.43	473.19	3.70	51.77	9.14	-17.60
C79	D4	19	5.34	6579	6787	7133	41.38	496.51	3.85	53.87	9.22	-19.03
C80	D4	25	5.4	6621	6877	7227	31.15	373.79	2.78	38.89	9.61	-18.91
C81	D4	31	5.46	6669	6969	7302	39.98	479.71	3.63	50.87	9.43	-19.64
C82	D4	37	5.52	6724	7062	7362	44.68	536.12	3.27	45.72	11.73	-17.01
C83	D4	43	5.58	6798	7152	7402	38.00	456.02	3.02	42.22	10.80	-19.03
C84	D4	49	5.64	6893	7243	7437	36.73	440.81	2.94	41.20	10.70	-18.29
C85	D4	55	5.7	7011	7336	7466	38.79	465.47	3.35	46.91	9.92	-19.12
C86	D4	61	5.76	7223	7436	7503	38.65	463.78	3.41	47.78	9.71	-18.62
C87	D4	64	5.79	7439	7480	7530	36.89	442.72	3.29	46.02	9.62	-18.95
C88	D4	67	5.82	7447	7493	7539	36.54	438.47	3.28	45.87	9.56	-18.93
C89	D4	73	5.88	7462	7520	7550	35.16	421.87	3.15	44.03	9.58	-18.74
C90	D4	79	5.94	7503	7577	7870	40.87	490.45	3.38	47.32	10.37	-19.08
C91	D4	85	6	7547	7710	8179	39.88	478.51	3.37	47.17	10.15	-19.16
C92	D4	91	6.06	7584	7834	8361	40.67	488.04	3.55	49.64	9.83	-17.37
C93	D4	97	6.12	7623	7952	8494	36.81	441.76	3.44	48.10	9.18	-16.78
C94	D4	103	6.18	7671	8068	8610	33.62	403.43	2.98	41.67	9.68	-16.09
C95	D4	109	6.24	7728	8188	8710	32.04	384.53	2.91	40.76	9.43	-18.71
C96	D4	115	6.3	7806	8306	8797	28.14	337.70	2.57	35.92	9.40	-20.91
C97	D4	121	6.36	7895	8425	8864	31.77	381.18	2.68	37.46	10.17	-20.89
C98	D4	127	6.42	8008	8545	8916	31.07	372.88	2.80	39.21	9.51	-22.12
C99	D4	133	6.48	8125	8662	8962	31.43	377.12	2.76	38.67	9.75	-22.74
C100	D4	139	6.54	8282	8782	8999	30.46	365.56	2.70	37.84	9.66	-23.18
C101	D4	145	6.6	8484	8903	9037	20.95	251.35	1.81	25.37	9.91	-21.86
C104	D5	7	6.62	8582	8947	9050	28.80	345.61	2.54	35.57	9.72	-22.32
C105	D5	13	6.68	9029	9087	9257	26.28	315.41	2.48	34.76	9.07	-23.47
C106	D5	19	6.74	9068	9197	9355	25.77	309.24	2.41	33.73	9.17	-24.09
C107	D5	25	6.8	9133	9296	9413	20.96	251.48	1.98	27.68	9.09	-25.04
C108	D5	31	6.86	9320	9435	9653	20.45	245.40	1.89	26.43	9.28	-25.97
C109	D5	37	6.92	9346	9504	9840	20.83	249.96	1.83	25.66	9.74	-26.67
C110	D5	43	6.98	9366	9574	9987	18.99	227.93	1.69	23.64	9.64	-27.16
C111	D5	49	7.04	9389	9645	10111	18.22	218.68	1.58	22.12	9.89	-26.63
C112	D5	55	7.1	9416	9715	10240	13.11	157.29	1.15	16.16	9.73	-26.88
C113	D5	61	7.16	9443	9784	10355	9.29	111.49	0.81	11.33	9.84	-27.10
C114	D5	67	7.22	9474	9856	10471	6.98	83.78	0.59	8.20	10.22	-26.65
C115	D5	73	7.28	9498	9926	10576	9.11	109.35	0.69	9.70	11.27	-25.59
C116	D5	79	7.34	9524	9995	10676	18.10	217.15	1.42	19.88	10.92	-26.81
C117	D5	85	7.4	9555	10063	10781	13.48	161.76	1.06	14.82	10.91	-28.21
C118	D5	91	7.46	9580	10135	10876	5.64	67.70	0.48	6.67	10.15	-19.68

Table 4. Lignin phenol extraction data

Sediment depth (m)	Sample name	2σ low	Median	2σ high	S/V	C/V	[Ad/Al]v	[Ad/Al]s	Λ8 (mg/ 100mg OC)	3,5-Bd (Lcmpd. (mg/100mg OC)
0.085	S9	-50	43	327	0.7693	0.5111	0.4877	0.4728	0.9534	0.0612
0.365	S37	34	325	775	0.6810	0.4763	0.4637	0.4891	1.0290	0.0636
0.530	S53	119	488	984	0.6527	0.4871	0.4684	0.4891	0.9774	0.0605
0.725	S72	255	686	1200	0.5913	0.4892	0.4851	0.4754	0.9028	0.0594
1.205	S120	671	1169	1646	0.6156	0.3992	0.4499	0.4383	1.1220	0.0487
2.340	C18	2247	2637	2964	0.5112	0.4661	0.4819	0.4626	0.9608	0.0434
2.680	C27	3109	3279	3662	0.6189	0.3126	0.3963	0.4187	2.0541	0.0659
3.520	C41	3892	4342	4631	0.6022	0.2726	0.3838	0.4458	1.8510	0.0573
4.000	C49	4974	5091	5242	0.4933	0.1983	0.3545	0.3558	2.8905	0.0443
4.640	C63	5664	5839	6119	0.5242	0.3456	0.3726	0.3694	1.7127	0.0280
4.760	C65	5734	5982	6220	0.4971	0.3748	0.3474	0.3637	2.1243	0.0430
4.880	C67	5850	6122	6290	0.4763	0.3038	0.3895	0.4140	2.4583	0.0395
5.300	C75	6549	6723	7057	0.6547	0.2351	0.3752	0.4317	1.8620	0.0247
5.400	C80	6621	6877	7227	0.4146	0.2061	0.3684	0.4519	1.9356	0.0391
5.520	C82	6724	7062	7362	0.2103	0.0762	0.3907	0.4252	6.5229	0.0401
6.000	C91	7547	7710	8179	0.5707	0.0920	0.4135	0.4509	3.3677	0.0390
6.680	C105	9029	9087	9257	0.5566	0.2727	0.5594	0.6072	0.6622	0.0266
6.800	C107	9133	9296	9413	0.7208	0.3428	0.4883	0.4918	0.8420	0.0237
6.920	C109	9346	9504	9840	0.7823	0.4222	0.4711	0.4659	1.1329	0.0344
7.340	C116	9524	9995	10676	0.3004	0.1659	0.4659	0.4143	1.3863	0.0703